



*DRIVING RESEARCH AND INNOVATION FOR
VEHICLE EFFICIENCY AND ENERGY SUSTAINABILITY*

U.S. DRIVE Highlights of Technical Accomplishments

2016





U.S. DRIVE

Highlights of Technical Accomplishments Overview

Through precompetitive collaboration and technical exchange, U.S. DRIVE accelerates the development and availability of energy-efficient advanced automotive and energy infrastructure technologies.

The U.S. DRIVE Partnership (*Driving Research for Vehicle efficiency and Energy sustainability*) is a voluntary government-industry partnership focused on precompetitive, advanced automotive and related infrastructure technology research and development (R&D). Partners are the United States Department of Energy (DOE); the United States Council for Automotive Research LLC (USCAR), a consortium composed of FCA US LLC, Ford Motor Company, and General Motors Company; five energy companies, (BP America, Chevron Corporation, Phillips 66 Company, ExxonMobil Corporation, and Shell Oil Products US); two electric utilities, DTE Energy and Southern California Edison; and the Electric Power Research Institute.

The Partnership benefits from a history of successful collaboration across multiple technical teams, each focused on a key area of the U.S. DRIVE portfolio (see below). These teams convene the best and brightest scientists and engineers from U.S. DRIVE partner organizations to discuss key technical challenges, identify possible solutions, and evaluate progress toward goals and targets published in technology roadmaps. U.S. DRIVE also has two working groups: (1) fuel properties for future engines, recognizing an important opportunity to evaluate how various fuel properties can increase the efficiency of advanced internal combustion engines; and (2) energy efficient mobility systems, a new focus initiated in late 2016 to understand transportation system-level opportunities for significant energy savings in the movement of people and goods. By providing a framework for frequent and regular interaction among technical experts in common areas of expertise, the Partnership accelerates technical progress, helps to avoid duplication of efforts, ensures that publicly-funded research delivers high-value results, and overcomes high-risk barriers to technology commercialization.

U.S. DRIVE technical teams selected the highlights in this document from many hundreds of DOE-funded projects conducted by some of the nation's top research organizations in the field. Each one-page summary represents what DOE and automotive, energy, and utility industry partners collectively consider to be significant progress in the development of advanced automotive and infrastructure technologies. The report is organized by technical team area, with highlights in three general categories:

Vehicles

- Advanced Combustion and Emission Control
- Electrical and Electronics
- Electrochemical Energy Storage
- Fuel Cells
- Materials
- Vehicle Systems Analysis

Crosscutting

- Codes and Standards
- Grid Interaction
- Hydrogen Storage
- Integrated Systems Analysis

Fuels

- Hydrogen Delivery
- Hydrogen Production

More information about U.S. DRIVE, including prior-year accomplishments reports and technology roadmaps, is available on the DOE (<https://energy.gov/eere/vehicles/vehicle-technologies-office-us-drive>) and USCAR (www.uscar.org) websites.

Table of Contents

VEHICLES	1
<i>Advanced Combustion and Emission Control</i>	<i>1</i>
New Low Temperature Oxidation Catalyst Test Protocol Validated	2
Spark Ignition Model Developed to Predict Engine Misfires.....	3
Gasoline Fuel Injection Modeling Improved	4
Simplified Chemical Representations for Diesel Fuels Developed	5
Exhaust Catalysts Demonstrated for Improved Performance on Lean Gasoline Engines.....	6
Wide Range of Low-Temperature Combustion Modes Shown to Be Varying Degrees of Same Phenomenon	7
New SCR Catalyst Formulation May Enable Higher Efficiency Vehicles.....	8
Combustion-Timing Control for a Low-Temperature Gasoline Combustion Concept Demonstrated	9
Discovery of Cool-Flame Wave Enhances Understanding of Diesel Combustion.....	10
A Viable Approach to Improve Controllability of High-Efficiency Gasoline Engines.....	11
<i>Electrical and Electronics</i>	<i>12</i>
Thermal Management of Wide Bandgap Technology Critical for Power-Dense, High-Temperature Systems	13
High-Power Density Ferrite Permanent Magnet Motor	14
Using Supercomputers to Develop Better Magnetic Materials.....	15
Materials Expertise Aids Manufacturers in Commercializing High-Performance Motors	16
High-Temperature DC Bus Capacitor Cost Reduction and Performance Improvements	17
Vehicle Electric Motor Design uses Permanent Magnets without any Rare-Earth Content.....	18
Application of Silicon Carbide Power Devices in Hybrid Electric Vehicle Drive Systems	19
High-Temperature Wide Bandgap Inverter for Electric Vehicles.....	20
<i>Electrochemical Energy Storage</i>	<i>21</i>
Silicon Nanowire Anodes Enable High Specific Energy, High Energy Density, and Long Cycle Life	22
Fluorinated Electrolyte for 5-Volt Lithium-Ion Chemistry	23
Pursuit of Cost-Effective, High-Capacity, Manganese-Rich, Lithium-Ion Cathodes.....	24
Fluorinated Electrolytes for Higher Voltage Cell Operation	25
Advanced Polyolefin Separators for Lithium-Ion Batteries used in Electric Vehicles.....	26
Manufacturing High-Performance, Low-Cost Protective Coatings for Long-Life Lithium-Ion Battery Materials	27
Assessment of Fast-Charging Impacts on Battery Life	28
Improved Cathode Materials for Lithium-Ion Batteries	29
12 Volt Start/Stop Lithium Polymer Battery Pack	30
Microstructure Simulation of Battery Electrode Design	31
Electron Beam Curing of Lithium-Ion Battery Electrodes	32
Enabling Fast Formation for Lithium-Ion Batteries	33
Alternate Reaction Pathway Enables Higher Performance Lithium-Sulfur Batteries	34
High-Performance Organosilicon-Based Lithium-Ion Electrolyte	35
Constructing a “Home” for Lithium-Metal Anodes	36
High-Energy, High-Power Battery for Plug-In Hybrid Electric Vehicle Applications	37
Reducing Interfacial Impedance in Solid-State Batteries	38
New Process is Demonstrated for End-of-Life Electric Vehicle Lithium-Ion Batteries	39
Silicon-Graphene Material Shows Promise for Electric Vehicle Batteries.....	40
<i>Fuel Cells</i>	<i>41</i>
Improved Membrane Performance and Durability.....	42

Enhanced Understanding of Platinum Alloy Catalysts	43
Materials	44
Low-Cost Carbon Fiber Commercialization	45
Predictive Engineering Tools for Injection-Molded Long Carbon Fiber Thermoplastic Composites	46
High-Performance Magnesium Alloys without Rare-Earth Elements	47
High-Speed Joining Method Delivers Lighter Weight Automobiles, Faster	48
Component-Level Validation of a Third-Generation Advanced High-Strength Steel Forming Model	49
Validation of Carbon Fiber Composite Material Models for Automotive Crash Simulation	50
Vehicle Systems Analysis	51
Impact of Connectivity and Automation on Vehicle Energy use	52
Analyzing Real-World Vehicle Efficiency	53
CROSSCUTTING	54
Codes and Standards	54
New Hydrogen Risk Assessment Model Toolkit Quantifies Hydrogen Risk for Global Code Development .	55
Grid Interaction	56
Adapter Enables Smart Networked Charging for Electric Vehicles.....	57
Testing Validated the Interoperability and Performance Requirements of SAE J2954™ Codes and Standards.....	58
Hydrogen Storage	59
First Demonstration of Multiple Hydrogen Molecules Adsorbed on a Metal Site in a Metal-Organic Framework	60
Hydrogen Materials—Advanced Research Consortium Supports New Storage Materials Discovery	61
Integrated Systems Analysis	62
Cradle-to-Grave Greenhouse Gas Emissions and Economic Assessment of U.S. Light-Duty Vehicle Technologies	63
FUELS	64
Hydrogen Delivery	64
World Record for Magnetocaloric Gas Liquefaction	65
New Hydrogen Station Equipment Performance Device.....	66
ASME Certification for Low-Cost 875 Bar Hydrogen Storage	67
Hydrogen Production	68
Economic Hydrogen Production Demonstrated Using a New Reformer-Electrolyzer-Purifier Technology ..	69
16% Efficient Direct Solar-to-Hydrogen Conversion Sets New World Record	70
Pathway to Economic Hydrogen from Biomass Fermentation	71

VEHICLES

Advanced Combustion and Emission Control



New Low Temperature Oxidation Catalyst Test Protocol Validated

Round robin study demonstrated new protocol for consistent and reproducible results across multiple testing laboratories.

ACEC Low Temperature Aftertreatment Group

The U.S. DRIVE/Advanced Combustion and Emission Control Technical Team (ACEC), in response to the low-temperature exhaust challenges that advanced powertrain technologies present, is taking steps to accelerate the pace of aftertreatment catalyst innovation and discovery. To this end, the ACEC Low Temperature Aftertreatment (LTAT) sub-team is developing catalyst test protocols to address the need for common metrics and strategies for catalyst testing. The catalyst test protocols will enable the exchange of consistent and realistic catalyst performance data between various research laboratories (industry, academic, and national laboratories) and to the open literature. As a first step, in 2014 the LTAT sub-team developed a low-temperature oxidation catalyst test protocol and in 2016, the team performed a round-robin study that validated the protocol's utility and its ability to yield reproducible results.

The utility of the test protocol depends on its ability to accurately screen candidate catalyst technologies for the application and provide consistent and reproducible results. The accuracy of the protocol was confidently verified by the intimate involvement of industry partners. The LTAT sub-team was then tasked to demonstrate the reproducibility of the protocol in the form of a round-robin study – recognizing that historically, comparing catalyst test results across multiple institutions has been difficult.

Four LTAT sub-team members participated in the study: Ford, General Motors, Oak Ridge National Laboratory, and Pacific Northwest National Laboratory. The goal was to demonstrate a standard deviation (SD) of less than 10% across the results from the various members. A production diesel oxidation catalyst was selected for the study; unique

mini-core samples were removed from a single aftertreatment part for testing at each organization's facility. Per protocol guidelines, the participants followed the procedures, in sequential fashion, for de-greening the catalyst, characterizing catalyst performance, aging the catalyst, and repeating catalyst performance characterization.

Figure 1 shows the results for the de-greened catalysts, as the temperature required to achieve 50% and 90% removal of each pollutant (T50 and T90, respectively). The compiled results showed that a maximum SD of 6.5% and 4.9% across the participants was demonstrated for T50 and T90 values, respectively, validating the utility of the protocol and its ability to yield consistent and reproducible results.

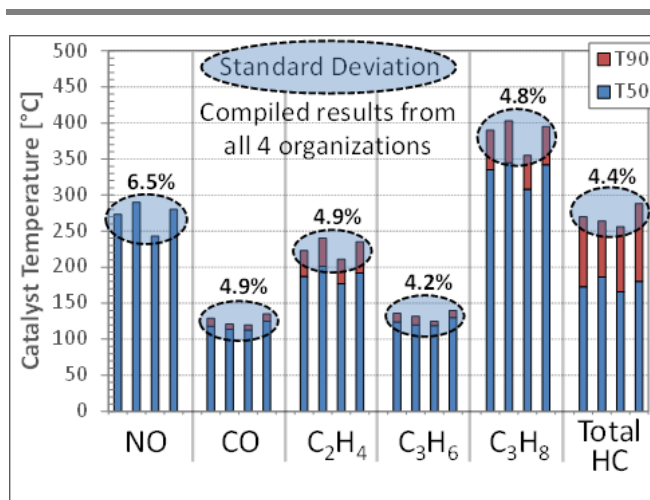


Figure 1. Results from de-greened catalysts, presented as temperature required to achieve 50% (T50) and 90% (T90) removal of each pollutant.

Spark Ignition Model Developed to Predict Engine Misfires

X-Ray imaging used to characterize ignition plasma and validate new ignition model for predicting ignition quality.

Argonne National Laboratory

Argonne National Laboratory (ANL) researchers developed a novel computational fluid dynamics (CFD) model as well as an advanced X-ray based measurement technique that was used to validate the thermal property predictions of ignition plasmas (see Figure 1). The validated CFD model presents a key capability for accurately evaluating advanced ignition concepts for high-efficiency spark ignition engines.

Because crucial features such as discharge energy amount, shape of the spark channel, and energy losses due to heat transfer are typically neglected, ignition models that are currently implemented in CFD codes are simplistic and are not able to correctly predict ignition success or failure. Nevertheless, these models are relied upon to describe the physical processes during plasma discharge events and determine whether or not the flame propagates. Validating improved ignition models requires accurate characterization of the chemical and thermal properties of ignition plasmas. Using innovative X-ray diagnostics, researchers quantified the physical properties of ignition plasmas with superior accuracy. Plasma density and the change of density during the ignition process was measured with high precision and used to validate the accuracy of CFD results employing a novel modeling approach.

CFD results were successfully validated against Schlieren images from an optical vessel at Michigan Technological University (MTU) for both firing and misfiring conditions. ANL researchers demonstrated that this comprehensive ignition model was able to accurately describe the flame kernel growth and capture the experimental transition from ignition success to failure (see Figure 2). This was achieved by modeling the entire ignition system with realistic

ignition system inputs to eliminate inaccurate modeling assumptions and combined with detailed chemistry calculations, thereby significantly improving the predictive capabilities necessary when simulating the ignition process in modern gasoline engines.

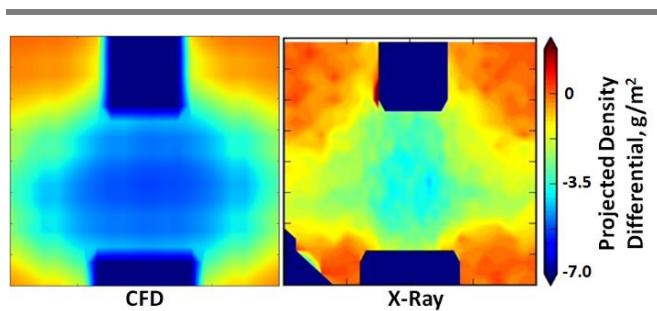


Figure 1. Calculated (CFD) and measured (X-ray) two-dimensional map of the differential of projected gas density in the spark-plug gap region during the ignition discharge.

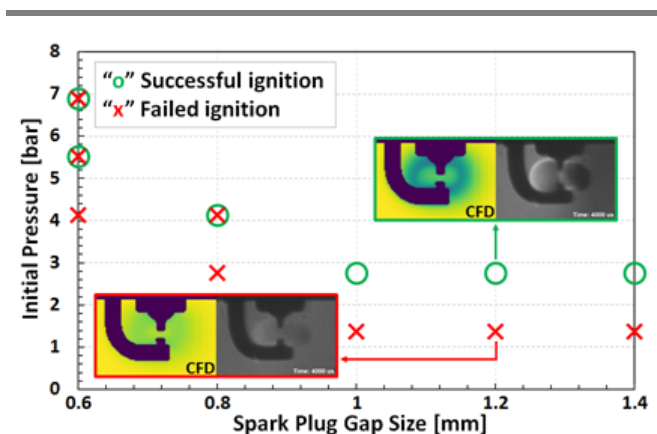


Figure 2. ANL ignition model predicted ignition success and failure (optical data from MTU).

Improved ignition models play a critical role in assessing the potential and accelerating the implementation of advanced ignition systems. These ignition systems hold the potential to enable further engine efficiency gains through improved dilution tolerance and performance at increased boost levels.

Gasoline Fuel Injection Modeling Improved

Spray collapse observed in experiments is correctly predicted by CFD modeling linking internal and external flow conditions.

General Motors and Oak Ridge National Laboratory

A research collaboration between General Motors and Oak Ridge National Laboratory (ORNL) demonstrated a computational fluid dynamics (CFD) modeling approach that predicted the structure of gasoline fuel sprays due to fuel temperature and ambient pressure including conditions with aggressive flash boiling. The key aspect of the approach was a single code that coupled models for internal nozzle flow and an external spray solver. The approach addressed a significant challenge in CFD modeling of spark-ignited direct injection (SIDI) engines to predict the onset of spray collapse induced by flash boiling. Spray characterization is critical to the in-cylinder mixing and subsequent performance of SIDI engines.

The computed spray structure matched experimental photographs of the spray in a vessel (Figure 1). At low fuel temperatures and higher pressures (non-flash in the figure), both the

calculated and measured individual spray plumes were discrete, distinguishable and had a well-defined pattern. At high temperatures and lower pressures (flare flash in the figure), the spray shape collapsed into a single, diffuse plume. This condition had aggressive flash boiling and occurred because superheated fuel was injected into a low-pressure environment created by a closed engine throttle. Between these two conditions is a transition zone of moderate flash boiling in which the spacing between the sprays plumes lessened.

Researchers performed computations on the Titan supercomputer at ORNL, one of the U.S. Department of Energy's Leadership Computing Facilities. The understandings from this work advanced knowledge of spray physics and increased confidence to apply modeling tools in the development of novel combustion systems.

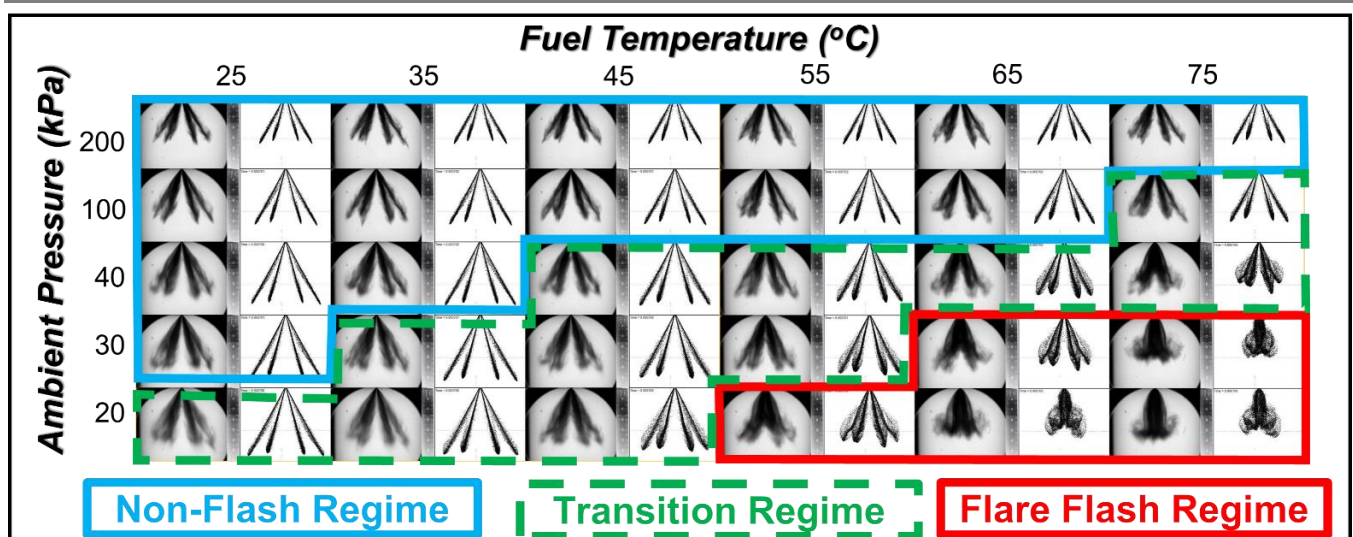


Figure 1. Comparison of experimental images (left) and CFD computations (right) of a six-hole gasoline spray under fuel temperatures and ambient pressures for non-flashing, transition, and flare flashing operation.

Simplified Chemical Representations for Diesel Fuels Developed

New “surrogate” fuels accurately capture relevant properties for efficient and accurate modeling to optimize engine design.

Lawrence Livermore National Laboratory, National Renewable Energy Laboratory, Pacific Northwest National Laboratory, and Sandia National Laboratories

Computational and experimental scientists and engineers have worked hand-in-hand with colleagues from industry and universities to develop methods to generate surrogate fuels that closely mimic the properties of typical diesel fuels. Development of these surrogate fuels enables exploration of the impact that fuel properties can have on engine efficiency and emissions, and provides the foundation for affordable yet realistic computer optimization of new engine designs.

New fuel-characterization techniques were applied to select a nine-component palette of compounds representative of those found in commercial diesel fuels. Next, the team employed a computational optimization algorithm to determine how much of each palette compound should be added to each surrogate to match the molecular structure (carbon bond types), reactivity (cetane number), and physical properties (distillation curve, density) of the target fuel. High-purity palette compounds were

then procured, blended according to the optimized “recipe,” and the resulting surrogate fuel was tested to verify that it adequately emulates the target fuel (see Figure 1). Finally, detailed kinetic mechanisms were crafted for each of the palette compounds, enabling simulation of the performance and emission characteristics of a range of surrogates. The research was conducted in collaboration with the Coordinating Research Council (www.crcao.org).

Colleagues at Yale University have subsequently tested these surrogates to see if the sooting tendency of the target fuel is adequately captured. All of the surrogates match the yield sooting index of the target fuel within 25%—one surrogate is within just a few percent.

The outcome of this work—an ability to faithfully incorporate both chemical and physical fuel properties into engine simulations—addresses a key barrier to computational engine design.

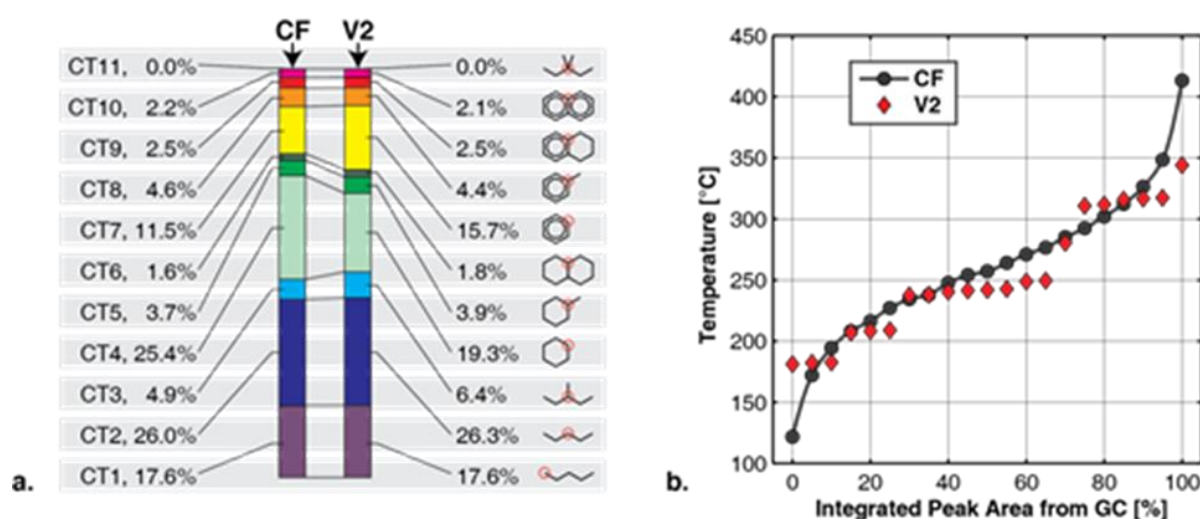


Figure 1. The surrogate diesel fuel (V2) closely emulates the 11 carbon bond types (a.) and distillation temperature distribution (b.) of the target diesel fuel (CF). See <http://pubs.acs.org/doi/abs/10.1021/acs.energyfuels.5b02879> for details.

Exhaust Catalysts Demonstrated for Improved Performance on Lean Gasoline Engines

Three-way catalysts produce ammonia at high efficiency and low exhaust gas temperature for enabling “passive SCR.”

Oak Ridge National Laboratory

Lean gasoline engines are more fuel efficient than the stoichiometric gasoline engines common in the U.S. passenger fleet, but controlling nitrogen oxides (NO_x) under lean exhaust conditions is challenging. Oak Ridge National Laboratory (ORNL), in collaboration with industry partners General Motors and Umicore, studied passive selective catalytic reduction (SCR) for lean gasoline engine emissions control. Studies at low temperatures demonstrated production of ammonia (NH_3), critical to the passive SCR approach, at more than 98% efficiency in the temperature range of 160°-180°C.

In passive SCR emission control, NH_3 production over a three-way catalyst (TWC) is critical because NH_3 is used to reduce NO_x emissions over a downstream SCR catalyst during lean engine operation. NH_3 production requires rich engine operation, which facilitates the reaction of reductants and NO_x in the engine exhaust to form NH_3 over the TWC. High-efficiency NH_3 production is desired so that rich operation can be minimized and fuel economy gains can be maximized.

In studies of TWCs on a synthetic exhaust flow reactor, NH_3 production at low temperatures was characterized for five unique TWCs. The catalysts studied had different composition; specific components varied included oxygen-storage capacity, platinum group metal loading, and NO_x storage capacity. During the TWC studies, simulated exhaust gases flowed over the catalysts representing different air-to-fuel ratios for engine operation. The catalyst temperature was increased to determine the efficiency of NH_3 production as a function of temperature and air-to-fuel ratio. If NH_3 can be produced during low-temperature operation, lower overall fuel use over the transient drive cycle

required for vehicle emissions and fuel economy compliance will be achieved.

As the TWC temperature increased, NH_3 formation dramatically increased to more than 98% efficiency in a TWC temperature range of 160-180°C with an air-to-fuel ratio of 14.06 (slightly rich operation) (see Figure 1). The efficient NH_3 production under these conditions demonstrates that TWCs can produce NH_3 efficiently during cold start and other low-temperature operation and thereby increase lean operation for fuel savings. The results were consistent over the wide range of TWC formulations studied.

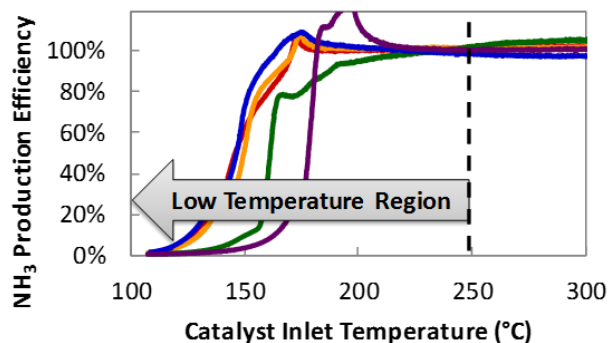


Figure 1. Efficiency of NH_3 production for five unique TWC formulations at a slightly rich air-to-fuel ratio of 14.06; all TWCs show highly efficient conversion of NO_x to NH_3 at low temperatures. Efficiencies over 100% occur from NO_x storage.

Wide Range of Low-Temperature Combustion Modes Shown to Be Varying Degrees of Same Phenomenon

Simulations and experiments show combustion modes comprise a continuum based on amount of fuel-air stratification.

Oak Ridge National Laboratory

Simulations and experimental research at Oak Ridge National Laboratory (ORNL) have led to the development of a new perspective on low-temperature combustion (LTC) that has changed the discussion of these strategies in the research community at-large. LTC strategies have been studied widely due to their potential for high efficiency with low nitrogen oxide (NO_x) and soot emissions. Previous LTC research classified the many variations as separate modes with many different names. ORNL's findings define a combustion mode continuum that shows how these combustion modes relate to one another based on the degree of air/fuel stratification at the start of combustion.

Figure 1 illustrates how these previously identified separate LTC modes are part of a continuum based on level of reactivity stratification for diesel-like fuels (high-reactivity), gasoline-like fuels (low-reactivity), and for dual-fuel approaches.

This new perspective of the LTC space has already had an impact on how LTC is discussed in the research community as well as government, industry, and academic institutions. This perspective of investigating LTC on a continuum of in-cylinder fuel stratification is critical to informing new research efforts focused on achieving potential efficiency gains and emissions reductions with LTC modes.

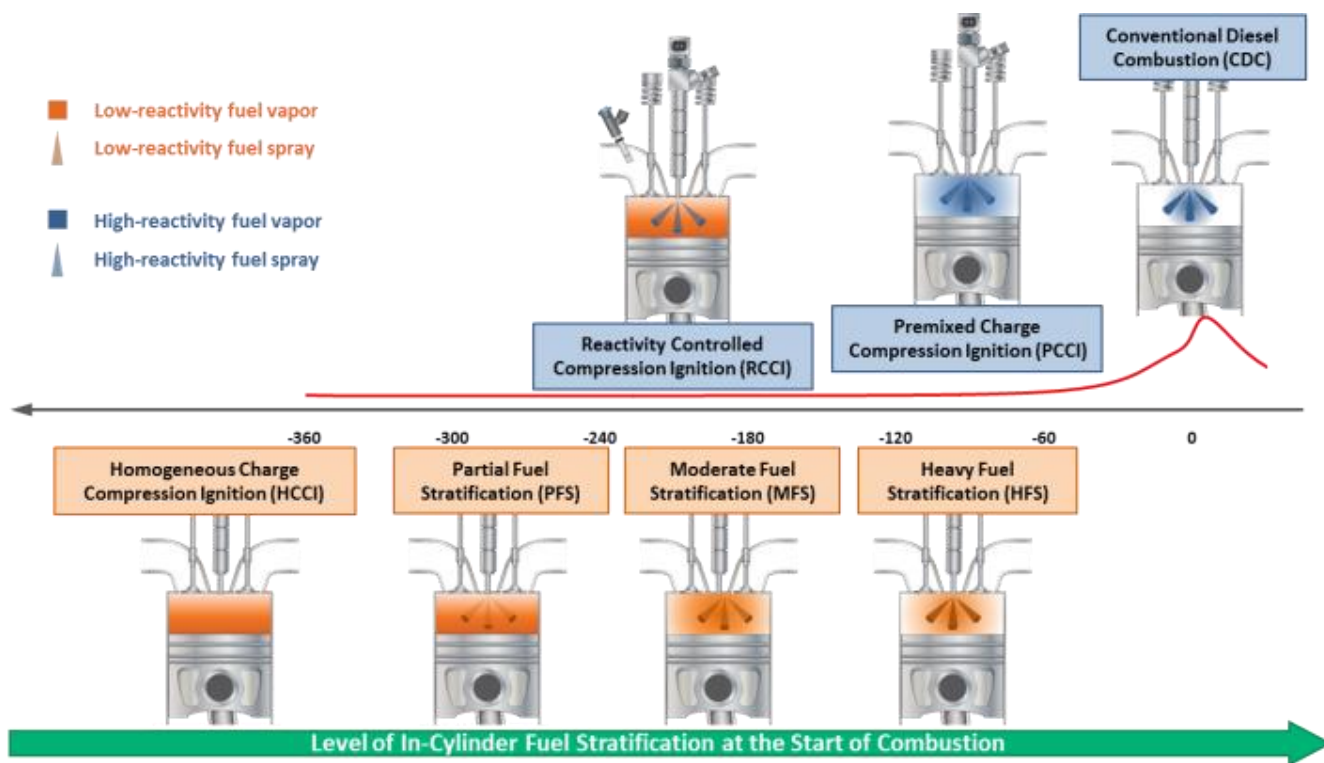


Figure 1. Advanced compression ignition combustion strategies are shown as a continuum based on the level of fuel stratification at ignition with gasoline compression ignition modes on the bottom and diesel and dual-fuel low temperature combustion modes on the top.

New SCR Catalyst Formulation May Enable Higher Efficiency Vehicles

Iron-zeolite catalyst shows high NO_x conversion at lower temperatures than previously possible.

Pacific Northwest National Laboratory, Cummins, and Johnson-Matthey

Lean-combustion gasoline and diesel engines provide reduced carbon dioxide (CO₂) emission and attractive performance compared to stoichiometric gasoline engines. However, meeting stringent emissions standards has been a major challenge with these engines. A new automotive catalyst has been developed at Pacific Northwest National Laboratory (PNNL), (in collaboration with Cummins and Johnson-Matthey (JMI)) for selective catalytic reduction (SCR) of nitrogen oxides (NO_x) that is a promising innovation for controlling NO_x at low temperature, and may become an enabling technology for future high-efficiency vehicles.

The fast-SCR reaction that consumes nitric oxide (NO) and nitrogen dioxide (NO₂) in equimolar amounts ($\text{NO} + \text{NO}_2 + 2\text{NH}_3 = 2\text{N}_2 + 3\text{H}_2\text{O}$) has long been recognized as efficient for low-temperature NO_x conversion. However, at under 180°C, this chemistry has historically been challenged by ammonium nitrate (NH₄NO₃) poisoning. A novel iron (Fe)-exchanged zeolite SCR catalyst has recently been developed at PNNL that eliminates NH₄NO₃ deposition under fast-SCR conditions at a temperature as low as 150°C.

In current SCR catalysts, below ~180°C, NH₄NO₃ forms as a solid poison under typical fast-SCR conditions and impedes NO_x reduction. NH₄NO₃ formation results from NO₂ disproportionation and a subsequent acid-base reaction. Under typical fast-SCR conditions, NO₂ disproportionation is unavoidable. However, PNNL's iron-SCR catalyst is successful at greatly eliminating the acid-base reaction by proper manipulation of the ammonia (NH₃) storage of the catalyst, allowing the fast-SCR reaction to proceed unimpeded at 150°C.

The work is occurring in parallel with advanced strategies of low-temperature NO-to-NO₂ oxidation to achieve ~50% NO₂:NO_x in the exhaust, and low-temperature reductant (NH₃) delivery. Together, these innovations will enable SCR aftertreatment to achieve greater than 90% NO_x reduction at 150°C.

As shown in Figure 1, at a relevant reaction space velocity (SV) and using NH₃ as the reductant under laboratory conditions, steady-state NO_x conversion exceeded 90% at 150°C. Furthermore, PNNL has developed a dual-bed catalyst concept to overcome inlet NO₂/NO_x ratio fluctuation, which is shown in Figure 1 to greatly improve NO_x conversion when NO₂/NO_x ≠ 0.5. No hydrocarbon inhibition or durability issues were observed with propylene at 150°C. The program is currently planning demonstration of the technology at relevant scale with the original equipment manufacturer partners (Cummins and JMI).

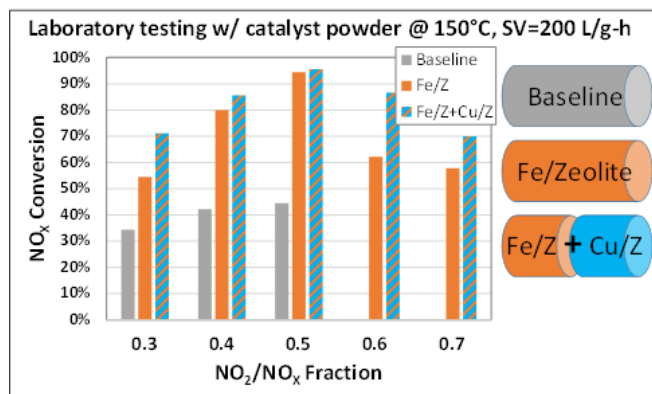


Figure 1. Steady-state NO_x conversion of a commercial baseline SCR catalyst, PNNL's Fe/zeolite, and the dual bed Fe/zeolite + Cu/zeolite concept.

Combustion-Timing Control for a Low-Temperature Gasoline Combustion Concept Demonstrated

Multiple gasoline direct injections create desirable fuel stratification to provide rapid adjustment of combustion timing.

Sandia National Laboratories

Low-temperature gasoline combustion (LTGC) engines can provide high efficiencies and extremely low nitrogen oxide (NO_x) and particulate emissions, but rapid, robust combustion-timing control remains a challenge to commercializing these engines. Recent research at Sandia National Laboratories has shown that partial fuel stratification (PFS) produced by double direct injection (DDI) can control the combustion timing over a wide range by altering the chemical-kinetic rates of autoignition. Using this DDI-PFS technique, the 50% burn point (CA50) could be adjusted as much as 8.5° CA, from near the misfire limit (overly retarded CA50) to beyond the knock/ringing limit (overly advanced CA50).

With this technique, a GDI-type fuel injector is used to inject 70% to 80% of the fuel early in the intake stroke, and the remainder from 200° – 325° crank angle (CA) after top dead center (TDC) intake. Combustion timing is controlled by adjusting the amount of mixture stratification, which is accomplished by varying the timing of the second (late-DI) injection and/or the late-DI fuel fraction. More retarded late-DI timings (or greater late-DI fraction) increase the stratification for higher fuel/air equivalence ratios (ϕ) in the richest regions. These higher- ϕ regions autoignite faster, driving the rest of charge into autoignition faster and advancing CA50. Thus, retarding the late-DI timing advances CA50, which is distinctly different from injection-timing control in a diesel engine or diesel-like engines operated on gasoline, in which autoignition occurs shortly after injection and retarded DI timings retard CA50.

Figure 1 demonstrates the ability of this technique to provide combustion-timing control for intake pressures (P_{in}) from naturally aspirated (1 bar) up to

2.0 bar absolute. The change in CA50 is shown relative to the combustion timing with the late-DI injection at 280° CA. As can be seen, the curves for $P_{in} = 1.2$ – 2.0 bar are quite similar. For a late-DI timing of 200° CA (near bottom dead center), the charge is relatively well mixed, and CA50 is quite retarded. Shifting the late-DI timing later in the compression stroke advances CA50, by as much as 8.5° CA for a late-DI timing of 315° CA. Control is robust, and it is rapid, because CA50 can be changed from one cycle to the next. $P_{in} = 1.1$ bar requires a little more stratification, with a late-DI timing= 320° CA for the most advanced CA50 shown. For $P_{in} = 1.0$ bar, good CA50 control is achieved by varying the late-DI timing from 270° – 325° CA, but late-DI timings earlier than 270° CA are not effective. Soot is at or below the detectability limit, and NO_x is ≤ 0.025 g/kWh for all points with acceptable ringing, reducing aftertreatment requirements.

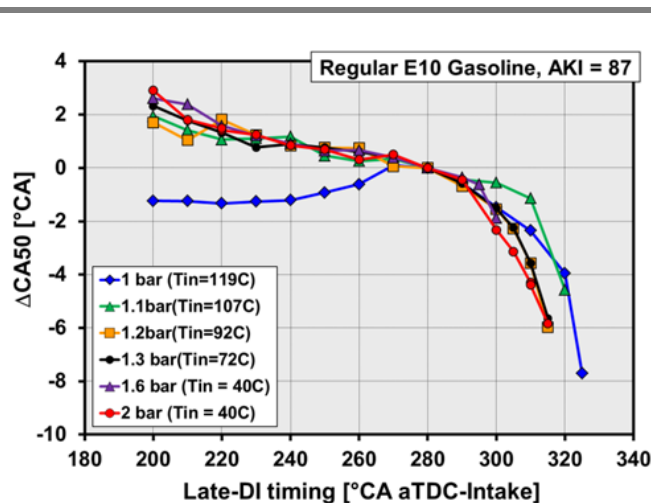


Figure 1. CA50 control as a function of the late-DI timing for intake pressures from 1.0 to 2.0 bar absolute. 1,200 rpm. 0° CA = TDC Intake.

Discovery of Cool-Flame Wave Enhances Understanding of Diesel Combustion

Interactions between combustion chemistry and intense turbulence in diesel sprays forms foundation for predictive auto-ignition model development.

Sandia National Laboratories

Both mixing and chemistry impact the auto-ignition process in diesel sprays; however, the interactions between these processes are poorly understood. Inevitably, this knowledge gap impedes the predictive quality of engine computational fluid dynamics (CFD) models. Recent work at Sandia National Laboratories has led to the discovery of a previously unrecognized interaction phenomenon—a cool-flame ignition wave—on which improved, physically realistic models can be built.

Experiments using high-speed Schlieren imaging and planar laser-induced fluorescence of formaldehyde consistently demonstrate initiation of ignition in the radial periphery of the spray where the fuel/air mixture is more fuel-lean and local temperatures are higher. Within the next 100-150 μ s, the experiments indicate that first-stage ignition proceeds throughout the entire spray head where local equivalence ratios exceed $\phi > 4$ (Figure 1). In a well-mixed scenario, without turbulence-chemistry interactions (TCI), these rich mixtures require more than 2 milliseconds to ignite. Thus, an interaction between the mixing and chemistry must exist to drive fuel-rich mixtures toward realistic (shorter) ignition delays.

To better understand TCI, researchers developed a first-principles analysis method based on high fidelity kinetics (see Figure 2). The analysis revealed that intense turbulence rapidly drives a “turbulent cool-flame wave” from the fuel-lean initiation regions throughout the entire vaporized mixture. This wave chemically activates the mixture, which significantly decreases the ignition delay of fuel-rich mixture regions in comparison to a well-mixed reference case. This new discovery demonstrates that the neglect of TCI in simulations fundamentally fails to capture key features of the experimentally

observed ignition process, and provides a phenomenological basis for improved models.

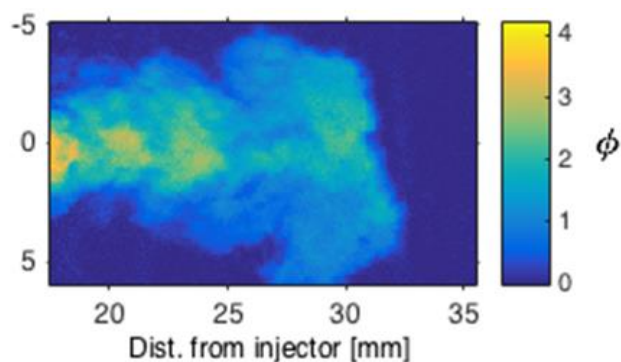


Figure 1. Equivalence ratio distribution of an n-dodecane spray depicting the ignition sequence in physical space.

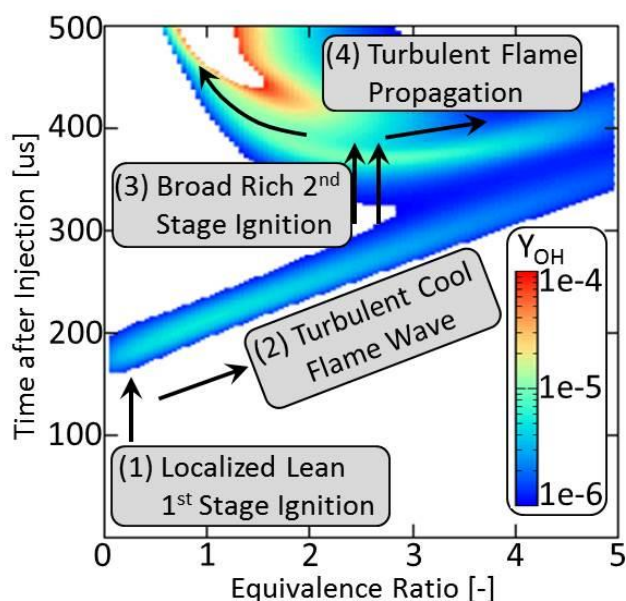


Figure 2. The hydroxyl radical mass fraction in ϕ -time space as it evolves during the ignition process in high-pressure spray flames. Beginning in fuel-lean regions (1), a cool-flame wave rapidly drives (2) temperature and reactive species into more fuel-rich regions (3) promoting combustion in a flame propagation regime (4).

A Viable Approach to Improve Controllability of High-Efficiency Gasoline Engines

How in-cylinder generated fuel reformat enhances fuel-air mixture reactivity.

Sandia National Laboratories

Strategies are needed to improve controllability for high-efficiency gasoline compression ignition concepts at low loads where combustion stability is problematic. One viable approach is to use in-cylinder generated fuel reformat from an auxiliary re-compression period to enhance overall charge ignitability. Research at Sandia National Laboratories has clarified the mechanisms responsible for increased reactivity when the reformat is mixed with main-period fuel-air charge. A modeling basis was also developed to enable optimization of the relevant processes.

Experiments were performed in a direct-injection, naturally aspirated, single-cylinder research engine. A five-component gasoline surrogate was used that matched the fuel properties and broad molecular composition of gasoline. The impact of the in-cylinder generated reformat on engine performance was evaluated and—unexpectedly—the lowest main-period fueling rates (leanest mixture) led to the fastest ignition for a fixed reformat quantity.

To investigate this behavior, researchers used an in-cylinder sampling apparatus to separately collect bulk-gas samples at the end of re-compression, with the reformat characterized in detail using a photoionization mass spectrometry (PIMS) diagnostic. PIMS uses soft X-rays to continuously ionize the sample gas, and various species are identified using a high-resolution time-of-flight mass spectrometer. Multiple X-ray (photon) energy scans were performed to distinguish between isomers with identical molecular composition. Over 80 sample constituents were identified and quantified based on their photoionization efficiencies.

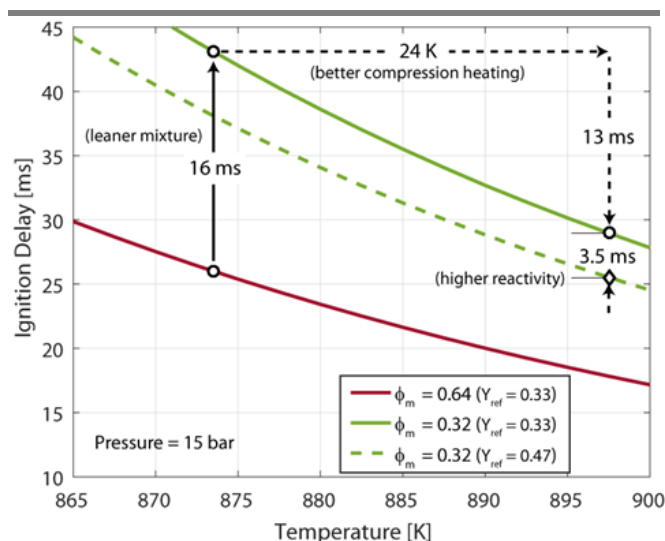


Figure 1. Calculated auto-ignition delays as a function of bulk-gas temperature for different charge mass equivalence ratios.

Thermodynamic and chemical kinetic modeling, using the comprehensive knowledge of the reformat composition, showed that the impact of reformat addition on the auto-ignition of the main-period charge was due to three effects. Figure 1 shows that—as expected—the ignition delay for a fixed reformat fraction Y_{ref} (solid lines) and bulk-gas temperature are 16 milliseconds (ms) slower for leaner charge mixtures (i.e., lower fueling rates). However, the increased reformat mass fraction associated with the leaner charge leads to increased compression temperatures (due to increased charge specific heat ratio and decreased main injection charge cooling), reducing the ignition delay by 13 ms. Moreover, increased reactivity due to higher Y_{ref} reduces the ignition delay an additional 3.5 ms through the production of more reactive species, namely acetylene, acetaldehyde, propene, and allene. Together, these three effects result in a modelled ignition delay that is 0.5 ms shorter than the richer mixture—a value that agrees well with the experiment data.

Electrical and Electronics



Thermal Management of Wide Bandgap Technology Critical for Power-Dense, High-Temperature Systems

New cooling solution will enable high-temperature and high-efficiency WBG devices within automotive power electronic systems.

National Renewable Energy Laboratory

Wide bandgap (WBG)-based power electronics will increase driving range and reduce the cost of electric drive vehicles by increasing efficiency, supporting higher junction temperatures, enabling higher switching frequencies, and increasing power densities in automotive power electronics systems (e.g., inverter). Achieving these benefits requires thermal management of the devices as well as the surrounding system components. A challenge with WBG devices is that although their heat losses are lower, the area of the devices is also reduced due to increased power density and reduced costs, which results in higher device heat flux. Additionally, the high junction temperatures of WBG devices will result in larger temperature gradients through the power module that will present reliability challenges and require high-temperature bonding materials. Another challenge with the higher junction temperatures is that they will expose other system components (e.g., capacitors and electrical boards) to higher temperatures. These challenges require system-level thermal management analysis and innovative thermal management solutions.

Using high-performance computing resources, the National Renewable Energy Laboratory (NREL) quantified an automotive inverter's three-dimensional steady-state and transient temperature and heat flow at the component and system level. The analysis quantified the inverter component temperatures resulting from the higher junction temperature enabled by WBG devices (from 175°C to 250°C). The results show that the capacitors, electrical boards, and module interface layers will exceed their allowable operating temperature limits under most WBG operating conditions. The resulting information is useful to component manufacturers and material suppliers working to commercialize WBG-based power electronics.

For example, capacitors are critical components in power electronics, but their low maximum operating temperature (85°C) poses thermal management challenges when packaged within high-temperature WBG environments. NREL demonstrated and compared the efficacy of capacitor thermal management approaches, demonstrating that cooling the electrical interconnections was a more effective thermal management strategy than directly cooling the capacitors. The electrical interconnect (Figure 1) cooling approach was predicted to enable capacitors to operate within their allowable temperature limits at WBG junction temperatures up to 250°C. The cooling solutions developed in this project will enable high-temperature WBG packaging within automotive power electronics.

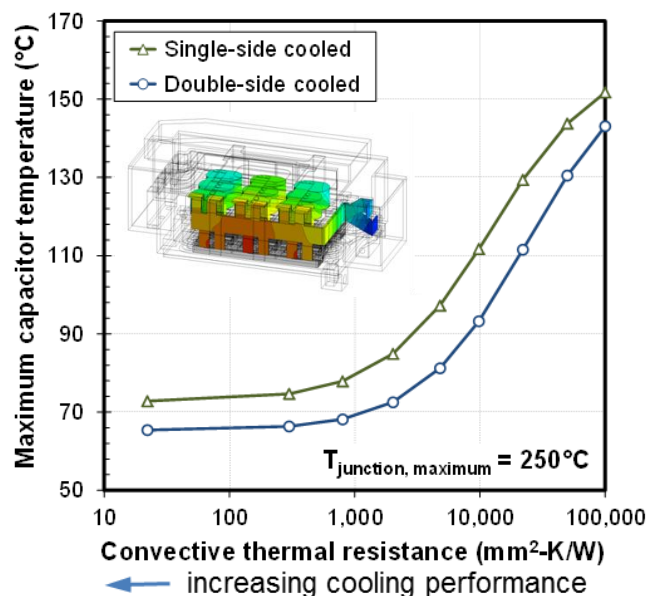


Figure 1. Simulation-predicted capacitor temperatures for a WBG operating condition with results showing that electrical interconnection cooling enables capacitor temperatures less than 85°C for WBG device temperatures up to 250°C.

High-Power Density Ferrite Permanent Magnet Motor

Non-rare earth motors are critical to achieving low-cost high-power density electric traction drives.

Oak Ridge National Laboratory

Most hybrid electric vehicle and electric vehicle motors (machines) use permanent magnets (PMs) with heavy rare-earth (HRE) materials such as neodymium and dysprosium because they enable high-power densities, specific powers, and efficiencies. However, there has been significant market volatility associated with HRE materials, including a price increase in dysprosium by a factor of 40 within one year (2011). Increasing the number of viable alternatives to HRE-based machines is a critical factor in providing greater certainty needed to enable mass production. Achieving competitive performance and efficiency with alternative motor technologies having comparable mass, volume, voltage, and other key metrics requires a highly advanced, multidiscipline research approach, including high accuracy modeling; researching, using, and developing soft and hard magnetic materials; and optimizing the comprehensive nonlinear computations of geometric features and winding parameters.

Oak Ridge National Laboratory (ORNL) implemented a novel guided random search method to optimize the design. To start, a population of candidate designs is drawn randomly from a joint Gaussian distribution with a given mean and standard deviation. After extensive optimization, the simulated peak power of the ferrite motor was 60 kW at 2,800 revolutions per minute (RPM), over 90 kW at about 4,500 RPM, and greater than 55 kW at 14,000 RPM. Table 1 summarizes key simulated and measured performance metrics. Researchers conducted detailed cost estimates that considered magnet grinding cost. Table 1 includes metrics associated with the measured power of 103 kW, and Figure 1 displays performance and efficiency data from dynamometer testing. ORNL estimated that

the manufacturing cost at 100,000 units is projected to be less than \$450.

The U.S. Department of Energy’s (DOE) 2020 targets for power density, specific power, and cost are 5.7 kW/L, 1.6 kW/kg, and \$4.7/kW, respectively; therefore, the ferrite motor met DOE cost and power targets. Further materials and design research is critical to develop advanced HRE free machines.

Speed (RPM)	Peak Power [kW]	Power Density [kW/L]	Specific Power [kW/kg]	\$/kW (Low)	\$/kW (High)
DOE 2020 Target	55	5.7	1.6	4.7	4.7
2800 (simulated)	60.8	6.08	1.83	3.3	7.4
4500 (simulated)	93.5	9.35	2.81	2.1	4.8
9000 (measured)	103	10.3	3.10	1.9	4.4

Table 1. Simulated and measured performance data.

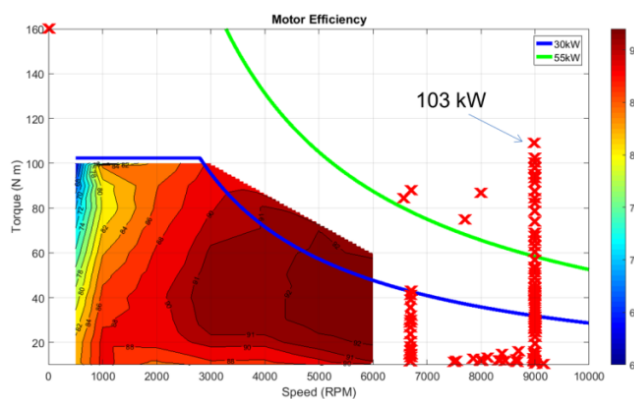


Figure 1. Performance and efficiency data from dynamometer testing of ORNL’s ferrite PM prototype motor.

Using Supercomputers to Develop Better Magnetic Materials

Unique tool leverages high-performance computing capability for high-accuracy simulations of motor performance and efficiency.

Oak Ridge National Laboratory

Oak Ridge National Laboratory (ORNL) conducted fundamental research to study the phenomena behind magnetization and loss characteristics of soft magnetic materials in electric motors to improve motor modeling accuracy. Stresses induced during manufacturing have a considerable impact on losses and permeability. Soft magnetic materials are characterized by a remnant magnetic structure that consists of magnetic domains—regions in which all atomic magnetic moments align in specific directions. The soft magnetic properties are determined by the ease with which the magnetic domains can respond to external magnetization and demagnetization—magnetic hysteresis loop. Magnetic materials are used in several critical applications, from data storage and computing to electric motors and power generators ranging in length scale from the nanometer (10^{-9} m) to several meters. Designing better devices that can meet the increasingly stringent demands of future

technologies requires a fundamental understanding of the material chemistry and processing defects on the magnetic behavior at the atomistic length scale, and the ability to predict magnetic behavior at the device-level length scale to accurately capture the underlying atomic level physics of magnetism as well as coupling with the microscopic state of stress in the material.

ORNL developed a unique simulation approach that uses supercomputers to predict the magnetic “constitutive properties” of materials used in electric motors to enable better motor design, as well as the development of high-efficiency, low-loss magnetic materials through optimizing new material compositions and processing technologies. Figure 1 illustrates the ability of the simulations to predict the hysteresis loop for polycrystalline iron at the micrometer (10^{-6} m) scale that can be directly coupled with motor performance simulations.

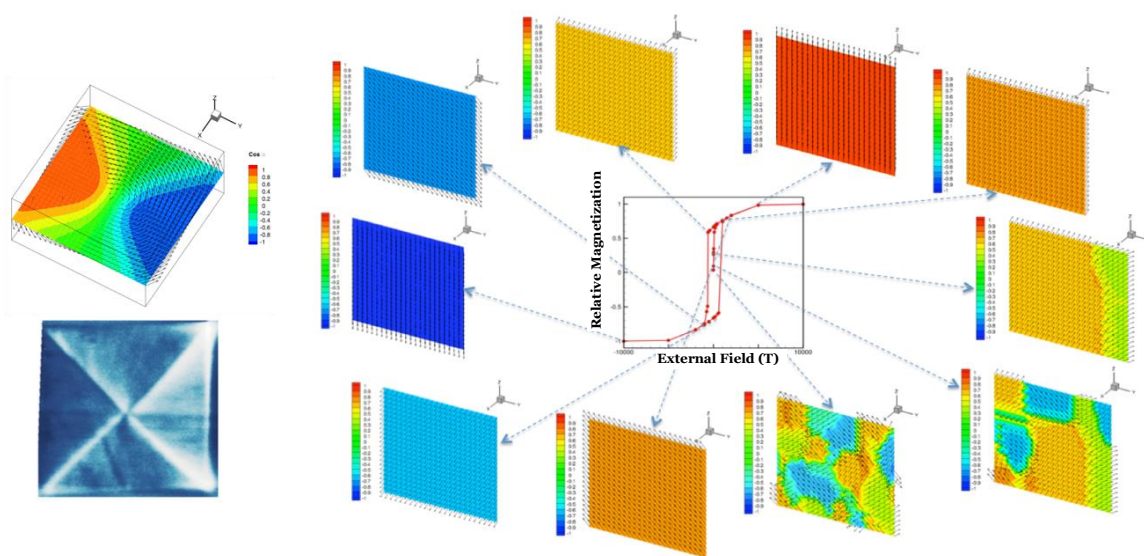


Figure 1. Simulation of a vortex domain structure in iron (top left) experimentally observed vortex structure in iron (bottom left), and simulation of hysteresis loop for a polycrystalline grain structure in iron (right).

Materials Expertise Aids Manufacturers in Commercializing High-Performance Motors

National Laboratories demonstrate methods for measuring the thermal conductivity of motor-winding materials, enabling characterization of new materials for high-performance motors.

Oak Ridge National Laboratory and National Renewable Energy Laboratory

Maximizing the efficiency, power density, and lifetime of motors requires thermal management of Joule-heating-losses in motor windings. Motor windings may be directly cooled via the exposed end turns of the winding, indirectly cooled with heat flowing into adjacent stator laminations to the motor housing, or both. Direct cooling applied to the motor end windings takes advantage of copper’s high thermal conductivity as heat flows parallel to the copper wire axis. However, the efficiency of indirect cooling (i.e., heat transfer from the copper wires into the adjacent stator) is limited by the heat transfer perpendicular to the wound-wire and affected by the interstitial constituents that can include insulating wire-coatings, organic fillers, and porosity, constituents that all typically have low thermal conductivity relative to copper. Additionally, interface thermal resistances between each constituent further impede heat transfer. New materials could improve heat transfer, but the highly anisotropic or direction-dependent thermal properties require specialized equipment for measuring the thermal conductivity of the composite windings.

Oak Ridge National Laboratory and the National Renewable Energy Laboratory measured the thermal conductivity parallel and perpendicular to the axis of the wire using laser flash, transient plane source, and transmittance test methods (Figure 1). Each test method was compared for a range of materials from monolithic homogeneous materials to anisotropic wire bundles with different wire diameters. The tested wire samples had a copper volume fraction between 50% to 60% and wire diameters of 670–925 μm. The thermal conductivity perpendicular to the wire axis was about 0.5–1 W/mK, whereas it was over 200 W/mK in the parallel direction.

Tests demonstrated that the anisotropic thermal conductivity of packed copper wire can be satisfactorily estimated with appropriate specimen preparation using the laser flash and transmittance test methods, as summarized in Table 1.

The thermal transmittance measurement uncertainty parallel to the wire axis was high for the tested sample geometry. The transient hot disk method did not consistently produce trustworthy and defensible apparent thermal conductivity results for these specimens and their architecture. The test results provide a baseline for comparing new materials and highlight methods for appropriately testing the thermal impact of new materials or winding structures relevant to motor windings.



Figure 1. Test specimens with thermal transmittance setup for thermal measurements perpendicular to the wire axis.

Test Approach	Parallel to Wire Axis	Perpendicular to Wire Axis
Laser Flash E1461	Y	Y
Transient Plane Source ISO 22007-2	N	N
Thermal Transmittance ASTM D5470	N	Y

Table 1. Comparison of test procedures and ability to measure direction-dependent thermal properties of winding samples.

High-Temperature DC Bus Capacitor Cost Reduction and Performance Improvements

Reduces the cost, size, and weight of the DC-link capacitor by greater than 50% while increasing durability in high-temperature environments.

Sigma Technologies International

Sigma and its partners Delphi Automotive (Delphi) and Oak Ridge National Laboratory have made significant progress in developing improved direct-current (DC) bus capacitors, fabricating and packaging these capacitors, and developing a business plan for production. The team has produced full-size (300 μF , 500 μF , and 700 μF) capacitors that meet or exceed technical targets for DC bus capacitor performance (see Table 1), and packaged life testing shows stability under various environmental conditions, including high-temperature automotive environments.

Sigma has developed a solid-state polymer-multi-layer (PML) capacitor (see Figure 1) composed of thousands of radiation-cured polymer dielectrics and aluminum electrodes to form a large-area nano-laminate that can be segmented into individual capacitors.

Characteristic	DOE Target	PML Capacitor
Temperature	-40 to 140°C	-40 to 140°C
Loss	1 %	< 1 %
Volume	< 0.6 L	< 0.3 L
Cost	< \$30	< \$20

Table 1. Sigma PML capacitor performance compared to U.S. Department of Energy capacitor development targets for a ~700 μF capacitor.

This PML technology represents a transformational and potentially disruptive technology. The current supply chain to manufacture metallized polypropylene capacitors involves a film manufacturing operation, an electrode metallizing operation and a capacitor manufacturing operation. Virtually all capacitor manufacturers use the same base polypropylene dielectric films, which leaves little room for innovation and advancement of the

technology to meet market needs. This PML material, which comprises a large sheet of multilayer material, is instead produced in a one-step process using a liquid monomer and aluminum wire into a process chamber. This allows a capacitor original equipment manufacturer (OEM) to control all key material and process parameters, including the dielectric formulation, dielectric thickness, electrode material, electrode thickness, capacitor shape, and capacitor size. This approach to capacitor production can reduce the cost of metallized polymer capacitors and allow a capacitor OEM to innovate and create application-specific products with different polymer dielectric properties.

Sigma is in the process of designing and fabricating a production scale machine to manufacture bulk PML capacitor material.

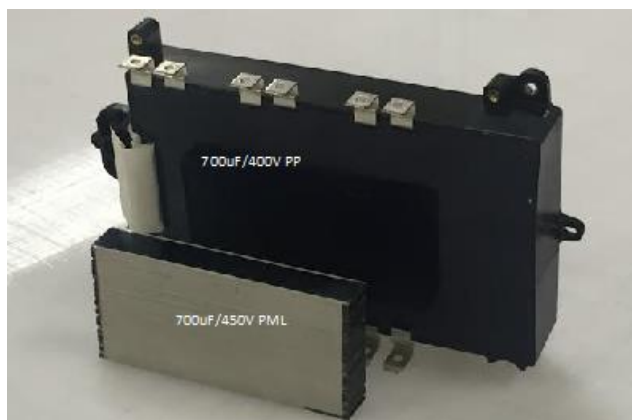


Figure 1. Comparison between current metallized polypropylene DC bus capacitor and the developed PML capacitor. Both are rated at 700 μF , but the PML capacitor can handle 140°C temperatures, an increase of 35° over current capacitors..

Vehicle Electric Motor Design uses Permanent Magnets without any Rare-Earth Content

Current motor designs use permanent magnets containing rare-earth materials, which have shown unstable prices, supply constraints, and temperature limits.

UQM Technologies

UQM Technologies, a company developing propulsion systems for electric, hybrid electric, plug-in hybrid electric and fuel cell electric vehicles, recently patented a new design for electric vehicle motors that use non-rare earth magnets (see Figure 1).

While most plug-in electric vehicles (PEVs) use motors with rare-earth magnets, these magnetic materials are expensive, prices have been highly volatile, and their supply may be short as future market demand is expected to be high. Electric motors that do not use rare-earth magnets will potentially be less expensive and rely more on domestic resources and processing capabilities, improving economic, environmental, and energy security. In the past six years, rare-earth magnet prices have fluctuated between \$80/kg to \$750/kg, while the metal that will be used in the new motor has a much more stable price. Reducing the use of rare-earth magnets in PEVs can also help alleviate future supply concerns for these materials, which have seen supply restrictions and reductions in recent years.

UQM’s new motor design performs comparably to rare-earth motors, helping the company meet critical size, weight, and efficiency targets for vehicle applications (see Table 1). It also provides the company flexibility to adapt to the market. Once UQM develops the design, it can either use the original rare-earth-based design or the new one, depending on the price and availability of rare-earth materials.

UQM is collaborating with DOE’s Ames National Laboratory to improve the magnets’ properties, the National Renewable Energy Laboratory to develop thermal management approaches, and Oak Ridge National Laboratory to test the motor.

UQM, a Colorado-based company, currently has the capability to manufacture at least 50,000 electric drive systems annually. The company is supplying motors to transit bus company Proterra and has supply agreements with energy management and vehicle companies around the world.



Figure 1. UQM patented motor with the internal rotor shown on the right. United States Patent Number 8,928,198

Characteristic	DOE Target	Achieved
Efficiency	>90%	Comply
Peak Power	55 kW	55 kW
Maximum Speed	10,000 rpm	10,000 rpm
Torque	262 N-m	235 Nm
Total Volume	≤ 9.7 L	9.59 L

Table 1. UQM motor performance compared to DOE’s 2015 motor targets.

Application of Silicon Carbide Power Devices in Hybrid Electric Vehicle Drive Systems

Silicon carbide MOSFETs can significantly reduce inverter losses and have the potential to improve drive system efficiency and reliability with reductions in power inverter weight and size.

Wolfspeed™, A Cree Company

Present-day traction inverters are expensive, heavy, and bulky, which ultimately can limit their adoption in the greater automotive market. Wolfspeed has demonstrated the benefits of reduced system cost and extended reliability for electric drive systems through the application of 900 volt (V) silicon carbide (SiC) metal-oxide semiconductor field-effect transistors (MOSFETs) into advanced power modules and demonstrated traction drive technology. This new SiC MOSFET-based module significantly reduces losses in an electric drive system modeled after the Ford Focus with project partner Ford, ultimately increasing vehicle fuel economy, range, and productivity.

The 900 V, 10 mΩ SiC MOSFETs were fabricated with a total chip area of 32 mm². In Figure 1, the advanced power module with SiC MOSFETs inside is shown. A record-low 1.25 mΩ on-resistance was measured, dramatically lowering on-state losses. The 900 V SiC MOSFETs room temperature on

resistance is approximately 41% less than the 650 V silicon (Si) MOSFET, and 63% less at 150°C. Significantly, the overall total die size of the SiC MOSFET is one-third the currently used Si insulated gate bipolar transistor (IGBT) and diode pair it replaced with similar power capability in power module testing. This reduction in required semiconductor area and losses for a similar power rating can significantly reduce costs associated with electric drive systems.

Figure 2 shows the comparison between a Si IGBT and Wolfspeed SiC MOSFET for traction drive operation. Compared to currently used Si devices, SiC reduces inverter losses by ~78% in electric-only drive mode for the U.S. Environmental Protection Agency metro-highway cycle combined. Energy savings from using SiC devices can vary significantly with different drive cycles, and savings are greatest for cycles that include city or urban driving patterns and more aggressive drive cycles. Estimated volume die pricing of SiC should be attractive for mass adoption in automotive systems once it reaches a cost of less than two times that of Si.

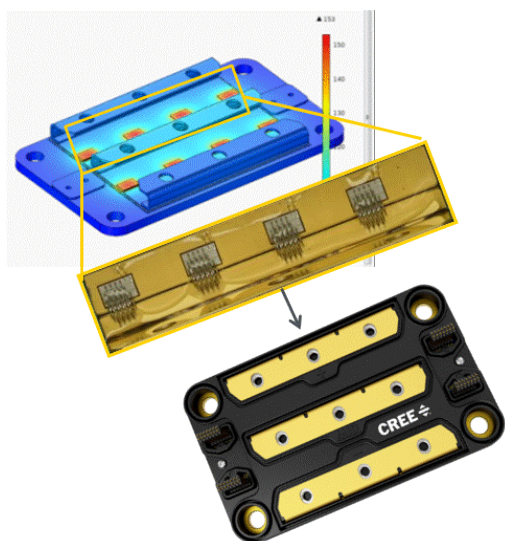


Figure 1. 900 V, 1.25mΩ SiC power module with record-low on-state losses, based on new 900 V SiC MOSFETs.

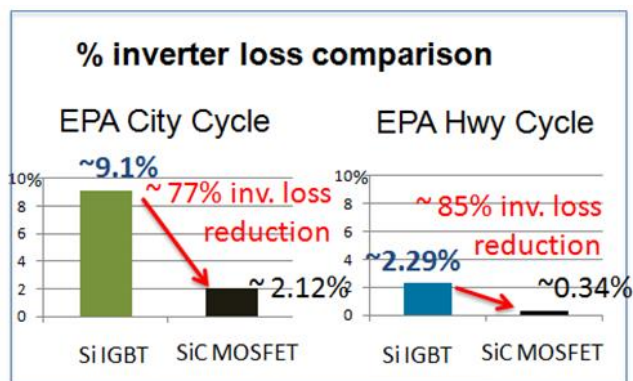


Figure 2. 78% combined inverter loss reduction is possible when using the 900 V SiC power modules in place of Si IGBT power modules for a 90 kW Ford Focus EV.

2016 U.S. DRIVE Highlight

High-Temperature Wide Bandgap Inverter for Electric Vehicles

New silicon carbide (SiC) inverter is the first traction drive optimized for wide bandgap devices that utilizes a commercially available SiC power module and can operate in high-temperature automotive environments.

Wolfspeed™, A Cree Company

Wolfspeed's high-temperature, wide bandgap (WBG) underhood inverter was developed to address the need for smaller, lighter, and more efficient systems with higher power density in the electric vehicle market (see Table 1). The device was developed in collaboration with the Toyota Research Institute of North America, the National Renewable Energy Laboratory, and the University of Arkansas National Center for Reliable Electric Power Transmission.

was named an R&D Magazine Top 100 Award winner as one of the top technical breakthroughs in 2015.

Characteristic	DOE 2020 Target	Achieved
Efficiency (over 4 bus voltages, 6 thermal cases, & 3000+ operating points)	>93%	Avg. 96.3% Peak 98.9%
Peak Power	55 kW	81.8 kW
Weight	≤ 3.9 kg	4.0 kg
Volume	≤ 4.1 L	4.4 L
Cost	≤ \$182	~\$192

Table 1. Wolfspeed's WBG technology has exceeded the U.S. Department of Energy's 2020 targets.

Underhood inverters (see Figure 1) convert the direct-current power stored in hybrid, plug-in hybrid, or all-electric vehicle battery packs to three-phase alternating current power that can be used to energize one or more electrical loads, and traditionally employ industry standard silicon semiconductors. Using Wolfspeed's WBG semiconductor devices and advanced packaging techniques in an underhood inverter allowed engineers to achieve faster switching with reduced system-level losses during high ambient (140°C) and high coolant (105°C) temperature operation (see Figure 2). This WBG-based system significantly outperforms silicon technology for vehicle inverters—especially at light load conditions, and



Figure 1. SiC-based traction drive inverter.

Wolfspeed's WBG technology increases the unit's peak power delivery by 2-3 times what is currently achievable with silicon-based devices, while operating at overall higher ambient temperatures.

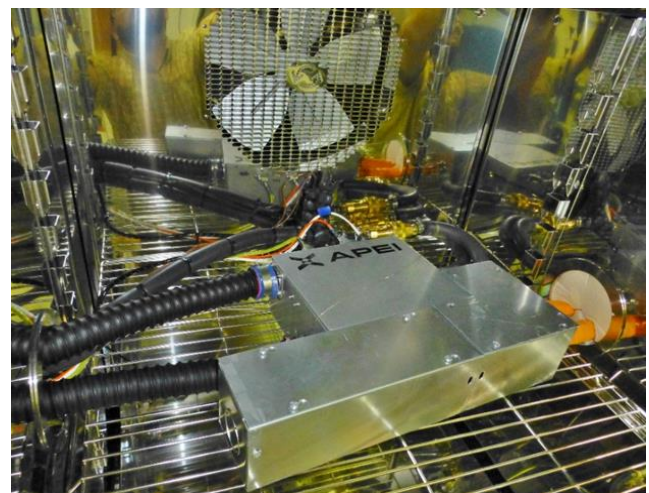


Figure 2. Inverter under test in an environmental chamber.

Electrochemical Energy Storage



Silicon Nanowire Anodes Enable High Specific Energy, High Energy Density, and Long Cycle Life

Amprius' growth-rooted silicon nanowire structure allows it to expand and contract internally, enabling long cycle life.

Amprius and the U.S. Advanced Battery Consortium

Active materials in today's commercial lithium-ion cells have limited room to improve specific energy or energy density. Their active materials—a graphite anode paired with one of several commercially available cathodes—are used at capacities close to their fundamental limits and their packaging has already been optimized. New active materials are needed to boost performance and extend driving range.

Silicon has significant potential as a new anode material, as it offers nearly 10 times the theoretical energy capacity of graphite. However, when charged with lithium ions, silicon swells up to four times its volume, causing capacity fade and mechanical failure. Because of swelling, conventional approaches to silicon anodes cannot be used in automotive applications due to inadequate cycle life.

Amprius' unique silicon structure—nanowires (see Figure 1) that are “growth-rooted” (i.e., grown directly on the current collector, without binders)—addresses swelling by enabling silicon to successfully expand and contract internally. Because the nanowires are attached to the current collector, Amprius does not rely on particle-to-particle contact and is able to achieve longer cycle life, energy and power.

Amprius is attempting to deliver cells sized for vehicle applications that meet the U.S. Advanced Battery Consortium's (USABC) technical requirements. Throughout the project, Amprius is improving its silicon nanowire anode material and cell performance in smaller baseline cells, and transfer those learnings to larger cells.

The project's first-year cells completed more than 550 cycles and exceeded USABC targets for Peak Discharge Power Density, Peak Specific Discharge

Power, Peak Specific Regen Power, High Rate Charge, Unassisted Operation at Low Temperature, and Maximum Self-Discharge. Figure 2 displays voltage drift at 500 cycles. The cells also met USABC's targets for Operating Environment and Survival Temperature Range (24 Hour).

During the second year, Amprius has demonstrated significant improvements in energy density and specific energy while scaling up the cell capacity from 2 Ah to greater than 10 Ah.

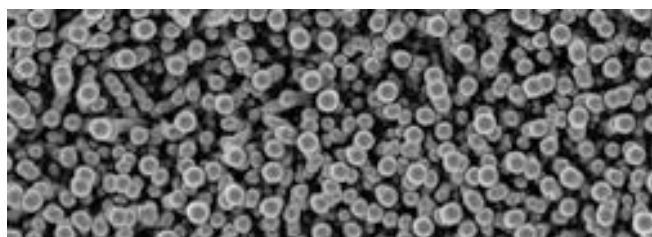


Figure 1. Top-down micro view of Amprius silicon nanowire structure.

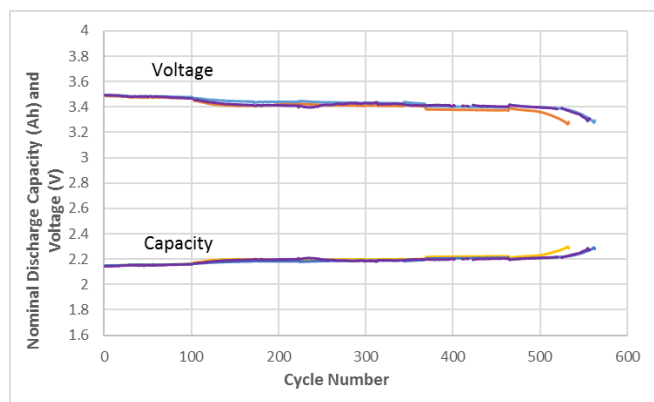


Figure 2. Voltage drift past 500 cycles was less than 4%.

Fluorinated Electrolyte for 5-Volt Lithium-Ion Chemistry

New electrolyte technology shows potential to overcome one of the key bottlenecks existing in the high-energy density lithium-ion battery through molecular engineering. Fluorinated carbonate electrolyte solvents have shown superior voltage stability over their non-fluorinated counterparts in 5-volt cells.

Argonne National Laboratory

The lithium (Li)-ion battery is an ideal power source for electric vehicles due to its long cycle life and high energy and power density. To further increase the energy density, one approach is to use cathodes with high operating voltages (5 volt (V) versus. Li^+/Li) and high specific capacity (250 mAh/g).

However, conventional electrolytes, typically composed of mixtures of ethylene carbonate with dimethyl carbonate, diethyl carbonate, and/or ethyl methyl carbonate dissolved in LiPF_6 salt, decomposes above 4.5 V versus Li^+/Li , leading to low Coulombic efficiency, rapid capacity fade, and severe self-discharge, which becomes even worse at elevated temperatures. The electrolyte instability limits the cathode chemistry that delivers high capacity at a high voltage. Therefore, the demand for a high-voltage electrolyte has become a high priority for the development of Li-ion batteries with high energy density.

Scientists at Argonne National Laboratory (ANL) have developed a new class of electrolytes based on fluorinated carbonate solvents. With strong electron-withdrawing fluorinated substituents, the highest occupied molecular orbital energy of the carbonate molecules is lowered and becomes more resistant towards oxidation. A variety of fluorinated carbonates (cyclic and linear) were synthesized and their superior voltage stability was examined by density functional theory calculation and electrochemical cyclic voltammetry. In addition to the improved voltage stability, the new electrolyte is also capable of forming a robust solid-electrolyte-interphase (SEI) on the graphite anode, an indispensable surface layer that protects against side reactions between the electrolyte and the charged graphite anode. Figure 1 shows cycling performance of the new electrolyte in a 5 V Li-ion battery using $\text{LiNi}_{0.5}\text{Mn}_{1.5}\text{O}_4$ as a 5 V cathode and graphite as an

anode. It is obvious that compared with the conventional electrolyte, the fluorinated electrolyte shows much improved performance both in Coulombic efficiency and capacity retention at 55°C.

Another desirable property of the new electrolyte is its reduced flammability, also imparted by the fluorination. ANL has observed a reduction in flammability of this fluorinated electrolyte. ANL attempted to ignite the electrolyte-soaked testing specimen (glass wool stick) by a torch and found that it would not catch fire.

Next steps include estimating the production cost of the fluorinated compounds, further improving the long-term anode SEI stability, and understanding the impact to other battery performance parameters such as general power capability and temperature dependence of rate capability.

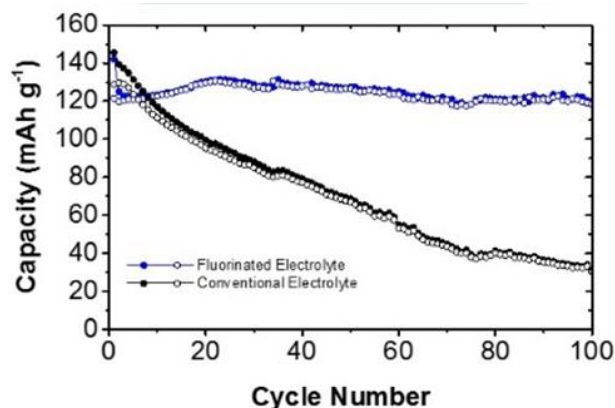


Figure 1. Capacity retention of $\text{LiNi}_{0.5}\text{Mn}_{1.5}\text{O}_4$ /graphite cells cycled at 55°C with fluorinated-electrolyte compared with conventional electrolyte at C/3 charge/discharge rates. (Voltage: 3.5-4.9 V).

Pursuit of Cost-Effective, High-Capacity, Manganese-Rich, Lithium-Ion Cathodes

Manganese-rich cathodes have the potential to lower cost and improve abuse tolerance but have been plagued by structural instabilities. A new platform may allow structurally stable manganese-rich cathodes, offering high capacity.

Argonne National Laboratory

Lithium (Li)- and manganese (Mn)- rich “layered-layered” (LL) cathode materials have been of interest for more than a decade due to the substantial capacity gains, increased abuse tolerance, and lower cost compared with their layered counterparts. As is now well-known, these high capacities come at the expense of structural stability, where the complex role of oxygen at high states of charge leads to oxygen evolution, cation migration, and the irreversible transformation of local structures accompanied by voltage fade. Voltage fade is, therefore, highly correlated to local structures (including defects) that dictate, to a large extent, Li site energies.

Following this line of thinking, researchers inferred that modifying local domain structures in the pristine materials might mitigate the structural transformations in these electrodes during cycling. The goal is to realize low-cost, Mn-rich cathodes with high capacities while maintaining good structural stability and energy over long-term cycling. But while some nickel-rich, layered oxides can deliver close to 200 mAh g⁻¹ at slow rates, a more cost-effective, Mn-rich oxide that can compete with these more expensive options is unavailable. The team initiated “bottom-up” strategy to create such an option. By starting with lower Li and Mn loadings and modifying local domain structures to mitigate the mechanisms of energy fade, a platform is being built toward the goal of practical, high-energy, Li- and Mn-rich cathodes.

Figures 1(a) and (b) show cycling data for a cathode with a targeted 15% “spinel” content, called layered-layered-spinel (LLS). Evident in the first-cycle charge (b) is the clear activation plateau associated with LL materials. On cycling (4.45-2.5 volt (V)), the LLS material maintains 195 mAh/g, good stability

and energy (~711/Wh/kg_{oxide}), with nearly all capacity being delivered above 3.0 V. In addition, the dQ/dV curves show minimal evidence of voltage fade. This material has been established as the baseline for future LLS research with further improvements already realized.¹ Figure 1(a) inset shows an example of the “next-generation” of this type of cathode particle, synthesized at Argonne National Laboratory. This material has been scaled to the 1 kg level and will be evaluated in larger-format pouch-cells under DOE protocols.

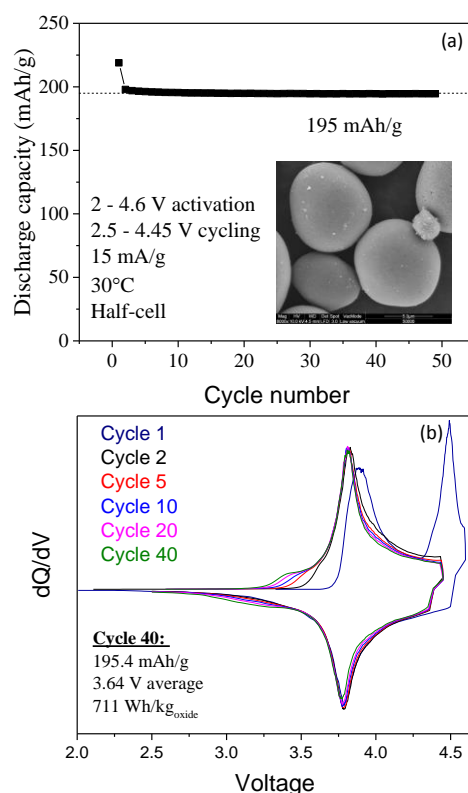


Figure 1. (a) Cycling and (b) dQ/dV plots of a Li- and Mn-rich, LLS material. The dQ/dV plot shows the stability of the charge/discharge curve after 40 cycles.

¹ Croy et al., *J. Power Sources*, 334, 213 (2016).

Fluorinated Electrolytes for Higher Voltage Cell Operation

Typical hydrocarbon electrolytes are unsuitable for battery operation above 4.35 volts with traditional cathodes, but introducing fluorocarbons into the electrolyte permits cycling of traditional cathode-based batteries up to 4.5 volts.

Daikin Industries

As part of a recent effort, Daikin has shown that a typical hydrocarbon electrolyte is not suitable for battery operation above 4.35 volt (V) due to gassing of the electrolyte. The introduction of fluorocarbons into the electrolyte allows cycling up to 4.4 V and significantly reduces gassing in cells with both nickel-manganese-cobalt oxide (NMC) and lithium cobaltate cathodes. The failure mechanism for the fluorocarbon electrolyte at 4.6 V is unknown. However, it has been noted that the cell thickness (non-gas related) increases due to swelling of the anode. The NMC111/graphite couple was chosen over higher nickel varieties due to its commercial availability in dry pouch cells.

Researchers initiated cycle life testing (at both 25°C and higher temperatures) in multiple cell chemistries to determine whether cell failures at higher voltages occurred independently of cell chemistry. Figure 1 shows the cycle life of hydrocarbon and fluorocarbon electrolytes in 1 Ah NMC/graphite pouch cells cycled to 4.2, 4.35, and 4.5 V at 60°C. At all voltages tested here, the fluorinated electrolytes yield better or equivalent cycle life to the cells with standard carbonate electrolytes.

Test data on silicon (Si) composite/lithium cobalt oxide (LCO) cells (not shown) indicates that cycle life at 4.2 V for both hydrocarbon and fluorocarbon electrolytes are similarly stable. Cycling at 4.4 V shows that fluorocarbon maintains capacity retention above 80% out to 1,000 cycles while the hydrocarbon electrolyte begins to fail earlier, with 80% capacity retention reached at 425 cycles. Both electrolytes show very poor capacity retention when cycled at 4.6 V.

Non-gas related cell swelling (not shown) was measured after cycling the LCO/Si composite cells.

At 4.2 V, the cells with hydrocarbon electrolyte exhibited a 14% increase in cell thickness, while the fluorocarbon cells showed no signs of swelling. This trend continued at 4.4 V, with the hydrocarbon cells having a 28% increase in thickness, while the fluorocarbon cells showed no thickness increases. Both hydrocarbon and fluorocarbon cells cycled at 4.6 V exhibited non-gas cell swelling of 18% to 20%. The trends in increasing cell thickness are consistent with the decrease in cycle life of the cells.

It is interesting that both the Si composite/LCO cells and the graphite/NMC cells show the same general behavior regarding both cycle life and gas generation. Thus, the fluorinated electrolyte appears to enable higher voltage cycling in a wide variety of cathode classes.

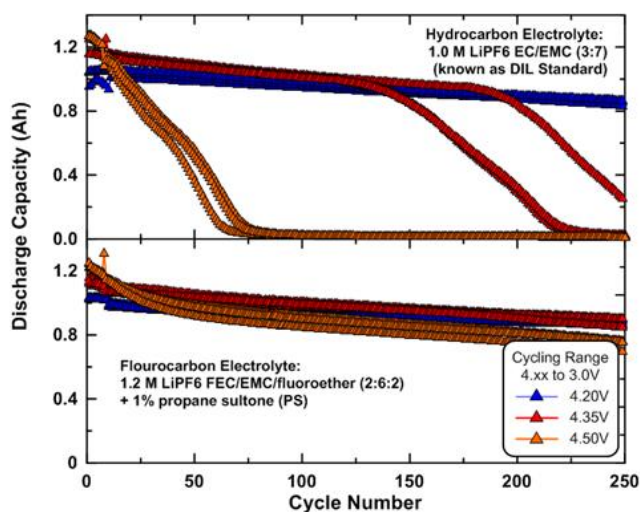


Figure 1. Cycle life showing capacity of 1 Ah NMC/graphite cells with both standard carbonate (top) and fluorinated (bottom) electrolytes at cycled at a Vmax of 4.2, 4.35, and 4.45 V.

Advanced Polyolefin Separators for Lithium-Ion Batteries used in Electric Vehicles

Separator ionic conductivity and safety features have been significantly enhanced by incorporating ceramic nanoparticles into the bulk structure and by applying a nanoparticle-based ceramic coating on the surface of the separator.

ENTEK Membranes and the U.S. Advanced Battery Consortium

ENTEK is developing an advanced separator with improved safety features, improved rate performance capability, high-voltage oxidation resistance, and reduced cost to meet the lithium (Li)-ion battery requirements for electric vehicle applications. In order to enhance the features of the separator, ENTEK used an innovative approach of incorporating nanoparticle filler into the bulk structure of the separator and of applying an alumina nanoparticle coating on top of the separator.

Figure 1 shows the effect of incorporating filler into the bulk of the separator. Adding filler into the separator resulted in increased porosity while maintaining a similar pore size distribution and mechanical properties. Higher porosity translates into improved ionic conductivity, and thus higher power capability in the cell. The main advantage of this approach is achieving a high porosity without sacrificing the mechanical strength of the separator.

Figure 2 illustrates that ENTEK's nanoparticle alumina coating approach requires 60% less coating mass compared to conventional coatings (with ~0.5 μm diameter particles) to achieve high temperature dimensional stability (less than 5% shrinkage in the separator at temperatures above the melting point of the base polyolefin separator). The nanoparticle alumina coatings may enhance safety features, improve energy density, and reduce cost. Additionally, ceramic coatings may allow for higher voltage stability, which will improve the stability in high voltage cells. This work is currently underway.

At the conclusion of this program, ENTEK will validate the advanced separator technology by its incorporation into high voltage (greater than 4.9 volt) Li-ion cells for improved energy density. This

will be achieved through a collaborative effort with Farasis Energy Inc.

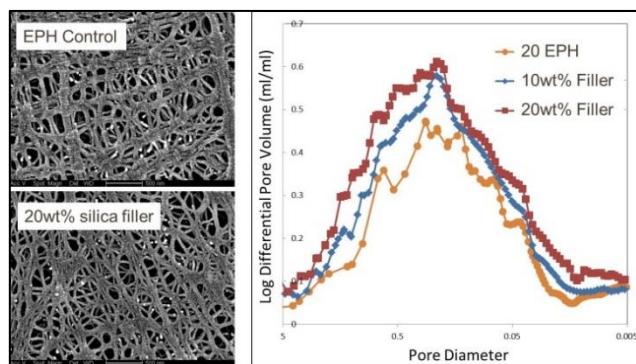


Figure 1. Effect of filler concentration on pore size distribution. Incorporating 20 wt% inorganic filler resulted in an increase in porosity from 48% to 65%, without significantly effecting pore size or mechanical properties.

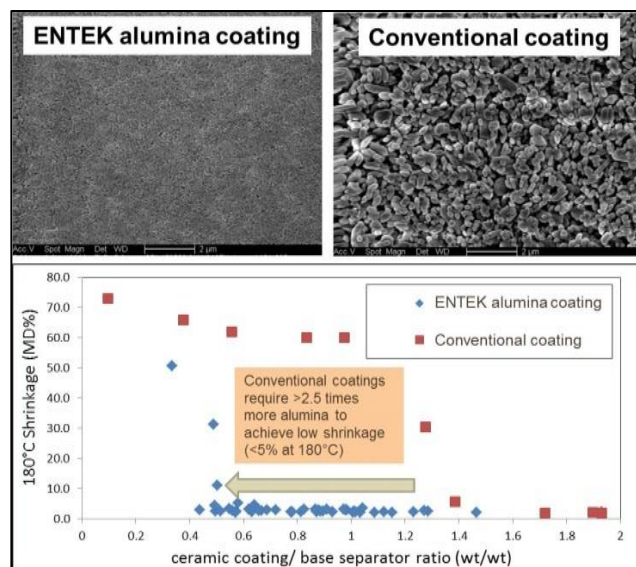


Figure 2. Coating with nano-alumina allows for a substantial reduction in coat weight required to achieve high-temperature dimensional stability, thus improved safety features in the separator, reduced cost, and improved energy density.

Manufacturing High-Performance, Low-Cost Protective Coatings for Long-Life Lithium-Ion Battery Materials

Forge Nano has successfully scaled its innovative high throughput production systems to metric ton levels, delivering nano-structured protective coatings for cathode and anode particles with unprecedented performance at low cost.

Forge Nano LLC

Forge Nano LLC (FN) has developed a fully automated, high-throughput material coating system that allows for rapid processing of cathode and anode powders, which significantly reduces the production costs of atomic layer deposition (ALD) encapsulated powders. FN has also significantly improved the electrochemical performance reliability of ALD coated cathode and anode particles through close process development in conjunction with battery partners. FN's coatings can increase cathode material lifetimes while enabling higher capacity nickel-rich battery chemistries. FN is also demonstrating similar gains to anode materials such as conventional graphite and emerging silicon-based materials. FN's technology can enable higher energy densities and longer lifetimes, enabling battery manufacturers to build a better, safer battery. In addition, the reduced impedance buildup throughout life enables higher charge and discharge rates.

FN is industrializing the ALD process by offering a unique value proposition toward upgrading material performance. ALD is a process that deposits a uniform and ultrathin encapsulating coating around any material. The process can be applied to many materials, including powders utilized to fabricate electrodes for lithium-ion batteries. ALD allows for coating thicknesses down to Angstroms (1/100,000th the thickness of a human hair). Such control allows for applying coatings that are thick enough to eliminate unwanted reactions that cause degradation within Li-ion cells, yet thin enough to not adversely affect wanted battery material properties (Figure 1). ALD coatings are one of the most compelling coating solutions for eliminating performance fade and enabling higher overall performance in batteries.

ALD is a process that has existed for decades with hundreds of publications demonstrating its capability as a process to improve material properties for a wide variety of applications. However, due to a lack of manufacturing innovation, it has remained a lab-scale process utilized primarily by academics. FN has developed, patented and successfully demonstrated a high-throughput, fully automated process for applying ALD, which reduces the overall cost of energy storage devices while improving their performance and safety.

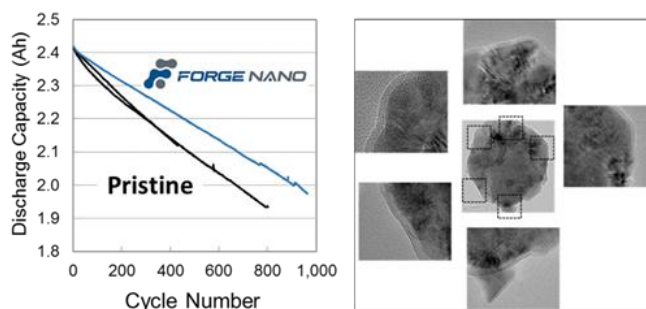


Figure 1. Third-party data showing how FN's coatings on high energy cathode materials can increase the lifetime of a 2 Ah nickel- manganese-cobalt 811/graphite cell by 40%, and images of the coating uniformity at the particle level delivered by FN's innovative manufacturing systems.

FN maintains the world's largest manufacturing capacity for ALD-enabled materials, and is expanding 10-fold to a 300 ton per year commercial production plant. This plant will come online in mid-2017 and will be capable of meeting demand volumes and price points for large-scale integration into the Li-ion market, while 3,000 ton per year systems are designed and constructed. XALT Energy is currently designing cells incorporating FN's ALD coated active materials.

Assessment of Fast-Charging Impacts on Battery Life

Understanding the impacts of fast-charging reinforces the need for consideration in future electric vehicle battery and charging system designs.

Idaho National Laboratory

The ability to quickly charge an electric vehicle (EV) is seen as one key to advancing consumer adoption. Idaho National Laboratory (INL) has found that while increasing the rate of charging from Level 2 (6.2 kW AC) to a scaled 50 kW direct current (DC) fast charge has minimal impact on performance at 30°C, there is a distinct increase in energy fade for the faster charge at higher temperatures. This work, which shows strong correlations between in lab cell and pack testing and on-road evaluation, supports design considerations for future EVs with fast-charging capabilities.

Previous work at INL entailed on-road operation of several Nissan LEAF EVs that were charged using either alternating current (AC) Level 2 or 50 kW DC fast charging. Batteries of the same type were cycled in the lab under constant temperature conditions, with discharge power cycles simulating the on-road duty cycle. The in-lab pack testing removed temperature and driver aggressiveness as uncontrolled variables. The work has recently been extended to include the investigation of individual cells under scaled use conditions, but with an expanded set of environmental conditions (20°C, 30°C, and 40°C). These cells have even greater temperature control.

Comparing the on-road vehicle data with data collected in the lab for packs and individual cells (Figure 1) shows that there is a distinct aging influence related to the incremental increase in cell temperature due to DC fast-charging at 30°C ambient. At higher temperatures (not shown) for Cells Lab Cycled the rate of performance fade is increased between AC Level 2 charging condition and 50 kW DC fast-charging condition. This negative impact to performance illustrates the potential for more severe response to significant amounts of DC

fast-charging during the summer season in hot climates. It also suggests that fast charging-capable vehicles may benefit from more robust thermal management systems to maximize battery performance and life.

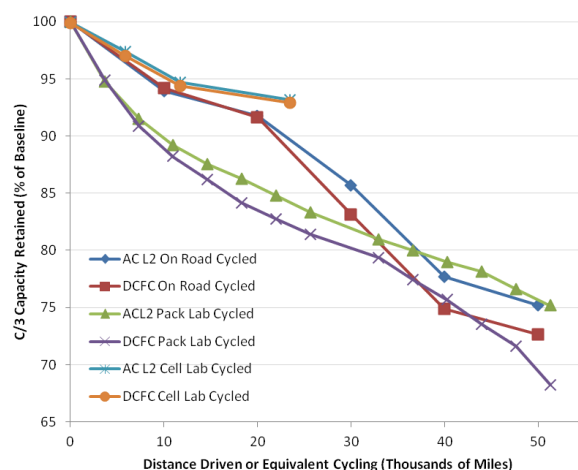


Figure 1. Relative capacity fade is shown for pack and cell level lab testing at 30°C, alongside on-road testing that had variable temperatures both above and below 30°C. DC fast-charging generally shows higher fade than Level 2 charging. Lab cell fade is slower than on road ad pack lab fade, possibly due to lower cell temperatures as cells in large packs general dissipate heat more slowly than individual cells.

The cell-based study has also expanded the earlier vehicle-based study to investigate additional charging scenarios, including charging above 50 kW and where combinations of DC fast-charging and AC Level 2 charging are used. It has also been expanded to look at other cell chemistries and designs to generate a more complete data set. As expected, the more aggressive charging regimes both increase the cell's temperature and the overall performance fade. Understanding the extent of temperature increase during these experiments will support the need for design consideration in future fast-charge capable EVs and related systems.

Improved Cathode Materials for Lithium-Ion Batteries

A simple one-step synthesis procedure results in high-capacity cathode materials with graded compositions. The new materials have less highly reactive nickel on particle surfaces in comparison with conventionally prepared cathodes, which results in enhanced cycle life.

Lawrence Berkeley National Laboratory

Nickel-manganese-cobalt oxide (NMC) is a cathode material for lithium-ion batteries (LIBS) with the general formula $\text{LiNi}_x\text{Co}_y\text{Mn}_z\text{O}_2$ ($x+y+z \approx 1$). Because NMCs contain a smaller quantity of expensive cobalt (Co) compared to lithium-cobalt-oxide, the cathode used in LIBS for some consumer electronics devices, they are of interest for use in cost-sensitive applications such as electric vehicles. The practical capacities of NMCs generally increase as the nickel (Ni) content is raised, resulting in higher specific energies (longer range in vehicles). Unfortunately, higher Ni content is also associated with reduced cycle life and abuse tolerance. This is due to the high reactivity of Ni ions with electrolytic solutions, as well as a tendency for Ni-containing oxides to lose oxygen. The latter results in structural transformation at particle surfaces (“surface reconstruction”), which is associated with poor cycle life. Under certain abuse conditions, such as over-charge, the evolution of oxygen from the cathode can exacerbate thermal runaway, resulting in explosions and fires.

Lawrence Berkeley National Laboratory (LBNL) has succeeded in synthesizing a high-Ni NMC with a graded composition by a simple one-step spray pyrolysis method, a continuous processing technique which enables high-throughput, making it commercially viable. In this technique, an aqueous solution containing precursors is ultrasonically sprayed into a hot furnace, resulting in the rapid formation of spherical particles. The particle size distributions are typically narrow (in this case, $\sim 5 \mu\text{m}$), which is desirable for battery applications. By using synchrotron transmission X-ray microscopy (TXM) or nanotomography, the distribution of transition metals in the particles could be spatially resolved (Figure 1). This revealed that the particle

surfaces were Ni-poor and manganese (Mn)-rich compared to deeper in the bulk.

The compositionally graded NMC showed better cycling performance than materials made by conventional co-precipitation techniques (Figure 2). Synchrotron X-ray absorption spectroscopy showed that there was less surface reconstruction on particle surfaces in the spray-pyrolyzed NMC compared to the conventionally prepared NMC, resulting in improved cycle life.

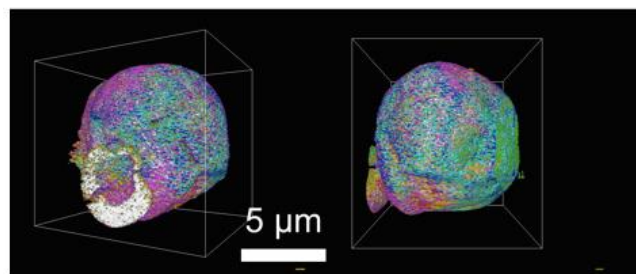


Figure 1. TXM (nanotomography) images of spray-pyrolyzed NMC particles, showing compositional variation on particle surfaces. Areas are color-coded as: blue=Mn, red=Co, green=Ni, purple=Mn+Co, cyan=Mn+Ni, yellow=Co+Ni, white=Mn+Co+Ni.

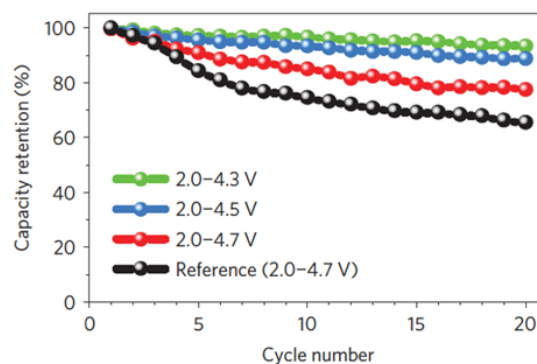


Figure 2. Cycle life of concentration gradient NMC materials at several maximum voltages (green, blue, and red curves) show improved cycling stability compared to traditionally prepared NMC cathodes.

12 Volt Start/Stop Lithium Polymer Battery Pack

Optimized material properties and pack designs for a lithium titanate/lithium manganese spinel battery have led to significantly improved cold-cranking power and durability in a 12 volt start/stop application.

LG Chem Power and the U.S. Advanced Battery Consortium

Start/stop batteries are gaining global attention as a cost-efficient solution for reducing carbon emissions. To achieve this goal, lithium (Li)-ion batteries are promising alternative to lead-acid or metal hydride batteries because of their higher specific energy and longer life. Key challenges for realizing this objective are cold-cranking power and cost. To achieve these objectives, LG sought to develop a highly abuse-tolerant and long-life cell using a Li titanate (LTO) anode and Li manganese spinel (LMO) cathode. Significant progress has been made by optimizing material properties, and by developing a low-cost battery pack incorporating a simple battery management system.

The three generations of cells developed in this program used LMO cathode materials that varied in particle size, surface area, dopants/dopant levels as well as surface coatings. A similar development approach applied to the negative electrode yielded a high power LTO anode. A number of electrolyte compositions and separators of different thickness and porosities were examined so the most effective could be implemented. In addition, studies carried out to improve processing conditions, such as electrode manufacturing and aging, proved critical to ensuring performance of cells using nano-materials such as LTO.

These efforts have led to considerable improvement in cell life and power. Figure 1 illustrates the significant improvement in storage characteristics achieved to date. Perhaps the greatest challenge for Li-ion batteries in start/stop applications is meeting the U.S. Advanced Battery Consortium's (USABC) cold-cranking power requirements. While the first-generation cells achieved the cold-cranking power only at ~100% state-of-charge (SOC), various cell modifications have resulted in significant improvement in the cold-cranking power capability;

for example, the latest cells can meet the cold-cranking power at 70% SOC. Another benefit of this approach is the cells' outstanding robustness under various abuse conditions. While testing has only been conducted on second-generation cells so far, they have met USABC expectations. The latest generation of cells are expected to match those results.

Another significant accomplishment was designing a battery pack to hold the cells in a mechanically rugged manner and simultaneously shield them efficiently from exterior heat while still being able to shed heat from the cells during operation. This novel design in conjunction with a low-cost, simplified battery management system has been incorporated into the battery packs for delivery to the USABC for full characterization, life and abuse-tolerance tests.

While this program has led to the development of a long-life and robust 12 volt start/stop Li-ion battery pack with significantly improved cold-cranking power, there are still gaps to the USABC targets for cost and cold-cranking power. Further development work is needed to bridge these gaps.

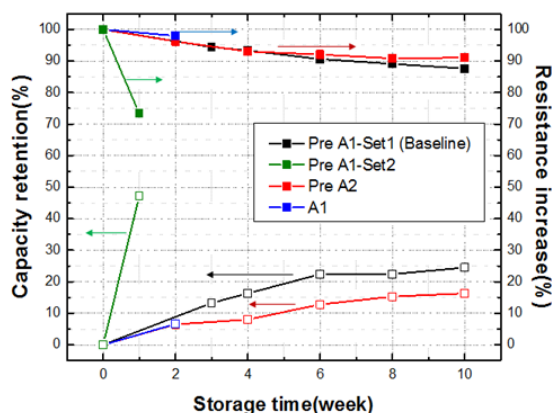


Figure 1. Illustration of the improvement in the storage properties of the LTO/LMO cells at 60°C and 70% SOC..

Microstructure Simulation of Battery Electrode Design

Computer-aided engineering models enable prediction of battery device-level performance based on material recipe, composition and morphology.

National Renewable Energy Laboratory

To achieve high energy, battery electrodes must pack in as much active material as possible. But for high power, the electrodes must balance a mixture of both active and inert materials. Carbon black dispersed in a polyvinylidene fluoride (PVdF) binder enhances the electrode's electronic conduction and an open pore structure provides ionic conduction when the electrode is filled with electrolyte. These inert materials improve battery power and lifetime at the expense of energy density. At present, optimizing a battery electrode requires time-consuming building and testing of prototypes.

While the electrochemical physics of lithium (Li)-ion batteries are relatively well understood, models generally only capture the average behavior of an electrode. Those homogenized models are unable to predict electrode response prior to actually building and characterizing a physical specimen. Under the U.S. Department of Energy's Computer-Aided Engineering of Batteries program, the National Renewable Energy Laboratory (NREL), Argonne National Laboratory (ANL) and Texas A&M University are developing microstructure-scale electrochemical models that predict the performance of battery electrodes based on their recipe, morphology, and manufacturing processes.

Under the NREL-led project, ANL is conducting X-ray tomography to map the three-dimensional architecture of electrodes. From these data, Texas A&M is extracting detailed geometry for NREL simulations. As tomography measurements are unable to separate PVdF binder and carbon black conductive additives, Texas A&M developed stochastic reconstruction algorithms that artificially grow this secondary phase amongst the active material primary phase (Figure 1). The structure closely matches structures observed in two-

dimensional scanning electron microscopy experiments. Next, using computationally generated microstructures, the team explored a range of different nickel-cobalt-manganese (NCM) electrode designs. Computer models showed that as additional secondary phase is added to an electrode design, electronic conductivity increases. Initially this improves performance; however, with too much secondary phase, performance decreases due to blockage of electrochemical active material surfaces and pores. The modeling results compare well to published experimental studies (Figure 2).

Moving forward, the team is conducting modeling and experimental validation studies for a range of next-generation electrode designs from ANL.

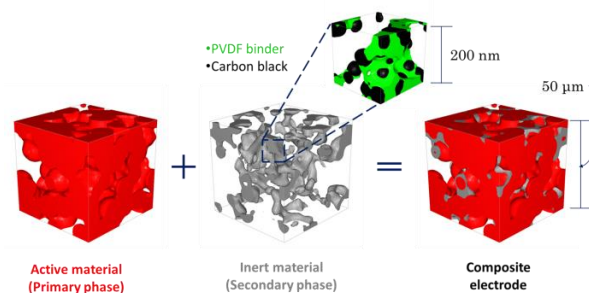


Figure 1. Microstructure geometry of computational model.

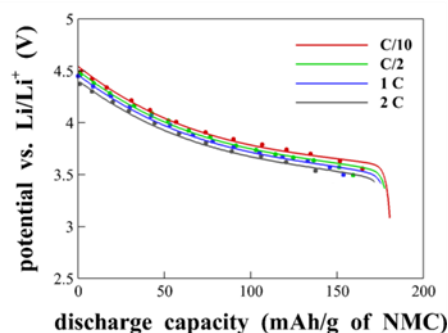


Figure 2. Validation of model (lines) with data (symbols).

Electron Beam Curing of Lithium-Ion Battery Electrodes

Electron beam curable polymers are demonstrated as aqueous binders for positive electrodes in lithium (Li)-ion batteries. Full Li-ion cells exhibit nearly identical initial cycling performance compared to cells using traditional binders, indicating the potential for future use of this new type of binder in Li-ion batteries.

Oak Ridge National Laboratory

Conventional lithium (Li)-ion battery electrodes are manufactured via a slurry-based process where N-methylpyrrolidone (NMP) and polyvinylidene fluoride (PVdF) are used as the solvent and binder, respectively. NMP is expensive, toxic, and requires a costly solvent recovery process.

Oak Ridge National Laboratory (ORNL) researchers are developing electron beam (EB) curing for electrode manufacturing where liquid polymer binders are utilized to replace PVdF. The liquid polymer binder also serves as the solvent and thus has the potential to eliminate extra solvent, which could reduce the cost and energy consumption associated with solvent recovery. Another advantage of this technology is that the polymer binders crosslink instantly when exposed to EB, allowing for high processing speed. ORNL researchers have successfully demonstrated EB curing of acrylated polyurethanes as binders in Li-ion electrodes. Comparable initial electrochemical performance has been obtained from the electrodes via EB-curing and NMP-based processing.

Figure 1a illustrates the EB curing process of Li-ion electrodes. $\text{LiNi}_{0.5}\text{Mn}_{0.3}\text{Co}_{0.2}\text{O}_2$ (NMC532) and carbon black are first dispersed in low molecular weight (MW) oligomers before coating on aluminum (Al) foil. Then the electrodes are exposed to an EB for cross-linking of the acrylated polyurethane (PU) resin. The high MW cross-linked polymer functions effectively as a binder to adhere the cathode coating to the Al foil.

Electrodes with PVdF binder or EB cured resins demonstrate similar voltage profiles (Figure 1b). The NMC532 cathode with PVdF as the binder retains 96.7% capacity after 100 cycles (Figure 1c). Similar cycling performance is observed for the NMC532 cathode using EB-cured binder with 97.1% capacity

after 100 cycles. Thus, Li-ion electrodes made via EB curing result in similar initial electrochemical performance and may enable faster electrode processing, potentially with thicker electrodes, and may reduce environmental impacts via eliminating toxic solvents.

ORNL has estimated that the cost of the EB curing step is \$0.056/kWh for a 100 μm cathode and \$0.034/kWh for a 200 μm cathode; based on a 3 meter roll width moving 400 m/min. Future work will involve monitoring the impedance and gas generation of cells containing EB cured electrodes over their life. ORNL plans to demonstrate both high line-speed and thick coatings with a nitrogen blanket (oxygen in the pre-dried, acrylated PU based coatings may result in incomplete crosslinking when entering the EB chamber at high speed), and will determine a “non-slot-die” coating method compatible with over 200 m/min lines.

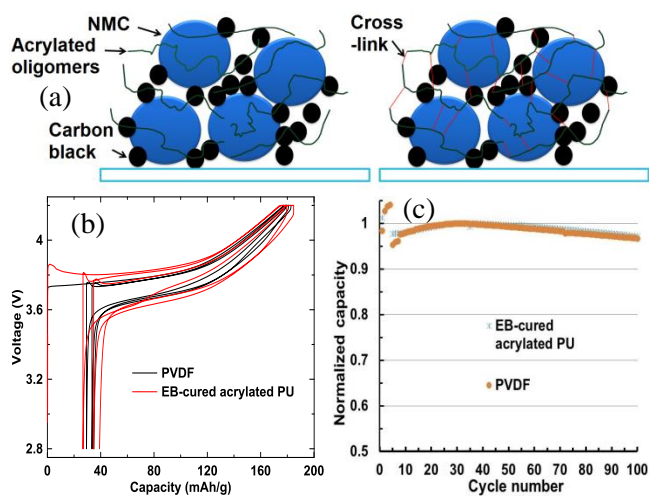


Figure 1. (a) Concept of using acrylated PU oligomers as binders in Li-ion battery electrodes. (b) Voltage profiles of NMC532 cathodes using PVdF and EB-cured acrylated PU as binders in Li half-cells. (c) Cycling performance of NMC532 cathodes using PVdF and EB-cured acrylated PU binders in full coin cells at C/3 and 30°C.

Enabling Fast Formation for Lithium-Ion Batteries

A new method of forming passivation layers on electrodes reduces the formation time from weeks to a day and results in similar cell capacity retention.

Oak Ridge National Laboratory

Electrolyte wetting and anode passivation film (solid electrolyte interphase (SEI)) formation steps are expensive processes (~\$7.5/kWh for wetting/formation cycling) due to the lengthy wetting and SEI formation period (e.g., 3-5 cycles at C/20 and 3-5 cycles at higher C-rate at an elevated temperature). This process may take up to 2-3 weeks, depending on the cell manufacturer, requiring a tremendous number of cyclers, large footprint, and intense energy consumption for the cyclers and thermal environment. These processes are a key production bottleneck and therefore, any significant reduction in wetting and formation time without sacrificing cell performance would be a key advancement.

Researchers at Oak Ridge National Laboratory (ORNL) have developed a new fast-formation method to generate the SEI in lithium-ion batteries consisting of graphite and nickel-manganese-cobalt oxide (NMC) 532 as the anode and cathode, respectively. The new formation method is shown in Figure 1 (top, orange line) and compared with a baseline method (top, blue line). The baseline method consists of a series of full charge and discharge cycles at a constant C-rate without any interruption between the lower and upper cut-off voltages (2.5 – 4.2 volt (V)). The new method, however, involves repeated cycling within a high state-of-charge region (4.2 – 3.9 V) after the first charge until the last cycle where a full discharge takes place. Compared to the baseline, the new method reduced formation time from more than nine days to less than a day.

The new method at ORNL resulted in similar capacity retention compared to the baseline (Figure 1, bottom). Thus, the new method not only reduced

the formation time by a great deal, but also resulted in similar cell capacity retention, which could significantly increase production throughput. This new SEI formation method could also result in capital equipment savings for new battery plants.

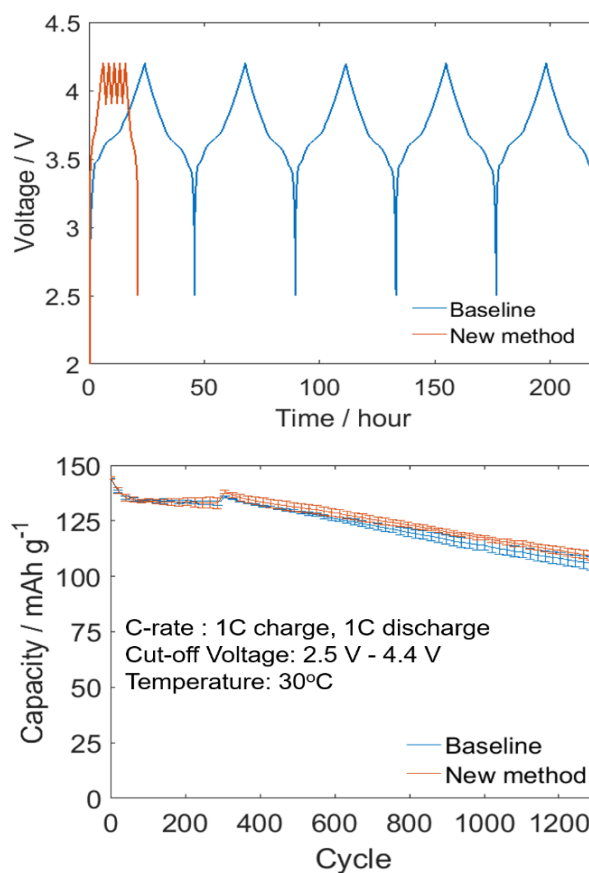


Figure 1. (Top.) The baseline and new formation method illustrated as voltage profiles, showing ten times faster formation time using the new method. (Bottom.) The capacity of 1.5 Ah pouch cells formed using baseline and new formation method. Error bars correspond to 90% confidence.

Alternate Reaction Pathway Enables Higher Performance Lithium-Sulfur Batteries

Dimethyl disulfide as a co-solvent is found to enable a new electrochemical reaction pathway for sulfur cathodes, which significantly boosts cell capacity and leads to improved discharge-charge reversibility and cycling of lithium-sulfur batteries.

The Pennsylvania State University

Lithium-sulfur (Li-S) batteries have attracted great attention because of their high specific energy, ~2,600 Wh/kg. However, dissolution of lithium polysulfide intermediates in conventional ether-based electrolytes forces large amounts of electrolyte to be used, significantly reducing cell energy density. Diffusion and side-reaction of lithium polysulfides are also known to be among the main technical barriers to long cycle life.

Penn State University researchers developed an electrolyte system using dimethyl disulfide (DMDS) as a co-solvent for Li-S batteries. DMDS promotes the discharge of sulfur through an alternate electrochemical reaction pathway by formation and subsequent reduction of dimethyl polysulfide species (Figure 1 a, b). The lack of any color change in Figure 1c (bottom) indicates the lack of traditional polysulfides, which has two major advantages.

First, the reaction pathway involves additional electron transfer to break the disulfide bond in DMDS molecules, boosting cell capacity. Second, the dimethyl polysulfide intermediates not only show better electrochemical kinetics than conventional polysulfides, but also avoid the large increase in electrolyte viscosity and cell resistance, enabling high performance with less electrolyte.

Combined, these advantages allow cells to reach high performance: a stable capacity of around 1,000 mAh/g sulfur at a very low electrolyte/sulfur (E/S) ratio of 5 mL/g using a high-sulfur-loading (4 mg S/cm²), almost double the capacity obtained with conventional electrolytes under the same conditions (Figure 2). These results highlight the practical potential of this electrolyte system to enable high-energy-density Li-S batteries. It is estimated that an E/S ratio of 3 mL/g is needed for a 300Wh/kg cell. This work achieves a large step in that direction.

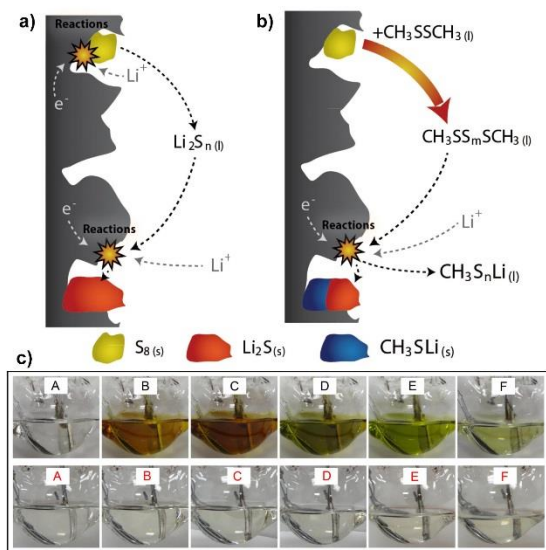


Figure 1. Schematic diagrams of the discharge mechanism of (a) conventional ether-based and (b) DMDS-containing Li-S electrolytes, and (c) photos showing the electrolyte color changes during discharge from A to F in conventional (upper) and DMDS-containing (lower) electrolytes.

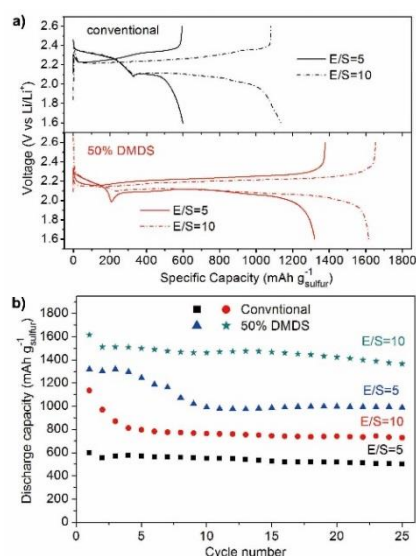


Figure 2. Electrochemical performance of high-sulfur-loading cathode with low electrolyte to sulfur (E/S) ratios of 10 and 5 mL g⁻¹ in conventional and DMDS-containing electrolytes.

High-Performance Organosilicon-Based Lithium-Ion Electrolyte

Organosilicon electrolyte material delivers cost effective lithium-ion battery performance improvement, while also improving battery safety and stability.

Silatronix

All automotive lithium (Li)-ion batteries use an electrolyte that contains Li hexafluorophosphate (LiPF₆), which has many advantages, including good conductivity over a wide temperature range, and good electrochemical stability. A major disadvantage is that under both high-temperature and high-charge voltage conditions, along with the presence of water, LiPF₆ in traditional carbonate solvents decomposes and creates very reactive and destructive compounds.

When carbonate/LiPF₆ electrolytes break down inside of a battery, a chemical reaction creating hydrogen fluoride (HF) is started. This creates three problems. First, hydrofluoric acid attacks battery materials. Second, decomposed carbonate material leads to gas generation. Third, electrolyte material is consumed. The result is swollen battery cells with reduced cycle life and reduced charge capacity.

Silatronix, improving upon technology licensed from Argonne National Laboratory, has developed a commercially available organosilicon material, OS3. This material has proven to inhibit LiPF₆ breakdown. OS3 benefits are particularly notable during high-temperature operation where traditional electrolytes decompose. OS3 provides benefits to Li-ion batteries in concentrations of just 2% to 5%. The minimal amount of material needed to impact cell performance makes OS3 cost-effective for all Li-ion applications.

Figure 1 demonstrates how OS3 material can reduce cell swelling due to gas generation in a Li-ion nickel-manganese-cobalt (NMC) cell. This 1.25 Ah cell had an initial volume of 12 ml. Thus, the cell with standard electrolyte increased in volume over 40%, while the OS3 containing one increased 20%. Figure 2 shows how adding OS3 material can significantly extend battery life during high-temperature

operation in Li-cobalt-oxide (LCO) cells. These observed performance improvements are achieved through OS3 inhibiting LiPF₆ breakdown and thus preventing HF creation in the battery.

Li-ion battery manufacturers are currently evaluating OS3 material. Silatronix will continue to develop organosilicon chemistry to enable next-generation electric vehicle batteries through U.S. Department of Energy support.



Figure 1. Li-ion NMC pouch cell battery. Reference cell represents a standard battery. Ref. +OS3 contains 2% OS3 material. Test conditions: Storage at 60°C, 10 weeks.

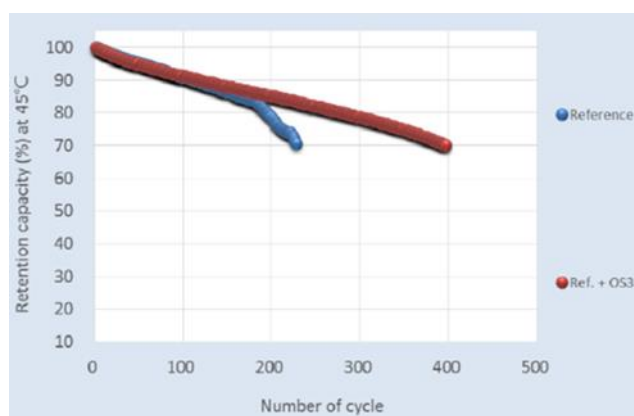


Figure 2. 4.45V Li-ion LCO pouch cell battery. Reference cell represents a standard battery. Ref. +OS3 contains 3% OS3 material. Test conditions: Charge to 4.45 V at 1C, current cut-off 1/20C, rest 10 min, discharge to 3.0V at 1C, rest 10 min at 45°C.

Constructing a “Home” for Lithium-Metal Anodes

Abuse tolerance and cycling stability are two major challenges for lithium-metal batteries. This work targets these two issues by designing a graphene-based “stable host.” Stable electrode dimensions with minimal volume change are designed for next-generation high-energy lithium-metal-based batteries.

Stanford University

Developing high-energy lithium (Li)-metal batteries with improved abuse tolerance is a prerequisite for more practical and affordable electric vehicles in the future. To achieve these goals, Li metal-based systems, such as Li-sulfur and Li-air batteries, hold great promise.

The Li-metal anode is known as the “Holy Grail” of battery technologies not only due to its high capacity (10-fold higher than the commercial material), but also due to the related grand challenges. The challenges lie mainly in two aspects, Li dendrite formation, which may result in internal short circuit, and the poor cycling stability leading to short cycle life. These problems stem from two roots: the high reactivity of Li and its significant volume change during repeated cycling.

Scientists at Stanford University have shown the importance of maintaining a constant volume of the Li metal anode. They have proposed a new principle for designing the Li metal anode: constructing a “stable host” to reduce the anode’s volume change during cycling. To achieve this goal, advanced nanotechnology plays a key role. Figure 1 shows the schematic drawing (a) and the real microscopic images (b,c) of the structure. Here, the designed structure consists of stacking graphene layers with uniform nanoscale interlayer gaps. The gaps provide room for storing Li-metal.

This layered stacking nanostructure offers several important advantages: First, due to the graphene “host,” the volume change with repeated cycling can be significantly reduced to less than 20%; second, the large surface area of the host can enable uniform Li deposition; and third, the graphene layers provide surface protection to reduce side reactions on highly-reactive Li-metal. This construct successfully suppresses Li dendrites, while at the same time

allowing for improved cycle life. Cells with commercial lithium-cobalt oxide cathodes further exhibit high-power output, with charging times of less than six minutes.

The “stable host” principle can be a promising platform for future studies, while further surface protection is still needed to meet the ultimate commercial standards.

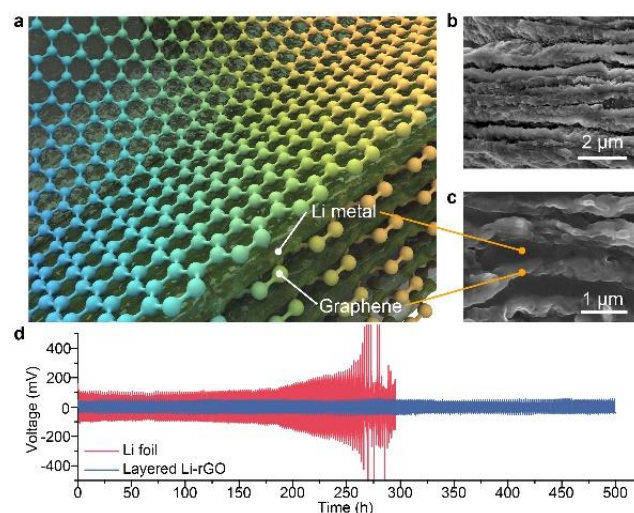


Figure 1. (a) Schematic of the Li metal anode with “stable host,” which exhibits layered stacking of Li metal and graphene. (b,c), Scanning electron microscopy images of the Li metal anode in cross-section view. (d) Cycling stability of Li-rGO and Li foil symmetric cells at 1 mA cm⁻² and 1 mAh cm⁻².

High-Energy, High-Power Battery for Plug-In Hybrid Electric Vehicle Applications

Demonstrating improved energy and power density, long life lithium-ion battery cells combining TIAX's high capacity CAM-7[®] cathode material with a silicon-based anode ideally suited for implementation in plug-in electric vehicles.

TIAX LLC

TIAX has developed long-life lithium (Li)-ion cells that exceed plug-in hybrid electric vehicle (PHEV) 40 battery cell energy and power targets (200 Wh/kg and 800 W/kg pulse power) set by the U.S. Department of Energy. To achieve these targets, we selected and scaled-up a high-capacity version of our proprietary high-energy and high-power CAM-7[®] cathode material. We paired the cathode with a blended anode containing silicon (Si)-based anode material capable of delivering high capacity and long life. We optimized the anode blend composition, cathode and anode electrode design, and selected inactive components to achieve not only the best performance, but also long life.

By implementing CAM-7 with a Si-based blended anode (with no prelithiation), we built and tested prototype 18650 cells that delivered higher specific energy and power than baseline cells employing CAM-7/Graphite (Figure 1). Program deliverable cell specific energy projected to 220 Wh/kg when scaled to state-of-the-art 18650 cell hardware and to 250 Wh/kg when scaled to 15 Ah pouch cells, which is substantially higher than the 100-160 Wh/kg typical of current PHEV Li-ion battery cells. Moreover, these program demonstration cells achieved excellent life, with 85% capacity retention after 1,000 cycles in on-going cycle life testing (Figure 2). Note that the PHEV40 cycle life target is 5,000 cycles. Thus, although this is an impressive achievement, more optimization may be needed to meet all PHEV targets. In parallel, we demonstrated that baseline CAM-7/graphite chemistry can sustain over ~4,000 cycles with 70% capacity retention in prototype 18650 cells.

By simultaneously meeting the PHEV40 power and energy targets and providing long life, we have developed a Li-ion battery system that can be

smaller, lighter, and less expensive than current state-of-the-art Li-ion batteries.

The demonstrated high energy density and long life of the CAM-7/Si-based Li-ion battery chemistry makes it ideally suited for PHEV and electric vehicle applications. While the program has concluded, we are investigating further ways of optimizing and scaling this CAM-7/Si-based Li-ion battery chemistry to accelerate its adoption and commercialization.

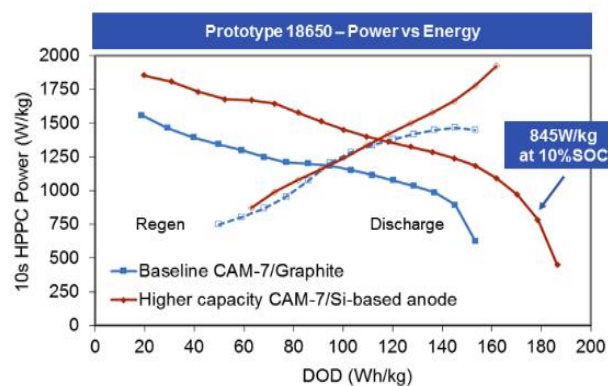


Figure 1. Implementing higher capacity CAM-7 with a blended Si-based anode yields prototype 18650 Li-ion cells with higher specific energy and power.

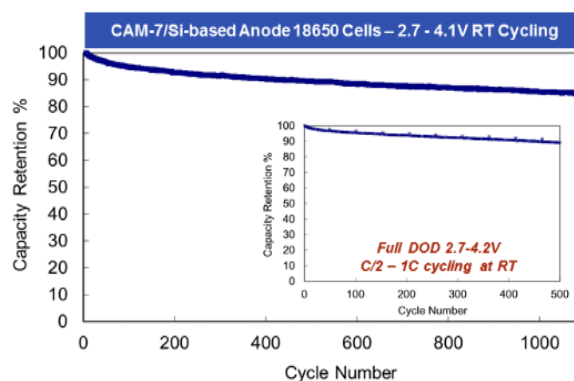


Figure 2. TIAX achieved excellent cycle life in the program demonstration 18650 cells with higher capacity CAM-7 and blended Si-based anode.

Reducing Interfacial Impedance in Solid-State Batteries

A University of Maryland team has developed engineered interfaces to dramatically reduce the interfacial resistance between solid-state electrolyte and electrodes, enabling both higher capacity lithium-metal anodes for higher energy density batteries and non-flammable solid-state electrolytes.

University of Maryland

Through modifying interfacial layers informed by computational modeling and controlled interfacial structures by three-dimensional (3D) printing, we have achieved low interfacial resistance in solid-state batteries comparable to commercial liquid electrolyte batteries. This attacks the large interfacial resistance problem, which is one of the primary issues with solid-state batteries. With these techniques, we can make intrinsically non-flammable solid-state batteries with high energy/power density, high efficiency, and long cycle life. While this work focused on garnet solid-state electrolytes (SSE), the findings have potential to be applied to other SSE materials.

We investigated different types of interfacial modifications between the garnet solid electrolyte and the electrodes. The materials included aluminum (Al), silicon (Si), and Al_2O_3 with both organic and aqueous electrolytes. With these interfacial layers, researchers made lithium (Li)-metal wet the garnet surface (Figure 1a) and decreased the garnet/Li interfacial resistance by three orders of magnitude to $1 \text{ Ohm}\cdot\text{cm}^2$ (Figure 1b). Note the inset of Figure 1b, which shows a voltage swing of just 10 mV during Li/Li symmetric cell cycling when using the atomic layer deposition (ALD) coated garnet electrolyte. Cycling the cell without ALD coated garnet results in voltage swings of 1 to 6 volt (V), red lines. We also decreased the cathode/garnet interfacial resistance to $7.5 \text{ Ohm}\cdot\text{cm}^2$, which is a dramatic improvement over the over $3,000 \text{ Ohm}\cdot\text{cm}^2$ resistance without surface modification.

Researchers applied first principles calculations to understand the interface stability between garnet electrolytes and electrodes and to predict new interlayer materials to further enhance interfacial

properties (Figure 1c). We studied multiple interlayers for wetting Li-garnet interfaces and computationally investigated other cathode coatings for improved electrochemical performance.

Finally, researchers printed 3D surface structures to increase the effective surface area relative to the planar areal surface area, forming structured ion-conductive pathways with varying line spacing. The resulting interfacial resistance decreased linearly with increased surface area, achieving a 52% resistance decrease (Figure 1d).

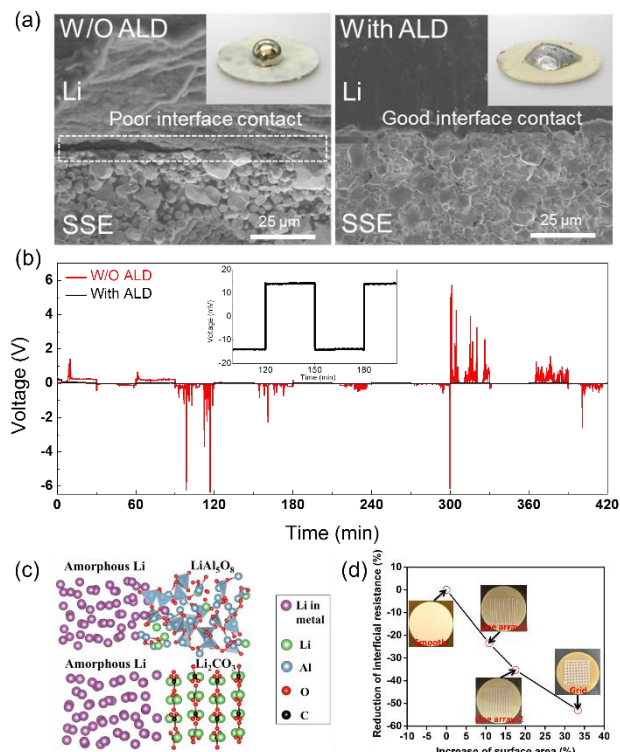


Figure 1. (a) Photos and scanning electron microscope figures of Li/garnet interface with and without ALD surface modification. (b) Voltage profile of DC cycling of Li/garnet/Li cell, showing lower and more stable interfacial resistance after ALD coating. (c) Interface model of Li metal on LiAl_5O_8 and Li_2CO_3 terminated garnet surface with and without ALD. (d) 3D printing of garnet increases surface area, linearly reducing interfacial resistance.

New Process is Demonstrated for End-of-Life Electric Vehicle Lithium-Ion Batteries

This closed-loop recycling process generates new cathode materials from spent lithium-ion batteries, providing new pathways for increased industry sustainability and potential vehicle cost reduction.

Worcester Polytechnic Institute and the U.S. Advanced Battery Consortium

The lithium (Li)-ion battery industry has been growing exponentially since its inception in the late 20th century. However, despite the continued rise of Li-ion battery technology development and commercialization, the battery recycling industry is lagging. Industrial battery recycling processes are limited and only capable of recovering secondary raw materials, which are not suitable for direct reuse in new batteries. Most recycling technologies also rely on high concentrations of cobalt to be profitable, and require costly and labor intensive battery sorting operations prior to processing. It is critical that a new recycling process be developed that is capable of recovering higher value materials at greater efficiencies, thus ensuring the full sustainability benefits of electrification are realized.

The goal of this U.S. Advanced Battery Consortium (USABC) project is to successfully recycle multiple 10 kg-size batches of end-of-life electric vehicle batteries consisting of different incoming cathode chemistries via the recycling process developed at Worcester Polytechnic Institute (WPI), and produce plug-in hybrid electric vehicle (PHEV) format cells using the recovered nickel-manganese-cobalt (NMC) 111 cathode. Over the course of the two-year development program, WPI will improve the performance of the recovered cathode materials so that they exhibit performance equivalent to current commercial materials, as confirmed by A123 and national lab testing using USABC PHEV test procedures.

Figure 1 shows the scanning electron microscope images of the NMC111 precursor, which has been synthesized from recycled Li-ion batteries. At 72 hours, dense particles are formed with a bimodal distribution. The synthesized NMC111 cathode material is similar to the precursor, and exhibits a dense morphology and a bimodal particle size

distribution. Measured impurity levels of synthesized NMC111 precursor and cathode materials are comparable to commercial NMC111. Feedstock consisted of GM Volt and Fiat 500-e batteries, with similar results. Table 1 shows the performance of recycled NMC111 versus commercial powder, which confirms that the performance of recycled NMC111 is equivalent to commercial powder. This recycling process has been scaled to the 10 kg level and will be evaluated in 25 Ah PHEV format pouch cells under U.S. Department of Energy protocols and using USABC PHEV test methods.

Scaling the process will provide valuable insight about the technology’s scalability and commercialization potential, and the scaled process and large-format cell data obtained will allow validation of WPI’s underlying economic model assumptions, which suggest potential savings of \$25.4/kWh for electric vehicle cells.

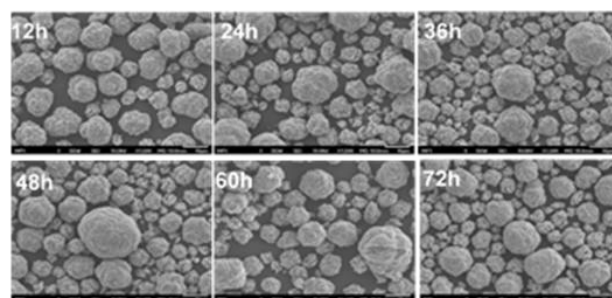


Figure 1. Morphology of NMC111 precursor with reaction time.

Test		Commercial Material 1	Commercial Material 2	WPI Sample 11022016
Tap Density	g/cc	2.28	2.84	2.36
D50 Particle Size	um	7.4	9.2	10.5
FCC/FDC	mAh/g	164.6 / 145.9	174.7/157.2	181.7/159.1
Efficiency	%	88.6	90.0	87.6
1C	mAh/g	132.9	130.9	129.1
2C	mAh/g	122.3	119.4	120.5
5C	mAh/g	36.7	40.4	39.6

Table 1. Comparison between recycled NMC versus commercial NMC.

Silicon-Graphene Material Shows Promise for Electric Vehicle Batteries

Significant progress towards practical application of silicon-based anodes with improved battery cycling stability and energy density.

XG Sciences, Inc.

Advanced batteries for electric vehicles (EVs) would benefit from greater energy density than in today’s lithium-ion batteries (LIBs). The U.S. Department of Energy/U.S. DRIVE defines cell specific energy targets of 350 Wh/kg with 1,000 charge-discharge cycles at a cost of ownership comparable to conventional vehicles. These targets cannot be met using materials in today’s LIBs—new advanced materials with increased storage capacity are required.

Silicon (Si) is considered a promising anode material due to its high charge storage capacity, low cost, and abundant supply. Si can store 10 times the charge of carbon and thus has the potential to help enable LIBs achieve the energy density needed for broad EV adoption. However, significant technical and cost challenges exist to Si commercial adoption. Poor cycling stability of Si-based LIBs is a foremost concern. XG Sciences (XGS) has developed XG SiG™, a Si/graphene composite anode material that is a potentially disruptive and enabling LIB technology. XG SiG™ features a unique nano-structured material design (see Figure 1) and an innovative, low-cost, scalable manufacturing process utilizing graphene to mitigate the cycling stability issues of Si in LIBs.

Many current Si production processes use expensive SI raw materials. XG can process low-cost, micron-sized Si in their existing one-step reactor. The design features a graphene platelet covering on the core Si material to provide chemical protection against reaction with the electrolyte and also mechanical support.

XGS’ optimization of the Si/graphene composite structure in this program led to improved LIB cycling stability. The XGS Si/graphene composite anode delivered high capacity (600 mAh/g), high

first cycle efficiency (~85%), and cycling stability of over 85% at 1m000 cycles in 2 Ah cells with a nickel cobalt aluminum (NCA) cathode produced and tested at A123 Systems (Table 1).

XG currently operates a 100 ton/year manufacturing plant in Lansing, Michigan and demonstrated the production of our Si/graphene composite in the production line.

In future work, the capacity retention must be improved to deliver 1,000 mAh/g and over 1,000 cycles.

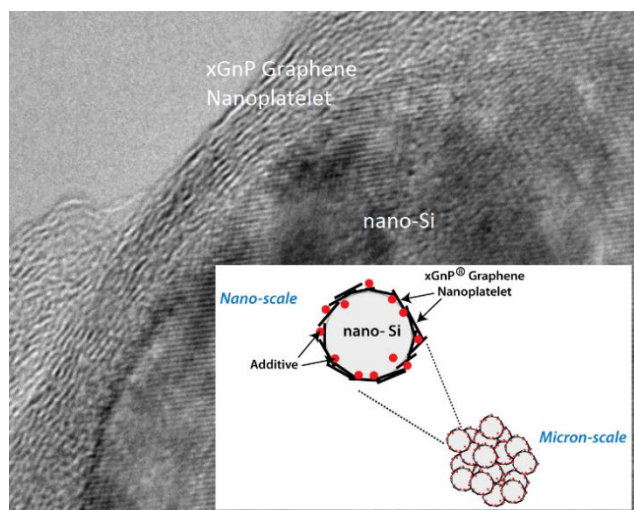


Figure 1. Transmission electron microscope image showing Si/graphene composite material in the region of the graphene Si interface and sketch illustrating nano-structured material design (inset).

Cycle	0	250	500	750	1000
% Cap	100	90	88.5	87.5	87

Table 1. 2 Ah pouch cell cycling data with 600 mAh/g Si/graphene anode/NCA cathode, 165 Wh/kg.

Fuel Cells



Improved Membrane Performance and Durability

New membrane achieves U.S. Department of Energy durability targets, while meeting the performance targets at all but the highest temperatures.

3M

The electrolyte membrane is a critical component of a proton exchange membrane (PEM) fuel cell. A good membrane must remain reliable and durable while maintaining a low protonic resistance over a wide range of temperature and humidity conditions. Existing membranes cannot perform under the most challenging (hot and dry) conditions, which drives up fuel cell system cost and creates challenges with respect to system packaging. The 3M membrane combines a novel multi-acid side chain ionomer with an improved nanofiber support to enable excellent fuel cell performance under hotter and dryer conditions while also meeting U.S. Department of Energy’s (DOE) mechanical and chemical durability targets.

The novel ionomer, perfluoro imide acid (PFIA), achieves low protonic resistance by packing two acid groups per side chain, compared to standard ionomers such as Nafion™ with one acid group per side chain. This allows for more proton conducting groups in the polymer without decreasing the backbone crystallinity necessary for mechanical strength.

Adding nanofiber supports increases the mechanical strength further and reduces membrane swelling and contraction stresses during hydration changes experienced over the automotive drive cycle. Based on mechanical strength tests, the time for failure under humidity cycling is projected to be longer for the membranes supported with the 3M nanofibers than for membranes supported with expanded Teflon™, the current state-of-the-art support. The increased mechanical strength allowed 3M to reduce membrane thickness from 15 to 10 μm, decreasing resistance and cost. Testing of these membranes indicates that the membranes can meet DOE mechanical and durability targets, while meeting the

low-protonic areal specific resistance targets for all but the most demanding high-temperature, low-humidity condition (see Table 1). The membranes have been produced at pilot scale and incorporated into membrane electrode assemblies that are undergoing stack testing.

Characteristic	Units	2020 Targets	3M PFIA Status
Maximum oxygen cross-over	mA/cm ²	2	3.5
Maximum hydrogen cross-over	mA/cm ²	2	1.9
Area specific protonic Resistance at:			
120°C, P _{H2O} 40 kPa	Ohm cm ²	0.02	0.054
120°C P _{H2O} 80 kPa	Ohm cm ²	0.02	0.019
80°C P _{H2O} 25 kPa	Ohm cm ²	0.02	0.02
80°C P _{H2O} 45 kPa	Ohm cm ²	0.02	0.008
30°C P _{H2O} up to 4 kPa	Ohm cm ²	0.03	0.018
-20°C	Ohm cm ²	0.2	0.2
Minimum electrical resistance	Ohm cm ²	1,000	1,635
Cost	\$/m ²	20	Proprietary
Durability			
Mechanical	Cycles with <10 sccm crossover	20,000	>24,000
Chemical	hrs	>500	614

Table 1. 3M PFIA status.

Additional experiments at 3M indicate further improvements are possible in both the fiber support and the ionomer. By varying fiber diameter 3M was able to decrease lateral swelling for a membrane that was 75% PFIA ionomer from 14% to less than 8% and increase tensile strength from 8.6 to 10.4 MPa. Ionomers developed at 3M with three and four acid groups per side chain have demonstrated potential for improved protonic conductivity, but durability of these ionomers has yet to be demonstrated.

Enhanced Understanding of Platinum Alloy Catalysts

Fuel cell catalyst performance and durability can be improved by tailoring operating conditions and binary platinum alloy catalyst properties.

Fuel Cell Performance and Durability Consortium

Performance of the proton exchange membrane fuel cell (PEMFC) electrocatalyst, primarily at high current densities, and its durability under load cycling and start-stop conditions, are major challenges to the widespread commercialization of automotive fuel cell systems. The Fuel Cell Performance and Durability (FC-PAD) consortium leverages the capabilities of five national laboratories to achieve high performance and durability in low-platinum (Pt) PEMFCs utilizing advanced Pt alloy catalysts. One of FC-PAD's approaches toward this overall goal is to provide foundational understanding of cathode electrocatalyst activity, performance, and durability by studying catalyst and catalyst support durability and degradation mechanisms, catalyst/support interactions, and the effects of catalyst instability on cathode-catalyst-layer properties.

The primary mechanism for loss of performance of Pt and Pt alloy electrocatalysts is dissolution of Pt and of the alloying transition metal (e.g., cobalt (Co) or nickel (Ni)). The FC-PAD team studied the dissolution behavior of state-of-the-art Pt and Pt alloy catalysts and utilized these data to develop a model for Pt and transition metal loss under various conditions. This model provides guidance for the development of more stable catalysts and defines operating conditions that will extend catalyst lifetime.

The particle morphologies of state-of-the-art alloy catalysts, studied by FC-PAD, which have catalytic activities exceeding the U.S. Department of Energy's (DOE) 2020 targets, range from solid particles to porous particles (see Figure 1-left). Researchers found that the dissolution of both Pt and the alloying transition metal are highly dependent on cell voltage and on the morphology and initial transition metal

content of the catalyst particles (Figure 1-right). For instance, the porous particles, which initially have higher catalytic activities and higher Co content, show lower Pt dissolution and higher Co dissolution leading to accelerated performance loss.

The FC-PAD studies linked the dissolution of both Pt and Co from the particles to the formation and reduction of Pt oxides. Researchers found that avoiding conditions that cause catalyst oxidation and also limiting the rate at which the oxides are reduced can extend catalyst lifetime. These studies also found that more extensive leaching of alloying transition metals from the catalyst particles prior to incorporation into the fuel cell is necessary to prevent the detrimental impact of in-cell leaching on performance. These guiding principles and others learned through FC-PAD research will enable the design of more active catalysts and systems to achieve the performance and lifetime goals for PEMFC systems.

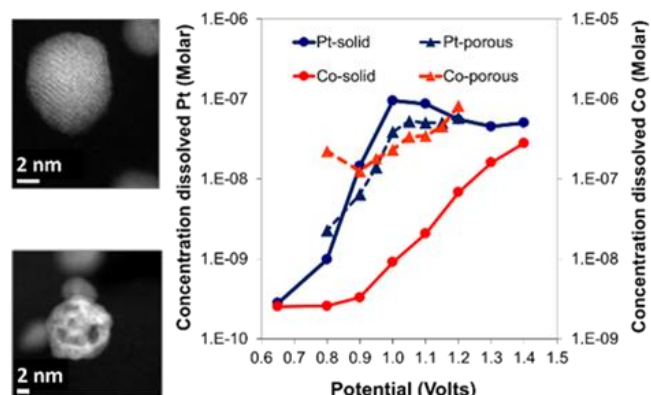


Figure 1. Example of the “solid” and “porous” morphology of PtCo alloy catalyst particles being studied in FC-PAD (left). Pt (blue lines) and Co (red lines) dissolution behavior as a function of cell voltage (potential) for a “solid” PtCo catalyst and a “porous” PtCo catalyst (right).

Materials



Low-Cost Carbon Fiber Commercialization

Facilitating the establishment of low-cost carbon fiber industry in the United States using alternative precursor materials.

Oak Ridge National Laboratory

In fiscal year 2016, the Carbon Fiber Technology Facility at Oak Ridge National Laboratory (ORNL) achieved breakthrough results in converting textile acrylic fiber to carbon fiber with mechanical properties at levels of commercial acceptance for vehicle and industrial applications.

Today, carbon fiber remains a low-volume, high-cost specialty material, prohibiting widespread adoption of carbon fiber-reinforced composites by the automotive manufacturing industry. In striving to reach the 2025 corporate average fuel economy standard of 54.5 mpg, vehicle light-weighting use of carbon fiber composites is essential.

Greater use of carbon fiber composites in high-volume automotive production and other clean energy applications can be substantially enabled through significant production cost reduction. The most direct approach to cost reduction is by reducing the cost of the precursor material, which comprises approximately 50% of the end-product cost. ORNL researchers were able to demonstrate large volume carbon fiber production (see Figure 1) by layering the precursor bands from 1 – 3, using three different acrylic textile precursors at semi-production scale (25 MT/year). The carbon fiber from textile grade precursors has demonstrated tensile strength, tensile modulus and strain to failure values exceeding 350 ksi, 35 Msi and 1%, respectively.

Based on new understandings of material chemistry and process kinetics, a reduction in production cost exceeding two times has been projected. Process energy input to achieve these results was also reduced, owing to additional heat of reaction from oxidation of the higher mass of precursor.

A patent was filed to protect this breakthrough technology and an opportunity to license rights to

the development was publicly announced. Significant work remains to reduce technical risk to enable licensees to design new plants or modify existing facilities to supply low-cost carbon fiber to the marketplace. ORNL pursued a path of licensing the patent semi-exclusively to as many as five companies. Two licenses have been issued to date with three others in negotiation. The intent is to stimulate interest for industry to collaborate in the further development of this and other technologies. As the technical risk is reduced to allow investment and deployment, the licensing program will continue to stimulate new domestic sources to serve anticipated growth in demand for lower-cost carbon fiber-reinforced composites.

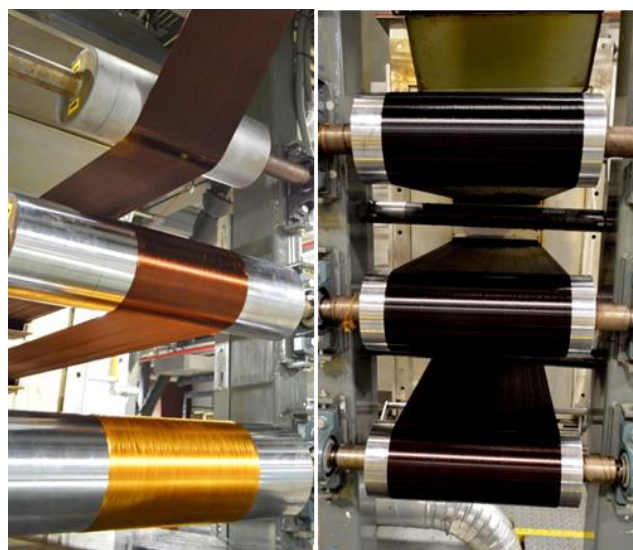


Figure 1. Showing increased throughput with textile acrylic fiber.

Predictive Engineering Tools for Injection-Molded Long Carbon Fiber Thermoplastic Composites

Validation of three-dimensional models to reduce development time for injection-molded composite components for vehicle light-weighting.

Oak Ridge National Laboratory

This project’s objective, led by Oak Ridge National Laboratory (ORNL) and conducted jointly with a U.S. automotive original equipment manufacturer (OEM), software developer, universities, and Tier 1 suppliers, was to validate three-dimensional (3D) models for long carbon fiber (CF)-reinforced, thermoplastic, injection-molded composites. Researchers used advanced characterization techniques to generate a database of experimental results for the CF orientation and CF length distribution within a component. Computational models were validated using a part with features representative of an automotive component, and the database of results will be available to the general public online. This predictive technology was used to create a demonstration part that may lead to production implementation of a separate part by the automotive OEM.

A seatback part was chosen as the prototype part (Figure 1). Plaques and seatback parts were molded using polypropylene (PP) and polyamide (PA) resins containing both 20% and 40% chopped CF. The complex part contains changes in thickness; ribs; holes, and changes in flow direction.



Figure 1. Complex part chosen for molding trials.

The team compared model predictions for fiber orientation and fiber length distribution at several strategically selected locations. A modified version of the method of ellipses for determining fiber orientation was used as well as new techniques for performing measurements in the lab. Eight of the nine 3D model predictions fell within 15% of experimental values, meeting the program validation goals.

The development of technologies for retaining fiber length during the injection molding process was critical for obtaining improved material properties. With modified screw design and processing inputs, the average fiber length maintained in the parts was 7.33 mm with the original input pellet length being 10 mm. The result is significantly longer fibers than had previously been possible and a higher retention of material properties.

Finally, a cost and mass analysis was performed for replacing an aluminum seatback with an injection molded seatback (Table 1). In summary, the CF/resin material substitution can deliver weight savings at a cost add of \$1.58 per pound of mass saved. The total weight savings opportunity for the replacement components on a vehicle would be 15.92 lbs. (7.24 kg).

	SI	English
Parts per vehicle	4	4
Mass saved per part	1.81 kg	3.98 lb
Cost add per part	\$6.29	\$6.29
Mass saved per vehicle	7.24 kg	15.92 lb
Cost add per vehicle	\$25.16	\$25.16
Total vehicle cost add per unit mass saved	\$3.48/kg	\$1.58/lb

Table 1. Cost and mass analysis.

High-Performance Magnesium Alloys without Rare-Earth Elements

Project aims to put low-cost, high-strength magnesium alloys on the road.

Pacific Northwest National Laboratory

At current rates, manufacturers produce over 235,000 cars and commercial vehicles each day worldwide. In the hunt for high-strength, lightweight materials to improve fuel economy, Pacific Northwest National Laboratory (PNNL) and a Tier 1 partner are developing a new, cost-effective means of creating magnesium alloys—the lightest known structural metal.

Auto manufacturers have yet to adopt high-performance magnesium due to the necessary addition of costly rare-earth elements and the slow throughput of processing techniques used to form the alloys. Funded by the U.S. Department of Energy (DOE), the PNNL team hopes to overcome both of these challenges and open more opportunities for magnesium components in cars and trucks.

In the initial phase of the project, PNNL demonstrated magnesium alloys that can replace aluminum alloys currently used in crush tube applications and reduce the weight of these components by 20% without compromising the energy absorption capability. The necessary processing conditions to make the desired magnesium alloy was obtained by modeling and verified experimentally.

PNNL determined that shear-plane enhanced precipitate formation yielded the best properties in the magnesium alloys. The technique developed, called “Shear Assisted Processing and Extrusion” (ShAPE), uses a rotating, axially-fed ram to plasticize a small region of billet material near the extrusion orifice (Figure 1). The patent-pending ShAPE manufacturing technique is currently being developed further to build extruded components for additional testing by the auto industry (Figure 2).

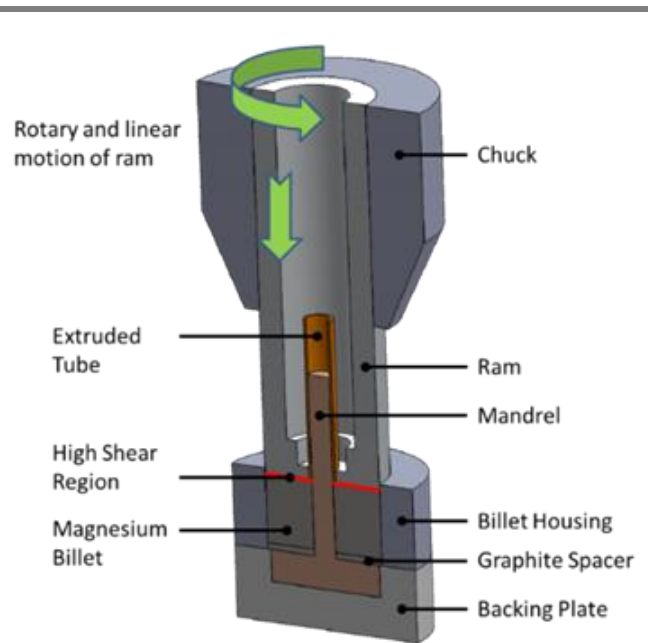


Figure 1. Novel ShAPE to form magnesium tubes.



Figure 2. A 30 cm length of ZK60 tubing extruded using the ShAPE process along with a cross section showing the 1.52 mm nominal wall thickness.

2016 U.S. DRIVE Highlight

High-Speed Joining Method Delivers Lighter Weight Automobiles, Faster

Friction stir welding technique joins aluminum sheets of dissimilar thicknesses 10 times faster than previously possible.

Pacific Northwest National Laboratory

Increasing the amount of aluminum in automobiles allows manufacturers to create lighter, more fuel efficient vehicles. A 10% reduction in weight can result in as much as a 6% to 8% increase in fuel economy. However, until recently, the inability to join sheets of dissimilar thicknesses at production speeds limited the use of aluminum in cars and trucks. As part of a U.S. Department of Energy-funded project, researchers at Pacific Northwest National Laboratory (PNNL) partnered with a U.S. automotive original equipment manufacturer, aluminum supplier, and Tier 1 supplier to develop a new, high-production friction stir welding technique.

In the past, auto manufacturers deemed friction stir welding—a solid-state joining method that uses a specialized rotating tool to weld metal together—as challenging for joining aluminum. The process was slow, especially when welding sheets of dissimilar thicknesses. The ability to join different thicknesses of aluminum enables parts like door panels to be produced more economically. Thicker gauge aluminum caused in sections requiring more strength and thinner gauges can be used elsewhere.

After developing and testing dozens of new tool designs against a variety of weld parameters, PNNL discovered a technique that increases the speed of friction stir welding from less than 1 m per minute to 10 m per minute—a 10 times boost in production speed (Figure 1). Based on the technology, a friction stir welding machine was manufactured that was capable of producing 250,000 lightweight, aluminum tailor-welded blanks per year.

Through ongoing development, PNNL seeks to further increase the speed of production and adapt the technique to curvilinear geometries (Figure 2), which would allow the joining of complex and

contoured auto parts that may not be feasible with competing techniques like laser welding. The project team is also working on developing high-speed joining of different aluminum alloys, such as joining automotive grade alloys like 5xxx to high-strength, lightweight alloys like 7xxx series typically used by the aerospace industry.

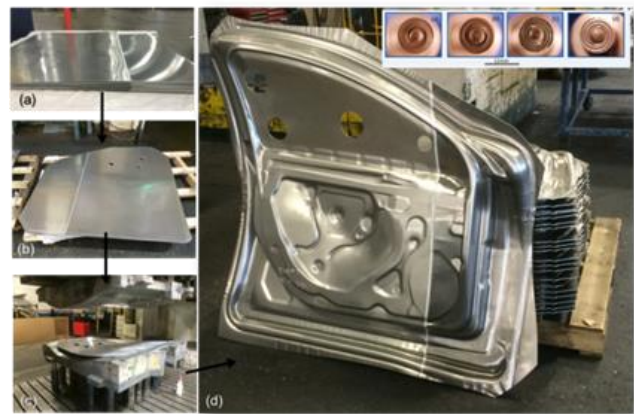


Figure 1. Production of a door using friction stir welding technique developed at PNNL: (a) welded blanks (b) welded blanks after cutting; (c) cut panels loaded for stamping; and (d) door panels after stamping.



Figure 2. Curvilinear welds made between (a) AA5182-O (1 mm-2 mm), (b) AA6022-T4 (1 mm-2 mm), and (c) AA5182-O (1 mm) to AA6022 (2 mm).

Component-Level Validation of a Third-Generation Advanced High-Strength Steel Forming Model

Formability of high-strength, exceptional ductility steel alloy designed using ICME was confirmed through physical testing.

U.S. Automotive Materials Partnership

The objective of the integrated computational materials engineering (ICME) third-generation advanced high-strength steels (3GAHSS) project is to demonstrate the applicability of an ICME approach for developing and deploying 3GAHSS. The project has both experimental and computer modeling components that cover the three primary manufacturing phases: materials by design, component fabrication, and assembly. Each of the modeling components must be calibrated and validated within 15% of experimental data.

At the component manufacturing length scale, the project developed a forming model based on a surrogate T-shaped component. The T-component was chosen for its automotive representative geometry (the lower portion of a safety-critical B-pillar); complexity of the deformation modes, such as uniaxial tensile, bending, plain strain, stretch bending, and bi-axial tension; complexity of strain paths that include linear, bilinear and non-linear; and the 200 mm wide 3GAHSS stamping blanks produced in the project.

The project designed and built a T-component die set to produce T-components for validating the forming model with respect to geometry and thickness and material models with respect to post-forming microstructure and mechanical properties. Researchers formed T-components from the baseline QP980 steel and the 3GAHSS high-strength, exceptional ductility Med. Mn (10 wt. %) steel produced in the project. Coupons for characterization were extracted from T-shaped stampings after strains were measured with digital image correlation and the retained austenite volume fraction (RAVF) was measured at Argonne National Laboratory using high energy X-ray diffraction. Coupled with other experimental work, the results of

this testing have enabled the project to validate both the material and forming models.

Figure 1a shows 10 locations from which coupons were extracted from a Med. Mn (10 wt. %) steel. The color contours denote the measured strain field. Figure 1b shows that the RAVF change depends upon deformation mode and strain path. For example, in uniaxial tension (Coupon #7) the RAVF change is 53%, but for a similar equivalent strain in bi-axial tension (Coupon #2) the retained austenite change is only 19%. The results suggest that local mechanical properties, such as ductility and strength, are dependent upon deformation mode and strain path.

These results enable the project to better predict post-forming microstructure and subsequent mechanical properties. This in turn enables optimization of the 3GAHSS lightweight component design and improved prediction of component and assembly crash performance. The project is on track and delivering excellent results.

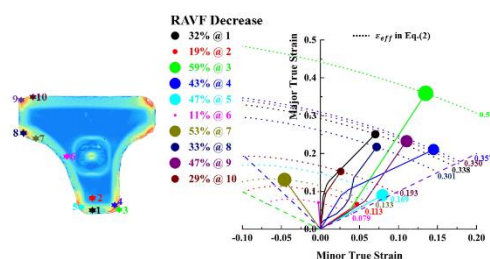


Figure 1. a) T-component and b) RAVF change versus strain.

Validation of Carbon Fiber Composite Material Models for Automotive Crash Simulation

Crash performance of lightweight carbon fiber front bumper-beam and crush-can assemblies evaluated using both experiments and simulations.

U.S. Automotive Materials Partnership

This validation project has completed the fourth year of an extensive analytical modeling and physical testing program to validate and compare constitutive models implemented in commercial crash codes and two models developed by the U.S. Automotive Materials Partnership's (USAMP) Automotive Composites Consortium in partnership with two U.S. academic institutions. Models include a meso-scale representative unit cell (RUC) model and a micro-plane RUC model. The project team is comprised of researchers from USAMP's original equipment manufacturer (OEM) members and academia, plus representatives from materials suppliers and composites' manufacturers, materials and crash testing facilities, and engineering design and computer-aided engineering (CAE) suppliers.

The project's goal is to validate material models for automotive carbon fiber composites for crash applications. The team chose a front bumper-beam and crush-can (FBCC) subassembly application to validate the material models by developing a composite FBCC that can be shown to absorb impact energy equivalent to a baseline steel FBCC under various crash modes, and then compared its actual performance to CAE simulations.

During year four (fiscal year (FY) 2016), the Validation of Material Models (VMM) project team completed all computational predictions for the composite FBCC using commercial crash codes (including multi-scale), and predictions using the ACC models. In tandem, the team manufactured the composite components from co-molded epoxy/carbon-fiber prepreg and chopped carbon fiber sheet molding compound, then used adhesive bonding to produce the final assemblies for testing (Figure 1). The FBCCs were tested in six crash modes (full frontal, frontal offset, frontal pole, angular, low-speed mid-point, and low-speed quarter). The VMM

team conducted a preliminary comparison of the experimental test results and computational predictions, and identified technology gaps that led to discrepancies between the data sets. This analysis will be finalized during the final year of the project in FY 2017. Non-destructive evaluations supported the post-fabrication and post-crash evaluations of FBCCs by providing ultrasonic scans, radiographic images, and computer tomography scans to identify areas of interest (Figure 2).

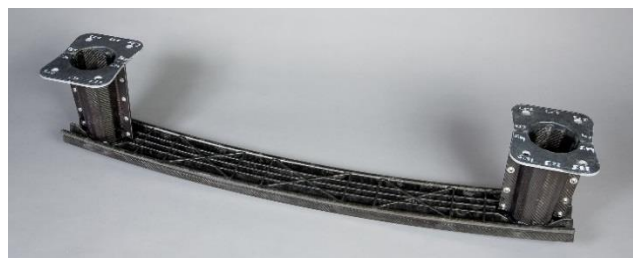


Figure 1. Carbon fiber FBCC, made from two compression-molded crush cans and a thermoset carbon fiber bumper beam with fabric C-channel and carbon sheet molding compound ribs.

The team began assessing thermoplastic crush cans made of nylon/carbon-fiber composite laminates that were also manufactured and evaluated as alternative material. Two types of carbon fibers were evaluated, including conventional carbon fibers and low-cost carbon fibers developed by Oak Ridge National Laboratory. Crash testing of these crush cans will be completed in FY 2017 and will be compared to the original thermoset FBCC crush can and steel FBCC designs.

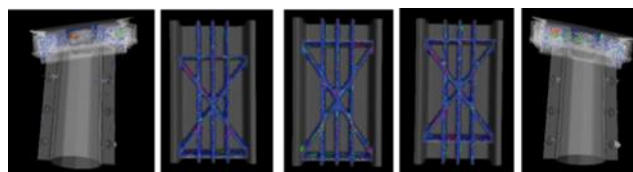


Figure 2. Non-destructive computer tomography imaging of a front-bumper/crush-can assembly showing four individual sections with superimposed porosity analysis shown in color.

Vehicle Systems Analysis



Impact of Connectivity and Automation on Vehicle Energy use

Vehicle connectivity and automation reduce vehicle energy use for a wide range of powertrains through smoother acceleration and braking and fewer stops, while enabling higher average vehicle speed.

Argonne National Laboratory

Connected and automated vehicles (CAVs) have the potential to significantly impact the transportation system. Knowledge of the environment (e.g., traffic signal timing, movement of other vehicles, etc.) will allow individual vehicles to accelerate and brake more smoothly, stop less often, and move at faster speeds, resulting in overall improvements to traffic flows. At the same time, the powertrain mix of the U.S. vehicle fleet is changing due to regulatory requirements and customer demands, which may result in increased levels of electrification.

This study's objective is to quantify the energy impact of connectivity and automation for different vehicle trip profiles considering multiple powertrain configurations ranging from conventional combustion-engine vehicles, to hybrid electric vehicles (HEVs) and battery electric vehicles (BEVs).

Using *Autonomie*, a state-of-the-art vehicle simulation software tool, a reference energy consumption value is calculated for constant, steady-state speeds to estimate an ideal state reached by the highest achievable connectivity degree. Real-world driving cycles (RWDCs) are then selected from the National Renewable Energy Laboratory database of recorded global positioning system (GPS) traces in the Chicago area to represent average driving styles. The original speed profiles are then mathematically transformed to represent the impact of varying degrees of connectivity: some stops are removed, speed is smoothed, and strong accelerations are limited. An overall increase in speed is also investigated to represent improved traffic flow. In each case, the driving distance is held constant to represent the same origin and destination.

For all the vehicles simulated, the results in Figure 1 demonstrate that connectivity leads to significant

reduction in fuel consumption. The reduction is higher at low speed than at high speed: fuel consumption is reduced between 10% and 30% at low speed depending on the degree of connectivity.

At the highest degree of connectivity achievable, BEVs have greater potential benefits than HEVs and conventional vehicles, as fuel consumption of BEVs can be reduced by 50%, by 40% for HEVs, and by 35% for conventional vehicles.

Future work will focus on identifying the impact of specific technologies such as eco-signal and platooning on the vehicle trip profiles and the resulting energy consumption reductions for different powertrain configurations.

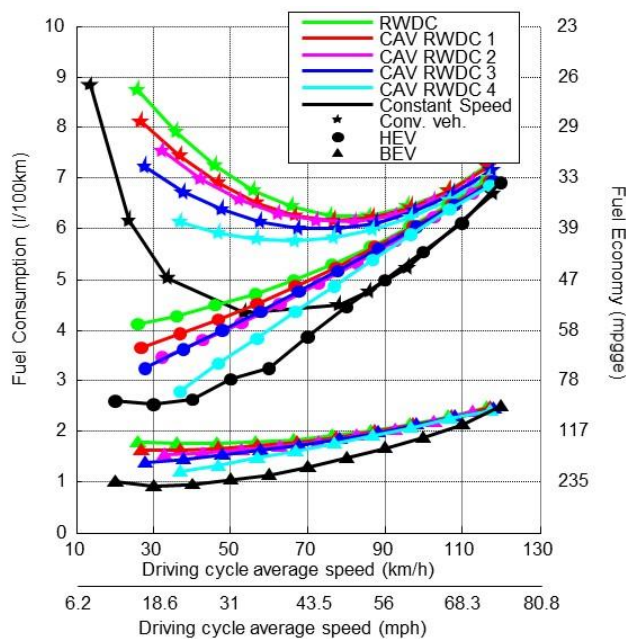


Figure 1. Impact of connectivity and automation on fuel consumption over multiple powertrains.

Analyzing Real-World Vehicle Efficiency

Evaluation underscores the importance of non-dynamometer effects on real-world fuel economy, and validates the National Renewable Energy Laboratory's real-world vehicle efficiency modeling approach.

National Renewable Energy Laboratory

It is well understood that “your mileage will vary” based on where and how a vehicle is driven. On-road testing that the National Renewable Energy Laboratory (NREL) conducted in collaboration with Argonne National Laboratory using a highly instrumented vehicle underscored the wide trip-to-trip fuel economy variations that occur in real-world driving. NREL has developed a methodology for modeling and rapidly simulating a vehicle’s fuel economy over wide-ranging real-world conditions, and the on-road test data has helped refine and validate the modeling approach (Figure 1).

The on-road testing included data collection from roughly sea level up to the Colorado mountains. One refinement revealed from comparing the data to initial modeling runs is that implementing air density as a variable parameter that depends on driving location, rather than a constant value as typically assumed for fuel economy modeling, allows for more accurate real-world fuel use estimation. This research showed that incorporating altitude together with road grade and weather effects can

improve real-world fuel economy modeling accuracy by over 10%.

An important application for NREL’s real-world fuel economy analytical methodology is objectively estimating the benefits of “off-cycle” technologies (those that provide greater on-road benefits than laboratory testing on standard test cycles can measure). The methodology can model a particular vehicle with and without a given technology enabled, and capture the varying benefits that the technology provides in different driving situations. Weighting the fuel economy results in different driving situations by the total amount of driving that occurs in each produces a national-level benefit estimate. Relevant technologies to which the analytical methodology can be applied include thermal management advancements that optimize the temperature of lubricants via active heating or thermal retention, and connected or automated vehicle technologies that can modify a vehicle’s operating profile.

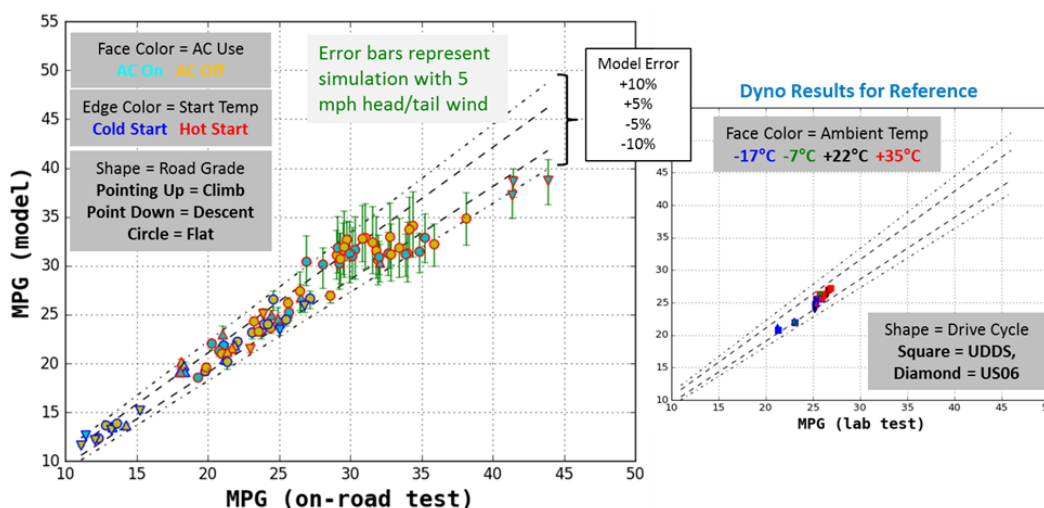


Figure 1. Testing shows much wider variation in real-world versus standard cycle fuel economy, but a simplified model trained on lab data is able to accurately predict real-world fuel use over a variety of driving conditions.

CROSSCUTTING

Codes and Standards



New Hydrogen Risk Assessment Model Toolkit Quantifies Hydrogen Risk for Global Code Development

Software package brings scientific rigor to support safety assessment for hydrogen infrastructure.

Sandia National Laboratories

In 2016, Sandia National Laboratories (SNL) released the HyRAM (Hydrogen Risk Assessment Models) software tool that integrates state-of-the-art models and data to quantify risks of accident scenarios, predict physical effects, and characterize hydrogen hazards (Figure 1). This quantitative risk assessment tool is a critical enabler for code committees as they pursue data-driven decisions to provide an objective basis for code requirements. Lack of information can be a barrier to the deployment of codes and standards resulting in a delay in hydrogen commercialization.

HyRAM formalizes the tools, data, and methods relevant to assessing hydrogen safety, risk, and consequence through risk assessment algorithms and physical models. It includes a documented quantitative risk assessment (QRA) approach with generic probabilities for equipment failures, including component leak frequencies and ignition probability (probabilities can be modified by users). HyRAM also contains computationally and experimentally validated models of hydrogen release and flame physics, including fast-running models of high-pressure hydrogen releases, jet flames, and accumulation and deflagration within enclosures causing overpressures for deterministic assessment of hydrogen hazards.

HyRAM was initially developed to enable SNL's Hydrogen Program to meet program goals, including providing science-based hydrogen safety distances and supporting harmonization of U.S. and international safety standards. In 2016, SNL packaged HyRAM for public release, making the prototype version available to stakeholders for free. By the end of 2016, HyRAM had been downloaded in 24 countries. HyRAM can be obtained at <http://hyram.sandia.gov>.

HyRAM is already having a direct impact on code development. For example, HyRAM models have been employed in assessing safety distances and indoor fueling requirements in the National Fire Protection Association's NFPA 2 *Hydrogen Technologies Code*. HyRAM has also been used to provide a harmonized, scientific approach to calculating and comparing region-specific safety distances within International Organization for Standardization's recent draft standard, 19880-1. Ongoing code development activities plan to utilize HyRAM to ensure code requirements are consistent, logical, and defensible.

The HyRAM toolkit has changed the way the hydrogen safety community approaches risk assessment by providing a rigorous tool that can be used early in the development stage to assess hydrogen failure mechanisms for consideration in the design and code requirements.

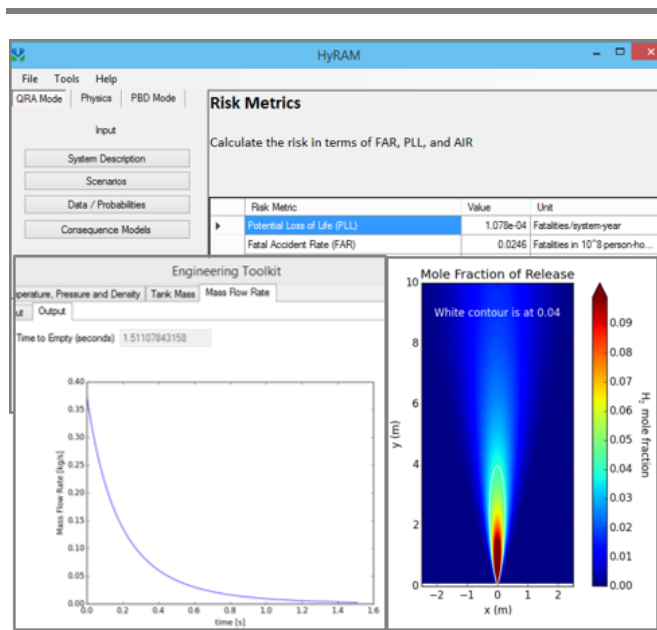


Figure 1. Output from the HyRAM tool supports code committees as they define safety.

Grid Interaction



Adapter Enables Smart Networked Charging for Electric Vehicles

Recently-developed smart charge adapter compatible with SAE J1772™-compliant connectors adds intelligent link to charging equipment and plug-in electric vehicles.

Argonne National Laboratory

Plug-in electric vehicles (PEVs) offer consumers the promise of long-term fuel cost savings, but concerns over when and how long it takes to charge PEVs remain an obstacle to their widespread adoption. Smart charging addresses these concerns by minimizing electricity costs and optimizing charging time. The trouble is that many existing PEVs and conventional electric vehicle supply equipment (EVSE) do not include such smart charging capabilities. The smart charge adapter (SCA) developed by Argonne National Laboratory (ANL) solves this problem by converting any legacy SAE J1772™ compatible, alternating current, Level 1 or Level 2 EVSE into a smart charging networked station. The SCA can also be used with existing networked EVSEs, allowing PEV drivers to choose network providers.

Figure 1 shows the white SCA prototype is a handheld, inline device that connects any PEV-EVSE combination. The SCA has a male and female SAE J1772™ coupler at either end for connecting the female with the EVSE and the male to the PEV. These two couplers make smart charging possible. A licensed electrician is not required for installation. The SCA also includes a processor, power delivery electronics, communications, an electric meter, and payment transaction controls.



Figure 1. Alpha prototype of SCA.

The SCA enables submetering, access control, billing, charging scheduling, and load control. The built-in electric meter meets the accuracy and other requirements of electric utilities to qualify as a revenue grade meter. The SCA enables start and stop, as well as increasing or decreasing any charge session seamlessly. Communications carried out through Wi-Fi networking permit SCA parameters to be displayed externally. Among the possible display modes are Communications and Monitoring, Manual Load Control, and Automated Load Following. Figure 2 shows the SCA Manual Load Control display.

In 2017, ANL will fabricate, test, and validate 30 alpha prototypes through pilot programs with commercial partners. The U.S. Patent and Trademark Office awarded ANL a patent for this invention (publication application #20160144728). The international patent application is still pending.

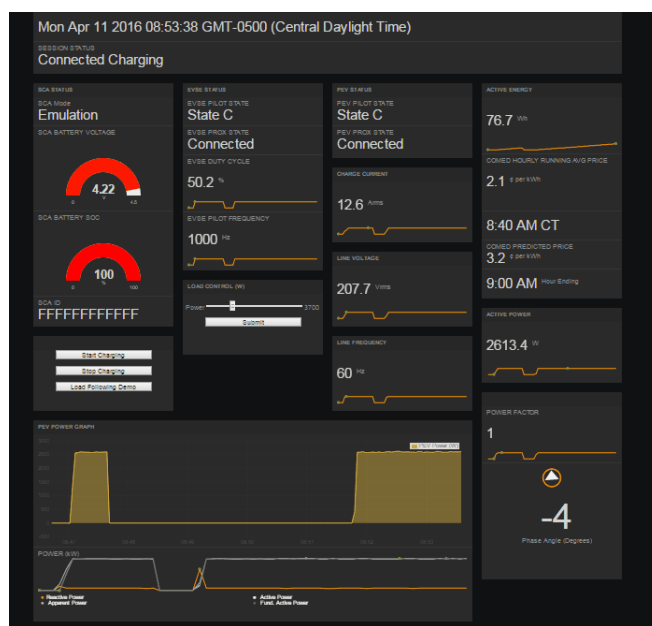


Figure 2. SCA external display for Manual Load Control.

Testing Validated the Interoperability and Performance Requirements of SAE J2954™ Codes and Standards

Testing of wireless power transfer systems provides detailed interoperable performance results to support and validate wireless power transfer codes and standards development and harmonization.

Idaho National Laboratory

Idaho National Laboratory (INL) collaborated with the SAE J2954™ committee, four vehicle manufacturers, and two wireless power transfer (WPT) system manufacturers through the testing of 22 combinations of WPT systems designed for electric vehicles (EV). The scope of the testing focused on determining interoperability performance and functionality, which directly supports the development and harmonization of WPT codes and standards. Standardization will help to ensure the interoperability of WPT systems and therefore prevent the undesirable multi-standard conundrum plaguing other EV charging formats, such as direct-current fast-charging. Multiple standards have led to EV owner confusion, frustration, and dissatisfaction. Additionally, robust codes and standards reduce the overall system cost by alleviating the need for the WPT systems to be built with multiple formats.

The collaborative companies in this testing effort include Daimler, Jaguar Land Rover, Nissan, Qualcomm, Toyota, and Witricity. The collaborative teams provided state-of-the-art WPT systems and collaborated in testing that spanned a wide range of test parameters, including coil misalignment, coil to coil gap, output battery voltage, primary and secondary coil control, and charge power level.

INL tested and evaluated the WPT system combinations using a standardized test apparatus, which enables the entire WPT system to be operated off-board a vehicle, as shown in Figure 1. The test apparatus accurately positions both of the WPT coils as well as absorbs the electrical output power via a battery emulator. The test apparatus incorporates a thin steel sheet to mimic a typical vehicle chassis undercarriage in which the vehicle-side coil is attached, and a thin aluminum sheet used to shield

the steel vehicle chassis from interacting with the electromagnetic field from the WPT charger.

High-accuracy laboratory equipment measured and recorded the charge efficiency, electrical power quality, and electromagnetic field strength outside of the primary to secondary coil energy transfer field. Sophisticated software controlled the test process as well as recorded the data from testing.

Testing results validated the interoperable functionality and system performance from the WPT primary and secondary coil combinations across the wide range of test conditions. Several lessons learned and recommendations were provided to the committee. The 4,500 test points will provide the SAE J2954™ committee with solid results to base decisions for the standardization of a reference coil design in which future designs will be certified for interoperable functionality in order to be considered SAE J2954™ compliant.



Figure 1. INL's test apparatus enables interoperable performance testing of WPT systems off-board the vehicle. Testing conducted by INL provides detailed results to support the development and harmonization of WPT codes and standards

Hydrogen Storage



First Demonstration of Multiple Hydrogen Molecules Adsorbed on a Metal Site in a Metal-Organic Framework

New material overcomes a long-standing challenge for efficient, onboard storage of hydrogen using adsorbents.

Lawrence Berkeley National Laboratory; University of California, Berkeley; and the National Institute of Standards and Technology

For the first time, the simultaneous binding of two hydrogen (H_2) gas molecules to a single metal site was demonstrated in a metal-organic framework (MOF), opening the door to significantly enhanced H_2 adsorption capacity and increased fuel cell electric vehicle driving range at a lower cost. These metal sites are referred to as coordinatively-unsaturated metal centers, and are known to be among the strongest binding sites for H_2 molecules in adsorbents such as MOFs. Stronger affinity for H_2 molecules is highly desirable as it enables higher capacity H_2 storage systems that can operate under more realistic operating conditions (lower pressure and higher temperatures). Consequently, a major goal of adsorption-based H_2 storage material research has been to increase both the density of these metal sites and the number of H_2 molecules adsorbed per site.

This breakthrough, achieved by researchers at Lawrence Berkeley National Laboratory, was observed using a MOF material, which is a compound consisting of metal clusters coordinated to organic ligands to form highly porous structures with tunable pore sizes. The specific MOF synthesized, $Mn_2(dsbdc)$, contains manganese (Mn) cations in two separate coordination environments. One of these is attached to two solvent molecules which can be thermally removed, leaving behind space for two H_2 molecules to bind simultaneously (Figure 1).

Confirmation that multiple H_2 molecules were adsorbing to the Mn sites was provided by in-situ neutron powder diffraction, carried out at the National Institute of Standards and Technology Center for Neutron Research. Loadings of deuterium (D_2) molecules were used as a proxy for H_2 to exploit

the higher scattering cross section of D_2 compared to H_2 . As shown in Figure 1, the interaction of two D_2 molecules with a single Mn site is clearly observed at adjacent locations on the four-coordinate Mn cation. While the binding strength of H_2 in this material is modest compared to other MOFs, this result provides an important proof of concept for designing adsorption-based H_2 storage materials with significantly enhanced H_2 capacity. Current work is aimed at extending this chemistry to materials that can bind more than two molecules per metal site, which modeling has shown to have the potential to yield materials that could meet the U.S. Department of Energy's 2020 H_2 storage system targets of 5.5 wt.% and 40 g/L H_2 .

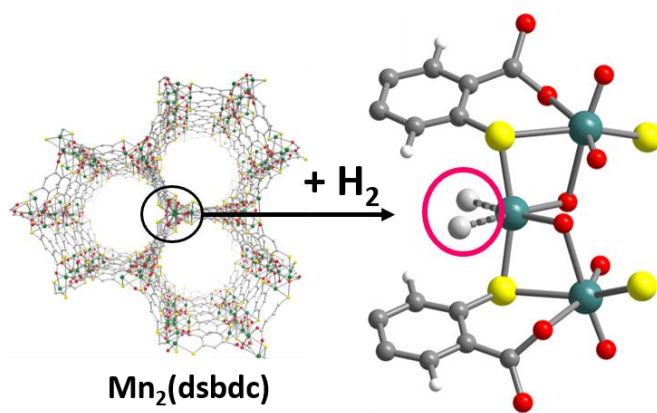


Figure 1. Illustration of multiple H_2 molecules bound to a single metal site. A portion of the $Mn_2(dsbdc)$ crystal structure shown on the left is zoomed in on the right showing where the two H_2 molecules are bound. Blue-green, yellow, red, gray and small white spheres represent Mn, sulfur, oxygen, carbon, and H_2 atoms respectively. The H_2 molecules bound at the open metal site are shown as larger white spheres inside the pink circle.

Hydrogen Materials—Advanced Research Consortium Supports New Storage Materials Discovery

The new Hydrogen Materials—Advanced Research Consortium accelerates development of onboard hydrogen storage materials to meet U.S. DRIVE's 2020 targets.

Sandia, Lawrence Livermore, and Lawrence Berkeley National Laboratories

In order to accelerate the discovery of breakthrough hydrogen storage materials, the U.S. Department of Energy (DOE) initiated the Hydrogen Materials—Advanced Research Consortium (HyMARC) as part of the Energy Materials Network in late 2015. The consortium is comprised of a core team of researchers at Sandia (lead), Lawrence Livermore, and Lawrence Berkeley National Laboratories. Through a highly coordinated combination of experimental and theoretical studies, HyMARC will elucidate fundamental understanding of key phenomena governing the thermodynamics and kinetics that have been impeding the development of hydrogen storage materials for transportation applications. HyMARC will offer a conduit to provide this foundational knowledge and key national laboratory resources to the hydrogen storage research community.

DOE-supported projects including the past material Centers of Excellence collectively synthesized and characterized hundreds of onboard storage material candidates. Many materials developed can meet a portion of DOE's targets, but progress towards identifying materials able to meet all of the targets simultaneously continues to be hindered by a lack of fundamental understanding of the physical and chemical processes governing the interaction of hydrogen with storage materials.

HyMARC's scientific activities aim to close this gap by focusing on the critical properties of storage materials, including mass transport, surface chemistry, and processes at solid-solid interfaces (Figure 1). It will leverage recent advances in predictive multi-scale modeling, high-resolution spectroscopic/structural in-situ characterization, and material synthesis techniques that were previously unavailable. These integrated and focused efforts will enhance development of all

classes of advanced hydrogen storage materials, including sorbents, metal hydrides, and liquid carriers.

The HyMARC core team will provide guidance and resources to other DOE hydrogen storage projects in the future to accelerate research. These separate material discovery projects, five of which were already selected separately by DOE, will benefit from close collaboration and access to unique capabilities within HyMARC. In addition, these projects will feed information into the core team's multi-scale modeling efforts.

In parallel, existing characterization and validation capabilities were consolidated into the Hydrogen Storage Characterization Optimization Research Effort. This team, led by the National Renewable Energy Laboratory along with Lawrence Berkeley and Pacific Northwest National Laboratories, and the National Institute of Standards and Technology, provides unique characterization techniques including neutron scattering, nuclear magnetic resonance, and electron microscopic techniques to supplement HyMARC's capabilities.

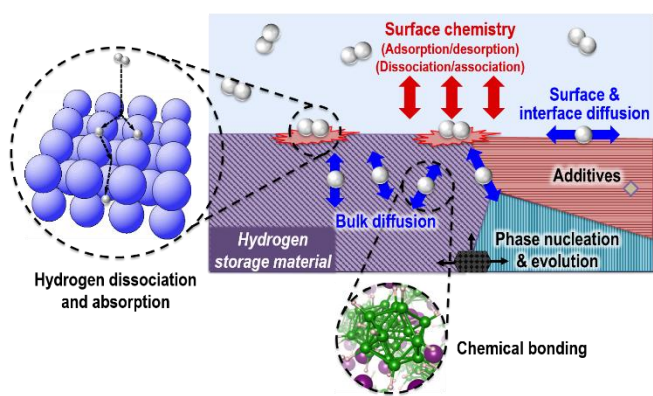


Figure 1. Illustration of various processes occurring during uptake and release of hydrogen by storage materials that influence material development.

Integrated Systems Analysis



Cradle-to-Grave Greenhouse Gas Emissions and Economic Assessment of U.S. Light-Duty Vehicle Technologies

A lifecycle analysis of current and future vehicle-fuel technology pathways.

Cradle-to-Grave Workgroup

The Cradle-to-Grave (C2G) Workgroup within the U.S. DRIVE Partnership completed a comprehensive lifecycle analysis, or C2G analysis, of the cost and greenhouse gas (GHG) emissions of a variety of vehicle-fuel pathways, as well as the levelized cost of driving and cost of avoided GHG emissions. The C2G study also evaluated the technology readiness levels of key fuel and vehicle technologies along various pathways. The C2G analysis spanned a full portfolio of midsize light-duty vehicles (LDVs), including conventional internal combustion engine, hybrid electric, plug-in electric, and fuel cell electric vehicles. In evaluating the vehicle-fuel combinations, the C2G study considered both CURRENT TECHNOLOGY (2015, low-volume and high-volume) cases and FUTURE TECHNOLOGY (2025-2030, high-volume) cases.

The selected fuel pathways were constrained to those deemed to be scalable to at least 10% of LDV fleet demand in the future. The C2G study strictly focused on possible vehicle-fuel combination pathways (i.e., no market scenario analysis was conducted). The C2G study is noteworthy in vetting its analysis through a broad set of major stakeholders in government, industry, and national laboratories. The study results were documented in a report¹ that was released in June 2016. Since its release, the report has been downloaded over 2,000 times.

The C2G greenhouse gas emissions evaluation was carried out by expanding and modifying Argonne National Laboratory's (ANL) GREET[®] model suite,² with inputs from industrial experts (Figure 1). The modeling of various vehicle technologies to estimate their cost and fuel economy was performed with the Autonomie model (also developed by ANL).

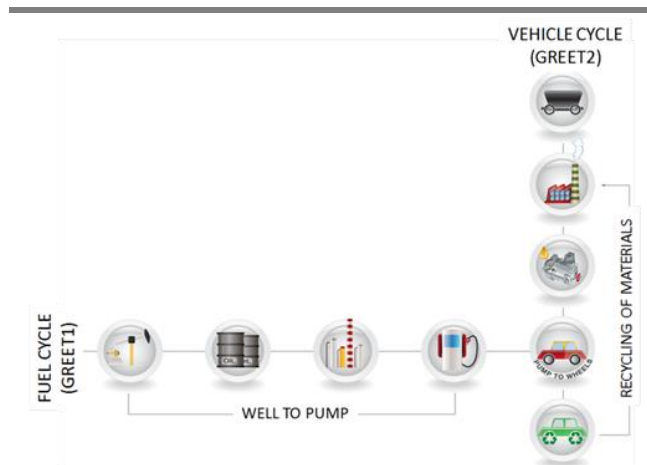


Figure 1. Scope of cradle-to-grave assessment.

The study estimated vehicle cycle emissions at approximately 8-12 tonnes carbon dioxide equivalent (CO₂e) for CURRENT TECHNOLOGY cases and 6-9 tonnes CO₂e for FUTURE TECHNOLOGY cases. Levelized costs of driving for high volume cases (~500,000 vehicles/year) were determined to be in the range \$0.20 to \$0.60/mi depending on technology, with vehicle cost being the major (60% to 90%) contribution and fuel cost a minor (10% to 40%) contribution. CURRENT TECHNOLOGY high-volume GHG emissions abatement costs were in the range of \$100s to \$1,000s per tonne CO₂e compared to a conventional gasoline vehicle baseline, whereas FUTURE TECHNOLOGY high-volume GHG abatement costs were in the range of \$100-\$500 per tonne CO₂e. The C2G study report noted that the cost of avoided emissions metric has limitations because the technologies considered in the analysis differed also in other important attributes, such as local air quality related emissions, reliance on different fuels, and vehicle functionality.

¹ <https://greet.es.anl.gov/publication-c2g-2016-report>.

² <https://greet.es.anl.gov/>.

FUELS

Hydrogen Delivery



World Record for Magnetocaloric Gas Liquefaction

Game-changing technology shows strong promise for efficient hydrogen liquefaction.

Pacific Northwest National Laboratory, Emerald Energy NW, LLC, and AMES Laboratory

Pacific Northwest National Laboratory (PNNL), together with Emerald Energy NW, LLC, and Ames Laboratory, conducted a groundbreaking demonstration of propane gas liquefaction from room temperature using only magnetocaloric materials, a process that is projected to be more than 40% more efficient than conventional liquefaction when applied to hydrogen (H₂) gas. Conventional H₂ liquefaction processes consume about 10-15 kWh/kg of H₂, which accounts for over 20% of the cost of liquefaction and has little room for improvement. While liquid tankers are one of the most economic methods of transporting H₂ over long distances, an increase in their use to meet future demand will be restricted by the high cost of liquefaction. Commercial liquefaction today implements the Claude cycle, a mature process that relies on repeated compression and expansion steps to cool heat transfer fluid that is then used to liquefy the gas. These steps generate inefficiencies that PNNL's liquefaction process is able to avoid.

In PNNL's new approach, "magnetocaloric" materials absorb heat in the presence of a magnetic field and cool down when removed from the magnetic field (Figure 1). This heat exchange characteristic can be used to cool heat transfer fluid that can subsequently be used to cool or liquefy a gas, eliminating the need to use the Claude cycle. In PNNL's design, magnetocaloric materials are layered in vessels known as active magnetic regenerators (AMRs). Heat transfer fluid is passed through the AMRs while they are cycled in and out of magnetic fields. In 2016, PNNL used two integrated AMRs to cool magnetocaloric materials by 100°C using magnets alone. This temperature span set a world record, and the system was then used to liquefy propane gas from room temperature using only magnetocaloric materials.

In 2017, PNNL will further improve the efficiency of this magnetocaloric liquefaction by implementing a "bypass," a design upgrade of AMRs that has also never been demonstrated to date. The "bypass" concept leverages an inherent property of magnetocaloric materials, wherein their ability to absorb heat changes below certain temperatures (i.e., the "Curie temperature") and with a change in the magnetic field. Due to this property, the AMR is able to cool more heat transfer fluid than necessary when it is removed from the magnetic field. This excess fluid can then be used to pre-cool incoming gas, i.e., "by-passed," thus improving system efficiency. PNNL projects that the bypass will reduce the amount of magnetocaloric material needed to ultimately liquefy H₂ by up to 88%.

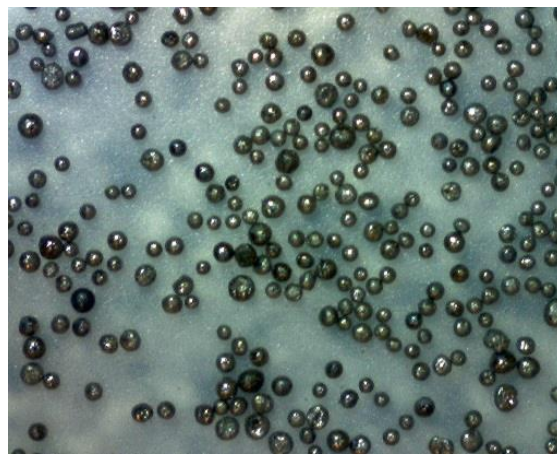


Figure 1. Spherical magnetocaloric particles (dia. ~200 μm) being used in PNNL's liquefier.

In 2018, PNNL will develop the third generation of their liquefaction system, which will implement the bypass configuration described above, along with 14 different magnetocaloric materials synthesized by Ames Laboratory. PNNL's GEN-III system will ultimately be used to liquefy H₂ gas from room temperature with an expected efficiency of 5-6 kWh/kg.

New Hydrogen Station Equipment Performance Device

Expedited commission of new hydrogen fueling stations by decreasing testing from months to one week.

Sandia National Laboratories, National Renewable Energy Laboratory, and PowerTech Labs

Cars powered by hydrogen (H₂) fuel cells are hitting the streets, but where are they getting their H₂ fuel? One of the greatest barriers to widespread acceptance of H₂ fuel cell cars is the availability of H₂ fueling stations. A challenge station developers currently face when opening an H₂ fuel station is the time it takes for the station to be accepted by auto manufacturers for dispensing into their fuel cell vehicles. Traditionally, each fuel cell vehicle manufacturer would test the station independently to ensure that it complied with the SAE J2601™ fueling protocol currently accepted by industry, SAE J2601. This testing could take months to complete, almost as much time as station construction. The Hydrogen Station Equipment Performance (HyStEP) device was developed to enable H₂ fueling station developers to perform these tests themselves, and thereby greatly expedite performance characterization. HyStEP was designed and built through a collaboration between the National Renewable Energy Laboratory (NREL), Sandia National Laboratories, and PowerTech Labs, with funding from the U.S. Department of Energy's Fuel Cell Technologies Office under the H2FIRST project.

HyStEP performs station tests defined in the CSA HGV 4.3 standard in one week. These tests characterize a station's ability to fill fuel cell vehicles in 3-5 minutes, per the SAE J2601 protocol. Parameters measured include fault detection, leak detection, infrared communications, and the temperatures, pressures, and flow rates of fueling both with and without communications between the dispenser and a vehicle tank. The device is mounted on a trailer so it is protected from weather and can be transported easily from one station to the next.

The HyStEP device includes three Type IV 70 MPa tanks that are capable of storing 9 kg of H₂ and are instrumented with pressure and temperature sensors. HyStEP uses an Infrared Data Association communications system to simulate a vehicle's communication with a dispenser, and a valve that simulates a leak in the vehicle or dispenser. Sensors record ambient temperatures that guide the pressure throughout a fill. Because most H₂ fueling stations today are equipped with nozzles for 350 bar and 700 bar fueling, HyStEP can perform tests at both pressures. The team validated HyStEP performance at NREL's Energy Systems Integration Facility in Golden, Colorado.

Subsequent to NREL's validation (see Figure 1), HyStEP has been used in the commissioning of multiple stations in California. Operators from the California Air Resources Board and Division of Measurement Standards have been trained to operate the device so it can be used for future H₂ fueling stations and all of its design documentation is publicly available. More information can be found at: <https://h2tools.org/h2first/HyStEP>.



Figure 1. NREL researcher Chris Ainscough prepares HyStEP for testing at NREL's Energy Systems Integration Lab. (Photo by Dennis Schroeder/NREL.)

ASME Certification for Low-Cost 875 Bar Hydrogen Storage

Innovative design and manufacturing technologies to reduce the cost of high-pressure storage vessels at hydrogen fueling stations by more than 30%.

WireTough Cylinders, LLC

WireTough, a small business in Virginia, has developed 875-bar hydrogen storage vessels that are expected to cost at least 30% less than the 2011 baseline and at least 50% less than those currently on the market. In 2016, WireTough's vessel design received a U3 stamp from the American Society of Mechanical Engineers (ASME), certifying their compliance with the ASME Boiler and Pressure Vessel (BPV) Code, Division 3. The ASME BPV Code is now adopted by all U.S. states in part or entirety, making compliance essential for a stationary pressure vessel to be installed and used at a hydrogen fueling station.

The U.S. Department of Energy's Fuel Cell Technologies Office began funding WireTough to develop low-cost high-pressure hydrogen storage in 2014. High-pressure gaseous storage is used at most fueling stations for fuel cell vehicles worldwide, regardless of whether the station is supplied by liquid or gaseous hydrogen. Today, high-pressure stationary hydrogen storage vessels cost about \$2,170 per kg of vessel capacity for a 16 kg vessel, sometimes accounting for over 10% of station capital cost. The development of low-cost vessel manufacturing technologies and broadening the very limited U.S. supplier base is therefore necessary to reduce the cost of hydrogen fuel.

WireTough's manufacturing process relies on using commercially available steel liners that are then overwrapped with ultra-high-strength steel wires to increase their pressure capability. WireTough currently uses this technique commercially to manufacture pressure vessels for compressed natural gas for pressures up to 300 bar, and developed the manufacturing process to build 875-bar hydrogen vessels. After wire wrapping, the steel liners are subject to a process known as "autofrettage," wherein high pressures are used to

generate permanent compressive stresses on the inside surface of the liners. These stresses decrease the tensile hoop stresses experienced by the liner when it is filled with pressurized gas, and thereby increase the tank's life. WireTough adapted this process for high-pressure hydrogen storage vessels through a combination of mechanical modeling and experimentation. Their design has been developed to account for the impacts of hydrogen embrittlement, vessel thickness, autofrettage pressure, and wire-wrap configuration on vessel performance. The life of their 875 bar hydrogen vessel at a fueling station is estimated at up to 30 years.

WireTough has manufactured two prototype vessels to date, and will manufacture one full-size 34-kg, 875-bar vessel in 2017, demonstrating the scalability of their design for commercial applications.

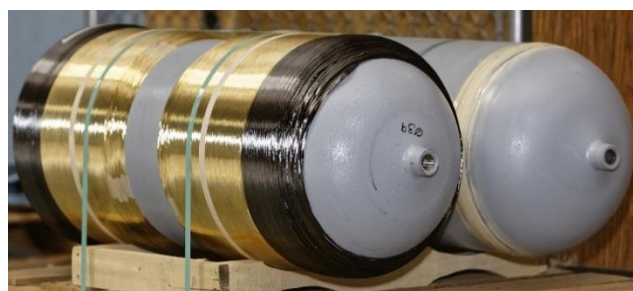


Figure 1. Wire-wrapped vessel for 875-bar hydrogen storage.

In addition to lowering storage costs, a secondary benefit of this project has been innovative research in the basic science of hydrogen embrittlement. In collaboration with Oak Ridge National Laboratory, Sandia National Laboratories, and other members of industry and academia, WireTough has studied the impact of cyclic compressive stresses on hydrogen assisted cracking. Researchers have presented their work at prestigious technical conferences, such as the 2016 International Hydrogen Conference, and will publish in technical journals.

Hydrogen Production



Economic Hydrogen Production Demonstrated Using a New Reformer-Electrolyzer-Purifier Technology

A commercial molten carbonate fuel cell stack operated in reverse as a reformer-electrolyzer-purifier generated more than 100 kg/day of hydrogen from natural gas and steam while removing carbon dioxide.

FuelCell Energy, Inc.

FuelCell Energy, Inc. (FCE) demonstrated an innovative hybrid reformer-electrolyzer-purifier (REP) technology for distributed production of low-cost hydrogen (H₂) with low greenhouse gas emissions. The new technology utilizes FCE's standard production molten carbonate fuel cell stack (MCFC/DFC[®]) operated in reverse in electrolysis mode. This process generates H₂ from both natural gas reforming and high-temperature electrolysis while simultaneously removing carbon dioxide (CO₂) from the H₂ product. The gas stream exiting the REP stack is 98% H₂ compared to less than 60% H₂ from conventional natural gas reforming (before water-gas-shift). The remaining gases (CO₂, carbon monoxide (CO), and methane (CH₄)) can be removed in a subsequent purification-plus-compression step to produce high-purity H₂ suitable for refueling fuel cell electric vehicles (FCEVs) or other fuel cell applications.

FCE successfully tested the REP technology in a nominal 100 kg/day H₂ production module (approximately equal to the refueling demand of 20 FCEVs). The module consisted of 30 production MCFC/DFC[®] cells demonstrating that standard MCFC/DFC[®] units can operate in the REP mode without the need to modify the cell/stack materials or architecture. The module (see Figure 1) demonstrated a production rate of 110 kg/H₂ per day at 97.5% purity. With CO₂-free power for electrolysis, the GHG emissions are 4,700 g CO₂/kg H₂, which is more than 50% lower than conventional steam CH₄ reforming. FCE projected up to five years of stack life based on an initial 4,000-hour test of a single REP cell; additional studies are needed to confirm and improve the granularity of this estimate.

FCE integrated the single cell with a methanizer and an electrochemical hydrogen compressor (EHC).

The methanizer converts CO and CO₂ in the reformed gas to CH₄, which can be recycled back to the REP feed. The EHC separates and compresses the H₂ producing 99.9+% purity H₂ at ~50 bar.

Strategic Analysis Inc., using H₂A analysis tools, projected an H₂ cost of \$3.10/kg H₂ for a standalone REP system operating on natural gas and grid electricity. This cost estimate includes pressure swing absorption and compressor components to bring the H₂ product to the standard H₂A conditions of 99.999% purity and 300 psi.

The REP technology is a flexible platform. FCE has identified a number of configurations that integrate REP with other processes, feedstocks (including biofuels), and power sources. As an example, a scenario for integrating REP with FCE's commercial MCFC system is projected to decrease the H₂ production cost to \$2.58/kg H₂.

FCE has successfully demonstrated this innovative and impactful technology on a commercially relevant scale, offering a promising pathway to produce low cost H₂ from a readily available domestic fuel with reduced CO₂ emissions.



Figure 1. Relative size of FCE's production MCFC/DFC[®] cell and stack capable of 2,000 kg H₂/day operation and sub-scale test cell and 100 kg H₂/day stack used in the project.

16% Efficient Direct Solar-to-Hydrogen Conversion Sets New World Record

High-efficiency semiconductors exceeded the previous world record by 33% for solar to hydrogen efficiency in photoelectrochemical water splitting—a step toward renewable economic hydrogen production.

National Renewable Energy Laboratory

The National Renewable Energy Laboratory (NREL) recently broke an 18-year-old world record for stand-alone photoelectrochemical (PEC) water splitting by demonstrating a 16% efficient cell, significantly exceeding the previous record of 12%.¹ PEC materials are specialized semiconductors that have the ability to convert light into electrochemical energy for directly splitting water into hydrogen (H₂) and oxygen. NREL's world-record PEC systems are made of high-quality “III-V” semiconductors, which are alloys combining Group III elements (e.g., indium, gallium, etc.) with Group V elements (such as arsenic, phosphorous, etc.).

PEC offers a promising route to inexpensive, sustainable, and low-carbon H₂ fuel by harvesting light from the sun, but challenges remain in performance and cost. Recent techno-economic analysis has shown that extremely efficient PEC systems (as high as 25%) are needed to meet the U.S. Department of Energy's Fuel Cell Technologies Office's H₂ production target of \$2 per kg.²

NREL's accomplishment demonstrates significant progress on the quest to high-efficiency PEC systems. To optimize efficiency, NREL stacked two III-V semiconductor absorbers in tandem (gallium indium arsenide and gallium indium phosphide) to separate the duty of absorbing short wavelengths (blue light) and long wavelengths (red light). This required two major innovations. The first employs inverted metamorphic epitaxy, which enables absorber layers to be grown in a fashion that minimizes interface defects and charge recombination. The second employs a transparent graded buffer to connect the two absorbers. This buffer slowly changes the lattice constant between absorbers, which enables the bandgap of each

junction to be varied independently and optimized to maximize efficiency.

The NREL team also made an important contribution to the measurement and benchmarking of these systems. They found that the research community has historically overestimated device efficiency due to common errors in simulating solar light and assumptions in defining the device active area.³ Having addressed these errors, the high efficiency (which would have been even higher under the previously standard practices) is even more impressive.

While the world record efficiency is an important achievement, PEC technology is still challenged by limited durability. The NREL team and PEC community as a whole are now placing a larger emphasis on increasing the durability of their PEC systems by modifying the electrode with protective coatings that will limit photocorrosion without sacrificing efficiency.

Continued significant advancements in efficiencies along with an increased focus on durability, surface area, and system cost will be critical to enable renewable, clean and cost effective H₂ production.



Figure 1. H₂ bubbles being generated in water from the illumination of a high-efficiency semiconductor-based PEC cell.

¹ Khaselev and Turner, *Science*, 1998, 280, 425.

² Shaner *et al.*, *Energy Environ Sci.*, 2016, 9, 2354.

³ Doscher *et al.*, *Energy Environ Sci.*, 2016, 9, 74.

Pathway to Economic Hydrogen from Biomass Fermentation

Case studies for modeling future hydrogen production scenarios from large-scale biomass fermentation identify the most impactful cost reducing steps.

Strategic Analysis, Inc.

Detailed cost analyses identified a potential pathway for fermentative hydrogen (H₂) production to reach less than \$4/kg. Achieving this cost will require significant research success and engineering optimization, which can be guided by this analysis. Strategic Analysis Inc. developed projected high-volume “current” and “future” case studies modeling H₂ production via large scale fermentation (50,000 kg/day) that will be made available on the Hydrogen Production Analysis Model (H2A) website.¹ The projected “current case” is based on 2015 lab-proven technology and the projected “future case” accounts for expected technology advancements by 2025 (see Figure 1).

The engineering systems model used as the basis for the analysis leverages existing knowledge from industrial-scale fermentation of biomass to produce biofuels. Because fermentation to H₂ is not yet commercial, the team worked with researchers from the National Renewable Energy Laboratory to estimate several inputs to the model.

The projected “current case” results in prohibitively high production costs of more than \$50/kg, but more importantly identifies real R&D opportunities to advance the current state-of-the-art and bring costs down significantly. The “current case” costs are dominated by the low feedstock loading (12.8 g cornstover/L). Feedstock loading directly influences the required volume of fermentation broth, which in turn effects the quantity of reactors required, total reactor capital cost, and heating requirements. The low concentration associated with the “current case” results in fermentation batches of 2.7 billion liters of broth required for 50,000 kg/day H₂ production, an unfeasible number of reactors (728), and cost

prohibitive energy and wastewater processing requirements.

The projected “future case” is based on technological advancements deemed feasible by 2025, including increasing the feedstock loading to 175 g/L, consistent with the U.S. Department of Energy’s Bioenergy Technologies Office target for biomass hydrolysis. This is the most significant contributor to the order of magnitude cost reduction seen between the “current” and “future” cases. The significance of the higher feedstock loading is reflected in the reduction in the number of required reactors to 12. Other key advances include increasing the H₂ produced per kg of feedstock due to microbes converting more types of biomass sugars (i.e., pentose in addition to hexose) into H₂, and a higher yield per sugar molecule. The combined improvements result in a projected cost of \$5.65/kg for a 50,000 kg/day H₂ production facility. The report also identifies several steps beyond the 2025 timeframe that could further reduce costs to less than \$4/kg, such as improved process efficiencies. Future analysis work is expected to build on these case studies, such as modeling integrated systems to address areas of high cost.

Case Study	Optimistic Value (2007\$/kg H ₂)	Baseline Value (2007\$/kg H ₂)	Conservative Value (2007\$/kg H ₂)
Current Case (2015)	\$59.76	\$67.71	\$75.67
Current Case (2015) with byproduct credit	\$40.88	\$51.02	\$61.16
Future Case (2025)	\$7.68	\$8.56	\$9.43
Future Case(2025) with byproduct credit	\$3.40	\$5.65	\$7.91

Figure 1. High-volume cost projections for fermentative H₂ production. Cases with and without byproduct credit are reported. Byproduct credit assumes excess thermal energy is converted to electricity in a gas turbine electrical generator and sold to the grid. Electricity byproduct selling price is set at 6.89¢/kWh average electricity price (levelized over 40 year life).

¹ https://www.hydrogen.energy.gov/h2a_production.html.